Mesomorphic and charge transport properties of novel fluorinated discotic liquid crystal

Sasada, Yasuyuki

(Degree)
博士（工学）

(Date of Degree)
2009-03-25

(Date of Publication)
2011-11-29

(Resource Type)
doctoral thesis

(Report Number)
甲4588

(URL)
https://hdl.handle.net/20.500.14094/D1004588

Doctoral Dissertation

博士論文

Mesomorphic and charge transport properties of novel fluorinated discotic liquid crystal

（新規フッ素化ディスコチック液晶の液晶性と電荷移動特性）

January, 2009

平成２１年１月

Graduate School of Science and Technology, Kobe University

神戸大学大学院自然科学研究科

Yasuyuki SASADA

笹田康幸

Contents

Preface

Intermolecular interactions are of essential for the morphological behavior of soft matters rather than the solid states of matter. In particular, intermolecular specific interactions such as hydrogen bond, dipole-dipole, charge transfer etc. make the molecular aggregations form a variety of orders and in the case of liquid crystals, the diversity of ordering are easily operated with such intermolecular interactions.[1-3]

Most of these are issues of molecular level segregations taking a place in the molecular aggregations and the fluorophilic and fluorophobic interactions are of typical and lead to a variety of molecular orders in mesomorphism involving its dynamical aspects.

Fluorine atom has been extensively studied so far and its unique properties have been revealed.[4] Some specific interactions have been proposed and for example, quadrapolar interactions working among aromatics and fluorinated aromatics are strongly supported in the system of benzene as a mostly simple example.[5-8] Even for dendric molecules with perfluoroalkyl chains the nano-segregation easily takes place to form a hierarchical columnar orders.[9] These surely indicate that fluorination of aromatics and alkyl tails are a good tool for making segregation in the molecular aggregations which is sometimes a drastic change of molecular orders and is involving structures suitable for functional properties.[10]

On the other hand, it is just in the midst of time for developing organic electronics and studies on organic semiconductors have been so extensively studied to give some compounds which show so high mobility of charged carriers (~ 10^{-1} $cm^2V^{-1}s^{-1}$), which is comparable to that of amorphous silicon.[11] A variety of solid materials have been reported as new organic semiconductors applicable to thin film devices such as transistors and solar cells.[12-15]

Recent studies on the application of organic semiconductors to thin film devices have been focused onto organic transistors and some striking materials such as pentacene[16] and rubrene[17-19] have shown to be a good candidature for such devices in a practical point of view. Furthermore, the

fabrication of thin film devices using organic semiconductors is expected as a new type of materials which could be ink. This requires the compound to have certain solubility into common organic solvents and easily forms to be a homogeneous thin film as the active layer in devices. However, most of solid organic semiconductors do never show the required solubility and thus new strategies at molecular design have been proposed like the introduction of alkyl chains and polar substituents. From this point of view, liquid crystals are so interesting because of the alkyl tails, which is an origin of self-assembling nature due to the fluctuations of molecules.

Columnar structures formed by molecular stacking are one of the important features of molecular orders for liquid crystalline semiconductors based on discotic liquid crystals. In 1994, Haarer et al. reported a first discovery of liquid crystalline semiconductors of which carrier mobility reaches to almost 0.1 $cm^2V^{-1}s^{-1}$ comparable to amorphous silicon, but for a plastic columnar mesophase having a 3-dimentional order with a helical structure.[20] Also indicated that the higher ordering within the columns in both orientational and dynamical aspects is essentially important for efficient charge transport in an electronic process (charge hopping among molecules). Increasing the fluctuation modes of molecules in mesophase surely leads to decreasing the efficiency, that is the lower carrier mobility is recalled.[21]

In this thesis, fluorinated phenyl groups are introduced to discotic liquid crystal molecules aiming the induction of molecular level segregation, which is expected to show in a columnar order by strong attractive interactions. Three types of discotic liquid crystals, which are fluorinated on the peripheral aromatic rings, were synthesized and the mesomorphic and charge transport properties was investigated.

Chapter 1; 2, 3, 6, 7, 10, 11-hexakis (4-alkyloxy-2, 3, 5, 6-tetrafluorobenzoyloxy) triphenylenes (**CnF4E-TP**) and the branched chain derivative were synthesized and investigated there mesomorphic properties. It was found that all compounds exhibit Col_h phase having a wide range of

temperature, though corresponding hydrocarbon homologue exhibit discotic nematic (N_D) phase accompanied with Col_r phase in the lower temperature region. On the other hand, the stabilities of mesomorphism for the compounds having the branched peripheral chains larger then corresponding non-branched peripheral chain homologues

Chapter 2; To reveal the alteration of fluorinated positions in the phenyl rings leads to a drastic change of the mesomorphism involving the thermal stability, hexakis (4-octyloxybenzoyloxy) triphenylene derivatives with mono- or di-fluorinated at the inner (2- and/or 6-) or outer (3- and/or 5-) positions in the peripheral aromatic rings were synthesized and studied there mesomorphic transition behaviors. Especially, the thermal stability of the columnar mesophase are extremely stabilized over 400 ºC in 3-fluoro and 3,5-difluorobenzoyloxy derivatives fluorinated at the outer positions of phenyl rings. On the other hand, the thermal stabilities of the mesophases for 2-fluoro and 2,6-difluorobenzoyloxy derivatives fluorinated at the inner positions are decreased in comparison with non-fluorinated and full fluorinated derivatives.

Chapter 3; Novel discotic liquid crystal, 2, 3, 6, 7, 10, 11-hexakis (4-alkyloxy-2, 3, 5, 6-tetrafluorobenzyloxy) triphenylenes (**CnF41O-TP**) were synthesized and investigated those mesomorphic behaviour. All compounds exhibit Col_h phase with a wide range of temperature and very large phase transitions enthalpies (>50 $kJmol^{-1}$).

Chapter 4; The carrier mobilities of **CnF4E-TP** (n=12, 14, 16) and **CnF41O-TP** in Col_h phase of these compounds were measured by TOF technique. For **CnF4E-TP**, the drift mobilities were observed in a wide range of temperature 30~180 ºC. The carrier mobilities were evaluated in the order of 10^{-3} $cm^2V^{-1}s^{-1}$ in the high temperature region, and 10^{-4} $cm^2V^{-1}s^{-1}$ in the low temperature region.

For **CnF41O-TP**, the carrier mobilities were evaluated in the order of 10^{-2} $cm^2V^{-1}s^{-1}$, very faster carrier mobilities as discotic liquid crystals. Their fast mobilities may be cause to be highly order in

inter-columns from XRD measurement result and their high transition enthalpies and entropies.

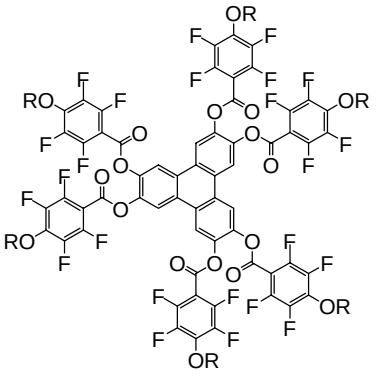

CnF4E-TP: R=C_nH_{2n+1} (n=6~10, 12, 14, 16)

C1(1C1)F4E-TP: R=

C6(2C2)F4E-TP: R=

C8(3, 7C1)F4E-TP: R=

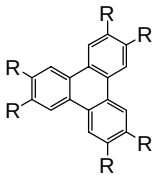

C8(2F)E-TP : R=

C8(2F6F)E-TP : R=

C8(3F)E-TP : R=

C8(3F5F)E-TP : R=

C8(2F5F)E-TP : R=

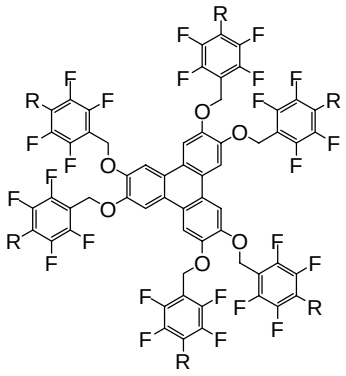

CnF41O-TP: R=OC_nH_{2n+1} (n=6, 8, 10)

References

[1] T. Kato, N, Mizoshita and K. Kishimoto, *Angew. Chem. Int. Ed.*, **2006**, 45, 38.

[2] I. M. Saez and J. W. Goodby, *J. Mater. Chem.*, 2005, **15**, 26.

[3] S. Laschat, A. Baro, N. Steinke, F. Giesselmann, C. Hägele, G. Scalia, R. Judele, E. Kapatsina, S. Sauer, A. Schreivogel, and M. Tosoni, *Angew. Chem. Int. Ed.*, **2007**, 46, 4832.

[4] *Organofluorine Chemistry Principle and Commercial Applications*, edited by R. E. Banks, B. E. Amart, J. C. Tatlow, Plenum, New York, **1994**.

[5] E. G. Cox, D. W. Cruickshank and J. A. Smith, *Proc. Royal Soc. London, Ser. A.*, **1958**, 274, 1.

[6] C. R. Patrick and G. S. Prosser, *Nature*, 1960, **187**, 1021.

[7] J. H. Williams, *Acc. Chem. Res.*, **1993**, 26, 593.

[8] J. H. Williams, J. K. Cockcroft and A. N. Fitch, *Angew. Chem. Int. Ed.*, **1992**, 31, 1655.

[9] V. Percec, G. Johansson, G. Unger and J. Zhou, *J. Am. Chem. Soc.*, **1996**, 118, 9855.

[10] V. Percec, M. Glodde, T. K. Bera, Y. Miura, I. Shiyanovskaya, K. D. Singer, V. S. K. Balagurusamy, P. A. Heiney, I. Schnell, A. Rapp, H.-W. Spiess, S. D. Hudson, and H. Duan, *Nature*, 2002, **419**, 384.

[11] P. G. LeComber and W. E. Spear, *Phys. Rev. Lett*., 1970, **25**, 509.

[12] L. Schmidt-Mende, A. Fechtenkötter, K. Müllen, E. Moons, R. H. Friend and J. D. MacKenzie, *Science*, **2001**, 293, 1119.

[13] L. Schmidt-Mende, A. Fechtenkötter, K. Müllen, R. H. Friend and J. D. MacKenzie, *Physica E*, **2002**, 14, 263.

[14] R. J. Bushby and O. R. Lozman, *Solid State and Materials Science*, 2002, **6**, 569.

[15] M. O'Neill and S. M. Kelly, *Adv. Mater.*, **2003**, 15, 1135.

[16] S. F. Nelson, Y. –Y. Lin, D. J. Gundlach and T. N. Jackson, *Appl. Phys. Lett.*, 1998, **72**, 1854.

[17] V. Podzorv, E. Menard, A. Borissov, V. Kiryukhin, J. A. Rogers and M. E. Gershenson, *Phys. Rev. Lett.*, **2004**, 93, 086602.

[18] V. C. Sundar, J. Zaumseil, V. Podzorov, E. Menard, R. L. Willett, T. Someya, M. E. Gershenson and J. A. Rogers, *Science*, **2004**, 303, 1644.

[19] M. Yamaguchi, J. Takeya, Y. Tominari, Y. Nakazawa, T. Kuroda, S. Ikehata, M. Uno, T. Nishizawa and T. Kawase, *Appl. Phys. Lett.*, **2007**, 90, 182117.

[20] D. Adam, P. Schuhmacher, J. Simmerer, L. Häulβing, K. Siemensmeyer, K. Etzbach, H. Ringdorf, and D. Haarer, *Nature*, 1994, **371**, 141.

[21] J. Simmerer, B. Glüsen, W. Paulus, A. Kettner, P. Schuhmacher, D. Adam, K. H. Etzbach, K. Siemensmeyer, J. H. Wendorf, H. Ringsdorf, and D. Haarer, *Adv. Mater*., 1996, **8**, 815.

General Introduction

1) Discotic liquid crystals

A discotic liquid crystal is generally the mesomorphic molecule, which has large π-conjugated system as central core structure, and peripheral chains such as alkyl chains.

It was generally though that mesomorphism could only be generated by molecules of a rod like molecule. However, in relatively recent years it has been shown that many other molecular architectures are also capable of generating mesophase, one of these is the disk-like structure. The existence of mesophase generated by disk-like molecules was theoretically predicted in 1970, and mesomorphism in discotic compounds of hexaalkanoylbenzens were first reported in 1977 by Chandrasekhar et al.[1] Up to the recent, an immense amount of research into the synthesis of disk-like molecules and into the structural characterization of the discotic mesophase generated have been carried out by many research groups all over the world. Two basic types of discotic mesophases have been widely acknowledged, these are columnar phase and the others. There are several different types of columnar phases; these are classified into hexagonal (Col_h), tetragonal (Col_t), rectangular (Col_r) and oblique (Col_{ob}) according to the different symmetry classes of two-dimensional lattice of columns (see Figure 1). Furthermore, Col_r is divided into four types therefore the arrangement of columns. The typical mesophase without columnar phase generated by disk-like molecule is the nematic phase. Discotic nematic (N_D) phase has only one phase axis similar to calamitic liquid crystal materials. The N_D phase is the least ordered discotic liquid crystal phase like its calamitic analog. As for the nematic phase of calamitic molecules, the N_D phase has only a statistically parallel ordering of molecular orientation with no translational ordering of the molecules (see Figure 2). Recently, a few disk-like materials have been reported that generate a columnar nematic (N_C) phase.[2-5] This phase is formed by short columns consist of few disk-like molecules that adopt a discotic nematic packing arrangement (see Figure 3).

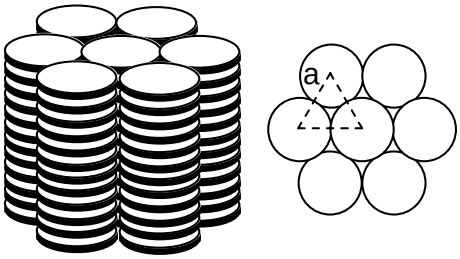

Hexagonal (Col_h) phase

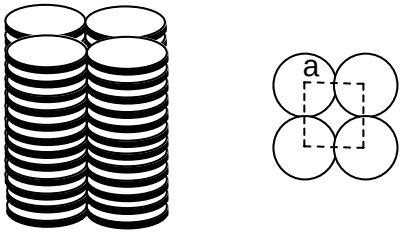

Tetragonal (Col_t) phase

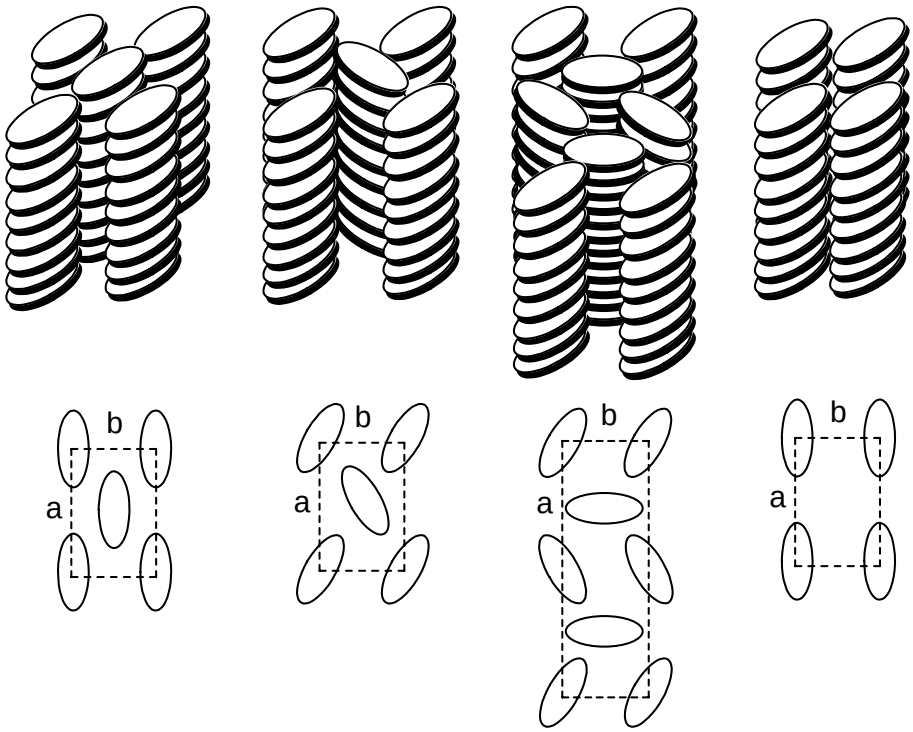

*C*2/m *P*2$_1$/a *P*2/a *P*2m

Rectangular (Col_r) phase

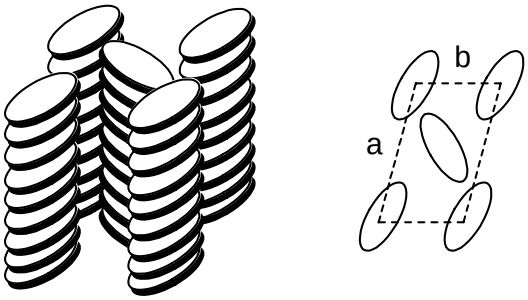

Oblique (Col_{ob}) phase

Figure 1 Classification of columnar phase.

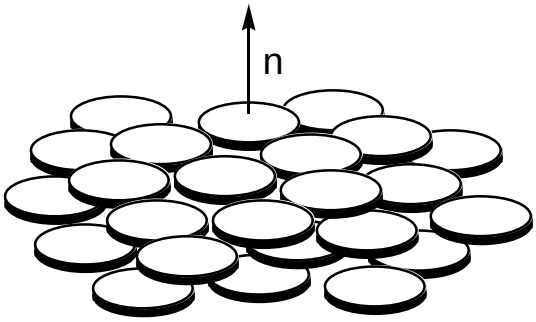

Figure 2 Molecular arrangement in discotic nematic (N_D) phase.

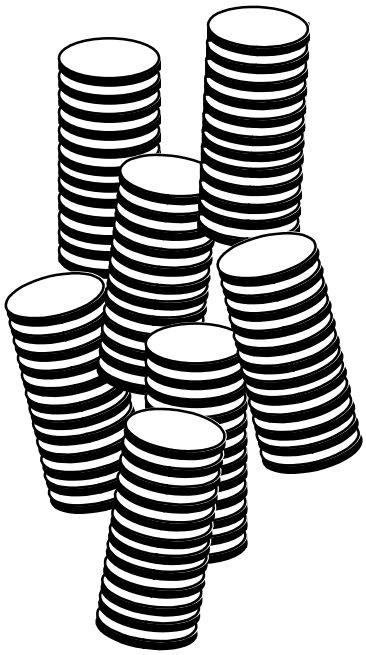

Figure 3 Molecular arrangement in columnar nematic (N_C) phase.

2) Liquid crystalline organic semiconductor

i) Organic semiconductor material

Recently it is expected that the Field-Effect-Transistor using organic semiconductor (OFET), which can be produced on a plastic substrate by printing technique with low cost, realize the electronic devices. The merit of OFET is an excellent flexibility, a lightweight, shock resistance, and so on. Organic semiconductor materials involve extended π-conjugated systems, and the carriers such as an electron and a hole migrate between molecules based on hopping or band conduction process. For the improvement of carrier mobility,

which is one of the important properties in OFET, it is necessary to make the π- conjugated system greatly overlapped among molecules. From these backgrounds, as an organic semiconductor material, molecular crystalline materials, such as pentacene and rubrene have been investigated so extensively. And the high-speed carrier mobility (>1.0 $cm^2V^{-1}s^{-1}$) has been reported in the single crystal of these in which the molecule is tightly packing. However, molecular crystals are generally unsuitable to the thin film production by a wet process owing to their low solubility into the common organic solvents. Additionally, in the thin film production by the vapor deposition, molecular crystals have many problems on element production processes that thin film production in which the molecules are aligned uniformly, is hard because of the difficult of crystal growth control.

On the other hand, liquid crystalline compounds which generally contain several alkyl chains, have a high solubility to common organic solvents, and therefore it is suitable for the solution process of thin film fabrication. Furthermore, liquid crystals are likely to exhibit a certain controllability of the molecular alignment due to the self-organization nature, and have an outstanding feature that their film formation with a uniform alignment of molecules could be attained to give a certain aria of uniformity in the film.

ii) Electronic conduction in mesophase -liquid crystalline organic semiconductor-

In organic semiconductors, the carrier mobility depends on the arrangement of molecule because the charge transport by molecules on elementary process of electronic conduction. The conduction mechanism is defined as two processes, band and hopping conductions according to the length for the localization of carrier on a molecule. The charge migration velocity between molecules depends on T shown in equation (1).[6-9]

$$T = \int \varphi_i H \varphi_{i+1} d\tau \qquad (1)$$

T: Transfer integral, φ_i, φ_{i+1}: molecular orbital, *H*: Hamiltonian

When T (transfer integral) is enough large, a carrier may be delocalized on molecules and charges migrate by band conduction. In molecular crystals, T is enough large owing to the dense highly ordered packing of most molecules and the molecular orbital interacted to each is degenerated into valence and conduction bands, leading to “band conduction”.

On the other hand, in amorphous materials, T is relatively small because each molecule is not approaching enough for extent of molecular orbital. So in those, the charges migrate in the hopping process conduction. T is lower than in crystal material and there is arrangement and energetic disorder owing to lower order of molecules in amorphous organic semiconductor. The electronic energy levels and T in the ordered aggregation are contributed due to participate in carrier hopping. Therefore, in hopping process conduction, the carrier is localized on molecule and hop to adjacent molecule by electric field and/or thermal assistance. The carrier mobility μ in hopping process conduction is formulated by H. Bässler (see equation (2)).[10]

$$\mu(\sigma, \Sigma, E, T) = \mu_0 \exp\left[-\left(\frac{2\sigma}{3kT}\right)^2\right] \exp\left[C\left\{\left(\frac{\sigma}{kT}\right) - \Sigma^2\right\}E^{\frac{1}{2}}\right] \quad (\Sigma \geq 1.5)$$

$$\mu(\sigma, \Sigma, E, T) = \mu_0 \exp\left[-\left(\frac{2\sigma}{3kT}\right)^2\right] \exp\left[C\left\{\left(\frac{\sigma}{kT}\right) - 1.5^2\right\}E^{\frac{1}{2}}\right] \quad (\Sigma < 1.5) \qquad (2)$$

σ: distribution of molecular orbital, Σ: disorder of distance between molecules

E: electric field, *T*: the absolute temperature

In mesophase, it is thought that the charge migrates between molecules on the hopping process. The highly packing of molecule and weakly disorder of molecular arrangement are effective to improve the carrier mobility. Therefore, it is thought that highly ordered molecular alignment and densified packing is

advantageous to first carrier mobility in columnar phase of discotic liquid crystals.

It was reported in 1994 that the hexaalkylthio triphenylene derivatives exhibit highly mobility of 10^{-1} $cm^2V^{-1}s^{-1}$ in helical columnar phase, which is equal to one of a-Si. Since then, many report of liquid crystal semiconductor using discotic liquid crystals have been shown. The example is shown in Figure 4.

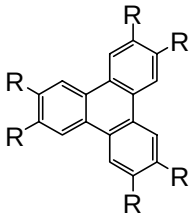

R=SC_6H_{13}; [11, 12] Cr 62 H 70 Col_h 93 Iso (°C)

μ=0.10 $cm^2V^{-1}s^{-1}$ (in H phase)

R=OC_4H_9; [13, 14] Cr 88.6 Colp 145.6 Iso (°C)

$\mu=2.5\times10^{-2}$ $cm^2V^{-1}s^{-1}$ (in Col_p phase)

R=OC_5H_{11}; [13, 14] Cr 69 Col_h 122 Iso (°C)

$\mu=1.9\times10^{-3}$ $cm^2V^{-1}s^{-1}$ (in Col_h phase)

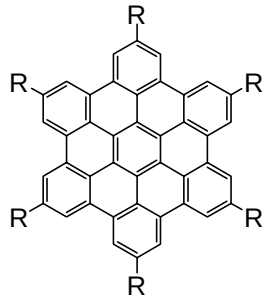

R=$C_{12}H_{25}$; [15] Cr 87 Col_h 417 Iso (°C)

$\Sigma\mu_{1D}$=0.38 $cm^2V^{-1}s^{-1}$ (in Col_h phase)

R=$C_{14}H_{29}$;[15] Cr 87 Col_h 417 Iso (°C)

$\Sigma\mu_{1D}$=0.31 $cm^2V^{-1}s^{-1}$ (in Col_h phase)

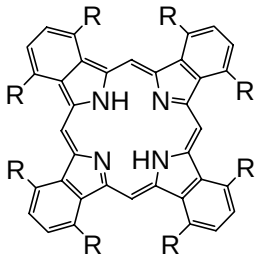

R=C_8H_{17}; [16] Cr 85 Col_r 101 Col_h 152 Iso (°C)

μ=0.1 $cm^2V^{-1}s^{-1}$ (in Col_r phase)

$\mu=9.0\times10^{-2}$ $cm^2V^{-1}s^{-1}$ (in Col_h phase)

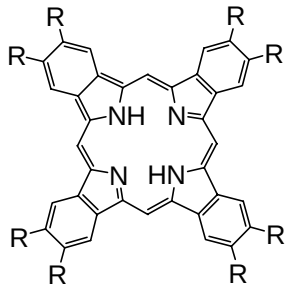

R=$C_{12}H_{25}$; [17] Cr 83 Col_h 309 Iso (°C)

$\Sigma\mu_{1D}=6.3\times10^{-3}$ $cm^2V^{-1}s^{-1}$ (in Col_h phase)

R=$C_{18}H_{29}$; [17] Cr 98 Col_h 247 Iso (°C)

$\Sigma\mu_{1D}=4.8\times10^{-3}$ $cm^2V^{-1}s^{-1}$ (in Col_h phase)

Figure 4 Mesomorphic and charge transport properties of discotic liquid crystalline semiconductors.

3) The effect of fluorination on liquid crystals

The fluoroline substituent in organic compounds is regarded as so interesting because of the combination of polar and steric effects, and the great strength of the C-F bond which confers stability on fluorinated compounds. Some quantitative parameters in respect of polarity and size of various substituent found in organic molecules are shown in Table 1.[18-21]

Table 1 Quantified polarity and size parameters for common substituent of organic molecules.

Property	H	F	Cl	Br	I	C	N	O
Electronegativity	2.20	3.98	3.16	2.96	2.66	2.55	3	3.5
C-X Dipole moment / D	0.4	1.41	1.46	1.38	1.19	–	–	–
Polarizability / 10^{-25} cm^{-1}	6.67	5.57	21.8	30.5	47	–	–	–
van der Waals Radii / Å	1.20	1.47	1.75	1.85	1.98	1.70	1.55	1.52
C-X bond length / Å	1.09	1.38	1.17	1.94	2.13	–	–	–
C-X Bond strength / KJ mol^{-1}	410	484	323	269	212	–	–	–

Fluorine atom has the highest electronegativity (3.98) all elements, and hence as a substituent confers a high dipole moment on the C-F bond. In an aliphatic or alicyclic environment the dipole moment is relatively large, *e.g.*, 1.85 D in fluoromethane, while in an aromatic environment the mesomeric effect cause a reduction of dipole moment, *e.g.*, 1.50 D for fluorobenzene. Despite such a high polarity of atom, the fluorine atom has a low polarizability, which lead to be the lower intermolecular dispersion interaction. The fluorine atom is the smallest in diameter, next to hydrogen atom. So although a fluoro substituent obviously cause a steric effect, the size influence is not too drastic, which enable it to be usefully incorporated into the original molecules for the beneficial modification of properties. The parameters of substituents that include carbon, nitrogen and oxygen are also shown in Table 1, but of course they must have other units bonded to them to give various different groups, which are much larger than a fluorine

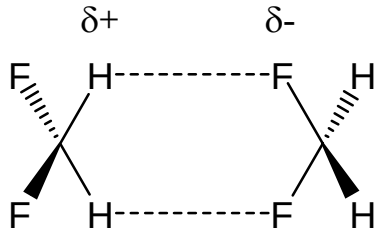

Figure 5 Interaction image in difluoromethane.

atom.

The interesting influence of fluoro substituents on properties as well exemplified by comparing hydrocarbon with perfluorocarbons, and such a comparison of behavior and properties is very applicable to liquid crystals, which almost always possess hydrocarbon chains in their molecular structure. For example, it have been shown that the introduction of perfluoroalkyl chains to the terminal chains enhances the mesomorphic thermal stability and facilitate smectic phase alignment in calamitic liquid crystals,[22-29] and the hexagonal columnar phase in discotic liquid crystals,[30-32] is probably owing to fluorophilic and fluorophobic interactions.

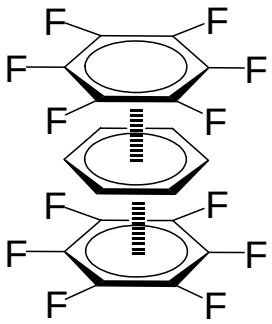

Figure 6 Interaction image between hexafluorobenzene and benzene.

Furthermore, the highly polar nature of the C-F bond can in turn causes polarization of the C-H bond of the same carbon, thus enabling the hydrogen to be involved in hydrogen bonding with the fluorine atom of a neighbor molecules. For example, difluoromethane has a significantly higher boiling point (-51.6 °C) than either the hydrocarbon (methane) or perfluorocarbon (tetrafluoromethane) homologues, which boil at

–161 °C and –128 °C, respectively.[33] This interaction image is schematically shown in Figure 5.

On the other hand as for interaction of fluorinated aromatics, remarkable influence is found for the complex resulting from an equimolar mixture of fully fluorinated and hydrocarbon aromatics. It has been reported that hexafluorobenzene (3.9 °C) and benzene (5.5 °C) form complexes in the mixture that have a higher melting point (23.7 °C), and is probably due to quadrapolar interaction[34, 35] as depicted in Figure 6.

Furthermore, compound **A** exhibit Col_h phase owing to the form action of the dimers by the hydrogen bond between fluorine atoms on fully fluorinated benzene ring and hydrogen atoms on the non-fluorinated benzene ring (image is shown in Figure 7).[36]

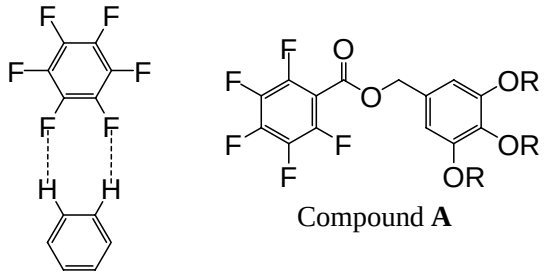

Compound **A**

R=C_8H_{17} Col_r 29 Col_h 46 Iso (°C)
R=$C_{10}H_{21}$ Col_h 42 Iso (°C)
R=$C_{12}H_{25}$ Col_h 40 Iso (°C)

Figure 7 Interaction image and mesomorphic properties of compound A.

Especially, the fully fluorinated aromatic ring is expected to exhibit various interactions owing to the nature of fluorine atom and has a potential for a construction of highly ordered molecular alignment.

4) References

[1] S. Chandrasekhar, B. K. Sadashiva, and K. A. Suresh, *Pramana*, 1977, **9**, 471.

[2] K. Praefcke, D. Singer, B. Kohne, M. Ebert, A. Liebmann, and J. H. Wendorff, *Liq. Cryst*., 1991, **10**, 147.

[3] H. Beings, O. Karthaus, H. Ringsdorf, C. Bashr, M. Ebert, and J. H. Wendorff, *Liq. Cryst.*, 1991, **10**, 161.

[4] K. Praefcke, D. Singer, and B. Kohne, *Liq. Cryst*., 1993, **13**, 445.

[5] H. Ringsdorf, R. Wustefeld, E. Zerta, M. Ebert, and J. H. Wendorff, *Angew. Chem*., 1989, **101**, 934.

[6] R. A. Marcus, *Rev. Mod. Phys.*, **1993**, *65*, 599.

[7] P. F. Barbara, T. J. Meyer, M. A. Ratner, *J. Phys. Chem.*, **1996**, *100*, 13148.

[8] V. Balzani, A. Juris, S. Campagna, S. Serroni, *Chem. Rev.*, **1996**, *96*, 759.

[9] J. L. Brédas, J. P. Calbert, D. A. da Silva Filho, J. Cornil, *Proc. Natl. Acad. Sci. U. S. A.*, **2002**, *99*, 5804.

[10] H. Bässler, *Mater, Phys. Stat. Solid. B*, 1993, **175**, 15.

[11] C. Destrade, M. C. Mondon, J. Malthete, *J. Phys. (Paris), Suppl. 40*, **1979**, C3, 17.

[12] H. Iino, Y. Takayashiki, J. Hanna, J. Bushby, and D. Haarer, *Appl. Phys. Lett.*, **2005**, *87*, 192105.

[13] H. Iino, J. Hanna, and D. Haarer, *Phys. Rev. B*, 2005, **72**, 193203.

[14] H. Monobe, Y. Shimizu, S. Okamoto, and H. Enomoto, *Mol. Cryst. Liq. Cryst.*, 2007, **476**, 31.

[15] A. M. de Craats, J. M. Warman, A. Fechtenkotter, J. D. Brand, M. A. Harbison, and K. Müllen, *Adv. Mater*., 1999, **11**, 1469.

[16] H. Iino, J. Hanna, R. J. Bushby, B. Movaghar, B. J. Whitaker, and M. J. Cook, *Appl. Phys. Lett*., 2005, **87**, 132102.

[17] P. G. Schouten, J. M. Warman, M. P. de Haas, C. F. van Nostrum, H. Gelinck, R. J. M. Notte, M. J.

Copyn, J. W. Zwikker, M. K. Engel, M. Hanack, Y. H. Chang, and W. T. Ford, *J. Am. Chem. Soc.*, 1994, **116**, 6880.

[18] A. Bondi, *J. Phys. Chem.*, 1964, **68**, 441.

[19] K. D. Sen and C. K. Jorgensen, *'Electronegativity'*, 1987, Springer, New York.

[20] J. K. Nagel, *J. Am. Chem. Soc.*, 1990, **112**, 4740.

[21] M. Hird, *Chem. Soc. Rev.*, 2007, **36**, 2070.

[22] H. Liu and H. Nohira, *Liq. Cryst.*, 1996, **20**, 581.

[23] A. C. Griffin and N. W. Buckly, *Mol. Cryst. Liq. Cryst.*, 1978, **41**, 141.

[24] S. Misaki, S. Takamura, M. Sufuji, T. Mitote and M. Matsumura, *Mol. Cryst. Liq. Cryst.*, 1981, **66**, 123.

[25] A. V. Ivashchenko, E. I. Kovshev, V. T. Lazareva, E. K. Prudnikova, V. V. Titov, T. I. Zverkova, M. I. Barnik and L. M. Yagupolski, *Mol. Cryst. Liq. Cryst.*, 1981, **67**, 235.

[26] E. P. Janulis Jr, J. C. Novack, G. A. Papapolymerou, M. Tristani-Kendra and W. A. Huffman, *Ferroelectronics*, 1998, **85**, 375.

[27] H. T. Nguyen, G. Sigaud, M. F. Achard, F. Hardouin, R. J. Twieg and K. Betterton, *Liq. Cryst.*, 1991, **10**, 389.

[28] M. Koden, K. Nakagawa, Y. Ishii, F. Fukuda, M. Matsuura and K. Awane, *Mol. Cryst. Liq. Crsyt*., 1989, **6(6)**, 185.

[29] A. Sakaigawa and H. Nohira, *Ferroelectronics*, 1993, **148**, 71.

[30] N. Terasawa, H. Monobe, K. Kiyohara, Y. Shimizu, *Chem. Lett*., 2003, **32**, 214.

[31] B. Alameddine, O. F. Aebischer, W. Amrein, B. Donnio, R. Deschenaux, D. Guillon, C. Savary, D. Scanu, O. Scheidegger, T. A. Jenny, *Chem. Mater.*, 2005, **17**, 4798.

[32] U. Dahn, C. Erdelen, H. Ringsdorf, R. Festag, J. H. Wendof, P. A. Heiney, and N. C. Maliszewskyj, *Liq. Cryst*. 1995, **19**, 759.

[33] W. Caminati, S. Melandri, P. Moreschini and P. G. Favero, *Angew. Chem. Int. Ed.*, 1999, **38**, 2924.

[34] V. R. Thalladi, H-C. Weiss, D. Bläser, R. Boese, A. Nangia and G. R. Desiraju, *J. Am. Chem. Soc.*, 1998, **120**, 2702.

[35] B. E. Smart, *J. Fluorine Chem.*, 2001, **109**, 3.

[36] K. Kishikawa, K. Oda, S. Aikyo and S. Kohmoto, *Angew. Chem. Int. Ed.*, 2007, **46**, 764.

Chapter 1

Mesomorphic properties of

2,3,6,7,10,11-hexakis-(4-alkoxy-2,3,5,6-tetrafluorobenzoyloxy)

triphenylenes

1-1. Introduction

The fluorinated compounds have attracted much interest because of their unique properties in chemistry and physics.[1] Especially in research field of LCDs technology, liquid crystal materials possessing the fluorinated aromatic rings or linkage groups have been synthesized and reported their properties such as dielectric anisotropy, rotational viscosity, etc.,[2-6] because the fluorination gives large dielectric anisotropy without the depression of the mesomorphic properties. On the other hand, for fluorinated discotic liquid crystals, only a few reports have been seen to show that a thermal stability of hexagonal columnar (Col_h) phase is enhanced by introducing perfluoroalkyl structures to peripheral chains of the central core part, probably due to the fluorophilic and fluorophobic interactions.[7-9]

On the other hand, for the fluorination of aromatic rings in discotic compounds, it has been reported that dodecafluorotriphenylene and triphenylene derivatives form complexes in the mixture that have a higher melting point, probably due to quadrapolar interaction. Moreover, columitic compound having fully fluorinated and non-fluorinated phenyl rings exhibit Col_h phase owing to form the dimmer by hydrogen bond between fluorine atom on fully fluorinated benzene ring and hydrogen atom on non-fluorinated benzene ring.[10-12] Thus, the fully fluorinated aromatic ring is expected various interaction owing to the nature of fluorine atom and has a potential for a construction of highly ordered molecular alignment.

A series of novel 2,3,6,7,10,11-hexakis(4-alkoxy-2,3,5,6-tetrafluorobenzoyloxy)triphenylene (**CnF4E-TP**s; see Figure 1-1) having non-branched and branched alkyl moieties as peripheral chain were

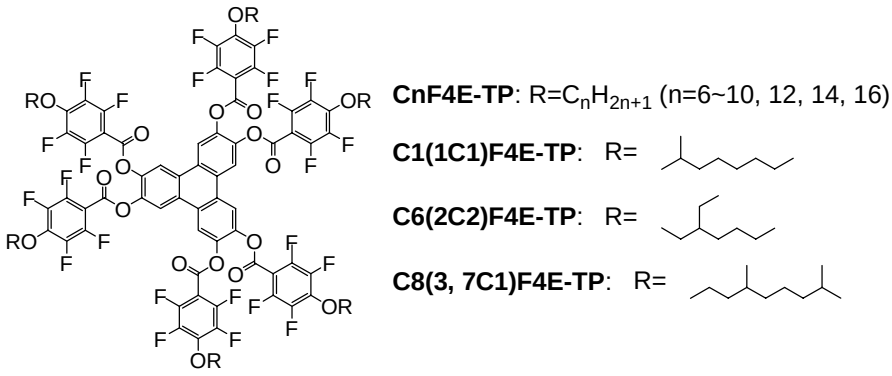

Figure 1-1 Chemical structure of hexakis (4-alkoxytetrafluorobenzoyloxy) triphenylene derivatives

synthesised (Scheme 1-1) to study the mesomorphic behavior and the corresponding non-fluorinated (hydrocarbon) homologues[13] were compared. The identification of these compounds was carried out by ^{1}H-NMR, ^{19}F-NMR, FT-IR, elemental analyses, and TOF-MS. And the mesomorphic behavior was investigated by polarized optical microscopy (POM), DSC measurement and X-ray diffraction technique.

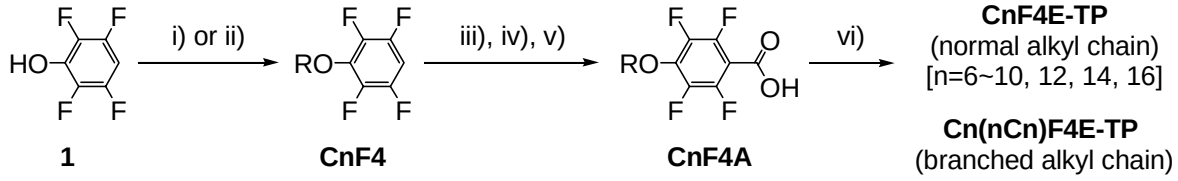

Scheme 1-1 Synthetic route of **CnF4E-TPs** and **Cn(nCn)F4E-TP**: i) RBr, K_2CO_3, TBAB, MEK, reflux; ii) ROH, PPh_3, DEAD, THF, rt.; iii) *n*-BuLi/Hexane, THF, -78 °C; iv) CO_2(S), -78 °C; v) 3M-HCl*aq*, rt.; vi) 2,3,6,7,10,11-hexahydroxytriphenylene, DCC, DMAP, CH_2Cl_2, rt.

1-2. Experimental

1-2-1. General measurement

^{1}H-NMR spectra were observed at 500.0 MHz on JEOL ECA500 FT-NMR spectorometer using $CDCl_3$ as solvent. Tetramethylsilane was used an internal standard.^{19}F-NMR spectra were observed at 470.6 MHz on the same spectrometer, Mass spectra was obtained on JEOL Accu TOF spectrometer. IR spectra were measured on Bio-Rad FTS6000 FT-IR spectrometer for the KBr pellet.

1-2-2. Measurement of mesomorphism

The phase transition temperatures and enthalpies of the compounds were measured by differential scanning calorimetry min (DSC, TA instrument DSC2920) for 5-10 mg samples of freshly recrystallised materials at a scanning rate of 5 °C/. Microscopic observations of the optical texture of mesophase were observed by a polarrized microscope (Olympus BH2) equipped with hot stage (Mettler FP90). The mesophases were identified by X-ray diffraction (Rigaku, RINT-2000) for non-arrigned sample in the mesophase temperature ranges.

1-2-3. Synthesis

1-2-3-1. 3-hexyloxy-1,2,4,5-tetrafluorobenzene (C6F4)

Following the addition of K_2CO_3 20.0 g (144.5 mmol) into a solution of 2,3,5,6-tetrafluorophenol (**1**) 20.1 g (121.3 mmol) in 2-buanone (100 mL), tetrabutylammonium bromide 4.7 g (14.5 mmol) and the solution of bromohexane 22.1 g (144.5 mmol) in 2-butanone (50 mL) here added into the suspension mixture, and was stirred with refluxing for 4 h. Water (100 mL) and diethyl ether were added to the reaction mixture at room temperature, and the sparated organic layer was washe with brine (100 mL) and dried over anhydrous $MgSO_4$. The solution removed under reduced pressure and the residue was purified by column chromatography on silica gel (300 g), eluting with hexane to yield 30.1 g (120.4 mmol) of **C6F4** as colourless liquid, yield 97.8 %. ^{1}H-NMR ($CDCl_3$, TMS, 500.0 MHz) δ 0.92 (t, J = 7.0 Hz, 3H), 1.27–1.36 (m, 4H), 1.47 (quintet, J = 7.5 Hz, 2H), 1.78 (quintet, J = 8.0 Hz, 2H), 4.22 (t, J = 6.5 Hz, 2H), 6.74 (tt, $^3J_{HF}$ = 10.0 Hz, $^4J_{HF}$ = 3.0 Hz 1H); ^{19}F-NMR ($CDCl_3$, $CFCl_3$, 470.0 MHz), δ –140.8 (dd, $^3J_{FF}$ = 14.8 Hz, $^5J_{FF}$ = 8.9 Hz, 2F), –157.6 (td, $^3J_{FF}$ = 13.6 Hz, $^5J_{FF}$ = 7.1 Hz 2F).

1-2-3-2. 3-hexyloxy-2,3,5,6-tetrafluorobenzoic acid (C6F4A)

A solution of 3-hexyloxy-1,2,4,5-tetrafluorobenzene (**C6F4**) 30.1 g (120.4 mmol) in dry THF (250 mL) was added 1.60 molL^{-1} *n*-BuLi in hexane 105 mL (168 mmol) at –78 ºC, and the reaction mixture was stirred for 2 h at –78 ºC, To the reaction mixture was added a solid of CO_2 (Dry Ice) as portionwise at –78 ºC, and the reaction mixture was stirred for 1h at –78 ºC and at room temperature over night. 3M-HCl*aq* (100 mL) and diethyl ether (200 mL) were added to the reaction mixture at 0 ºC, and the separated organic layer was washed with brine (100 mL) and dried over anhydrous $MgSO_4$. The solvent was removed under reduced pressure and the purified by recrystallization using n-hexane to yield 22.3 g (75.7 mmol) of **C6F4A** as colourless crystal (yield=62.9 %). ^{1}H-NMR ($CDCl_3$, TMS, 500.0 MHz) δ 0.91 (t, J = 7.0 Hz, 3H), 1.31–1.36 (m, 4H), 1.47 (quintet, J = 7.3 Hz, 2H), 1.80 (quintet, J = 7.1 Hz, 2H), 4.37 (t, J = 6.7 Hz, 2H), 9.3 (s, O*H*); ^{19}F-NMR ($CDCl_3$, $CFCl_3$, 470.0 MHz), δ –112.9 (d, $^3J_{FF}$ = 11.3 Hz, 2F), –131.3 (d, $^3J_{FF}$ = 10.8 Hz, 2F).

1-2-3-3. 2,3,6,7,10,11-hexakis(4-hexyloxy-2,3,5,6-tetrafluorobenzoyloxy)triphenylene (C6F4E-TP)

4-dimethylaminopyridine 1.50 g (12.24 mmol) was added into a solution of 4-hexyloxy-2,3,5,6-tetrafluorobenzoic acid (**C6F4A**) 4.29 g (12.24 mmol) and 2,3,6,7,10,11-hexahydorxytriphenylene (0.40g, 1.36 mmol) in CH_2Cl_2 (60 mL) and stirred for 1h at rt. *N*,*N*-dicyclohexylcarbodiimide (DCC) 2.53 g (12.24 mmol) in CH_2Cl_2 (20 mL) was then added, and the reaction mixture was stirred overnight at rt. The resulting mixture was filtlated and the filtlate was added to brine and stirred for 1 h and separated organic layer was washed with 3M-HCl*aq*, $NaHCO_3$*aq* and brine (50 mL, for each), and dried over anhydrous $MgSO_4$. The solvent was removed under reduced pressure and the residue was purified by column chromatography on silica gel (300 g), eluting with n-hexane/ ethyl acetate=3/1, followed by recrystallization using toluene (100 mL) and EtOH (400 mL) to yield 0.85 g (0.43 mmol) of **C6F4E-TP** as colourless crystal (yield=31.6 %). ^{1}H-NMR ($CDCl_3$, TMS, 500.0 MHz) δ 0.96 (t, *J* = 6.9 Hz, 18H), 1.38–1.41 (m, 24H), 1.52 (quintet, *J* = 7.0 Hz, 12H), 1.84 (quintet, *J* = 6.7 Hz, 12H), 4.33 (t, *J* = 6.5 Hz, 12H), 7.97 (s, 6H); ^{19}F-NMR ($CDCl_3$, $CFCl_3$, 470.0 MHz), δ –138.9 (s, 12F), –158.8 (s, 12F); MS *m/z*=1981.8 (Calc. 1981.7 for $C_{96}H_{84}F_{24}O_{18}$); FTIR (KBr, cm^{-1}) 2959, 2934, 2361, 2861, 2342, 1759, 1650, 1489, 1412, 1389, 1323, 1256, 1210, 1117, 1006, 939, 890, 835, 800; Anal. Calc. for $C_{96}H_{84}F_{24}O_{18}$: C, 58.19; H, 4.27; F, 23.01%. Found: C, 58.29; H, 4.29; F, 23.11%.

1-2-3-4. 3-heptyloxy-1,2,4,5-tetrafluorobenzene (C7F4)

Following the method employed for the synthesis of **C6F4**, 31.7 g (120.0 mmol, yield=99.6 %) of **C7F4** was obtained as colourless liquid by using 1-bromoheptane as the starting material. ^{1}H-NMR ($CDCl_3$, TMS, 500.0 MHz) δ 0.80 (t, *J* = 6.8 Hz, 3H), 1.26–1.38 (m, 6H), 1.46 (quintet, *J* = 7.5 Hz, 2H), 1.78 (quintet, *J* = 6.6 Hz, 2H), 4.21 (t, *J* = 6.4 Hz, 2H), 6.74 (tt, $^3J_{HF}$ = 10.2 Hz, $^4J_{HF}$ = 2.9 Hz 1H); ^{19}F-NMR ($CDCl_3$, $CFCl_3$, 470.0 MHz), δ –140.9 (dd, $^3J_{FF}$ = 24.6Hz, $^5J_{FF}$ = 13.6 Hz, 2F), –157.7 (td, $^3J_{FF}$ = 30.0 Hz, , $^5J_{FF}$ = 19.1 Hz 2F).

1-2-3-5. 3-heptyloxy-1,2,4,5-tetrafluorobenzoic acid (C7F4A)

Following the method employed for the synthesis of **C6F4A**, 12.9 g (41.8 mmol, yield=34.8 %) of **C7F4**

A was obtained as colourless crystal by using **C7F4** as the starting material. ^{1}H-NMR ($CDCl_3$, TMS, 500.0 MHz) δ 0.92 (t, J = 6.7 Hz, 3H), 1.36–1.43 (m, 6H), 1.51 (quintet, J = 7.6 Hz, 2H), 1.84 (quintet, J = 6.7 Hz, 2H), 4.34 (t, J = 6.5 Hz, 2H), 8.0 (s, O*H*); ^{19}F-NMR ($CDCl_3$, $CFCl_3$, 470.0 MHz), δ –112.9 (d, $^{3}J_{FF}$ = 11.3 Hz, 2F), –131.3 (td, $^{3}J_{FF}$ = 10.8 Hz, 2F).

1-2-3-6. 2,3,6,7,10,11-hexakis(4-heptyloxy-2,3,5,6-tetrafluorobenzoyloxy) triphenylene (C7F4E-TP)

Following the method employed for the synthesis of **C6F4E-TP**, 2.02 g (0.98 mmol, yield=72.1 %) of **C7F4E-TP** was obtained as colourless crystal by using **C7F4A** as the starting material. ^{1}H-NMR ($CDCl_3$, TMS, 500.0 MHz) δ 0.92 (t, J = 7.0 Hz, 18H), 1.33–1.41 (m, 36H), 1.51 (quintet, J = 7.5 Hz, 12H), 1.85 (quintet, J = 6.0 Hz, 12H), 4.34 (t, J = 6.5 Hz, 12H), 8.02 (s, 6H); ^{19}F-NMR ($CDCl_3$, $CFCl_3$, 470.0 MHz), δ –138.9 (s, 12F), –158.7 (s, 12F); FTIR (KBr, cm^{-1}) 2958, 2931, 2859, 2362, 1759, 1650, 1489, 1412, 1389, 1323, 1256, 1210, 1117, 998, 944, 889, 836, 802, 772, 725, 641; Anal. Calc. for $C_{102}H_{96}F_{24}O_{18}$: C, 59.30; H, 4.68; F, 22.07%. Found: C, 59.58; H, 4.59; F, 21.86 %.

1-2-3-7. 3-octyloxy-1,2,4,5-tetrafluorobenzene (C8F4)

Following the method employed for the synthesis of **C6F4**, 32.8 g (118.0 mmol, yield=98.0 %) of **C8F4** was obtained as colourless liquid by using 1-bromooctane as the starting material. ^{1}H-NMR ($CDCl_3$, TMS, 500.0 MHz) δ 0.80 (t, J = 6.8 Hz, 3H), 1.26–1.38 (m, 8H), 1.46 (quintet, J = 7.5 Hz, 2H), 1.78 (quintet, J = 6.6 Hz, 2H), 4.21 (t, J = 6.4 Hz, 2H), 6.74 (tt, $^{3}J_{HF}$ = 10.2 Hz, $^{4}J_{HF}$ = 2.9 Hz 1H); ^{19}F-NMR ($CDCl_3$, $CFCl_3$, 470.0 MHz), δ –140.9 (dd, $^{3}J_{FF}$ = 24.6Hz, $^{5}J_{FF}$ = 13.6 Hz, 2F), –157.7 (td, $^{3}J_{FF}$ = 30.0 Hz, , $^{5}J_{FF}$ = 19.1 Hz 2F).

1-2-3-8. 3-octyloxy-1,2,4,5-tetrafluorobenzoic acid (C8F4A)

Following the method employed for the synthesis of **C6F4A**, 21.4 g (66.2 mmol, yield=56.1 %) of **C8F4 A** was obtained as colourless crystal by using **C8F4** as the starting material. ^{1}H-NMR ($CDCl_3$, TMS, 500.0 MHz) δ 0.89 (t, J = 6.8 Hz, 3H), 1.29–1.36 (m, 8H), 1.46 (quintet, J = 7.0 Hz, 2H), 1.80 (quintet, J = 6.6 Hz, 2H), 4.37 (t, J = 6.3 Hz, 2H), 10.4 (s, O*H*); ^{19}F-NMR ($CDCl_3$, $CFCl_3$, 470.0 MHz), δ –112.9 (d, $^{3}J_{FF}$ = 10.9 Hz, 2F), –131.3 (d, $^{3}J_{FF}$ = 16.4 Hz, 2F).

1-2-3-9. 2,3,6,7,10,11-hexakis(4-octyloxy-2,3,5,6-tetrafluorobenzoyloxy) triphenylene (C8F4E-TP)

Following the method employed for the synthesis of **C6F4E-TP**, 1.44 g (0.67 mmol, yield=49.3 %) of **C8F4E-TP** was obtained as colourless crystal by using **C8F4A** as the starting material. ^{1}H-NMR ($CDCl_3$, TMS, 500.0 MHz) δ 0.94 (t, *J* = 6.5 Hz, 18H), 1.35–1.39 (m, 48H), 1.52 (quintet, *J* = 8.0 Hz, 12H), 1.85 (quintet, *J* = 8.0 Hz, 12H), 4.34 (t, *J* = 6.5 Hz, 12H), 8.00 (s, 6H); ^{19}F-NMR ($CDCl_3$, $CFCl_3$, 470.0 MHz), δ –138.9 (s, 12F), –158.7 (s, 12F); MS *m/z*=2148.7 (Calc. 2149.96 for $C_{108}H_{108}F_{24}O_{18}$); FTIR (KBr, cm^{-1}) 2958, 2929, 2858, 2361, 1759, 1650, 1488, 1412, 1389, 1323, 1256, 1209, 1117, 999, 951, 889, 835, 800, 771, 722, 642; Anal. Calc. for $C_{108}H_{108}F_{24}O_{18}$: C, 60.33; H, 5.06; F, 21.21 %. Found: C, 60.59; H, 4.88; F, 21.08 %.

1-2-3-10. 3-nonyloxy-1,2,4,5-tetrafluorobenzene (C9F4)

Following the method employed for the synthesis of **C6F4**, 34.9 g (119.4 mmol, yield=99.2 %) of **C9F4** was obtained as colourless liquid by using 1-bromononane as the starting material. ^{1}H-NMR ($CDCl_3$, TMS, 500.0 MHz) δ 0.88 (t, *J* = 6.8 Hz, 3H), 1.28–1.36 (m, 10H), 1.46 (quintet, *J* = 7.8 Hz, 2H), 1.77 (quintet, *J* = 6.8 Hz, 2H), 4.22 (t, *J* = 6.4 Hz, 2H), 6.74 (tt, $^{3}J_{HF}$ = 9.8 Hz, $^{4}J_{HF}$ = 2.9 Hz 1H); ^{19}F-NMR ($CDCl_3$, $CFCl_3$, 470.0 MHz), δ –140.9 (dd, $^{3}J_{FF}$ = 21.8Hz, $^{5}J_{FF}$ = 10.9 Hz, 2F), –157.7 (dd, $^{3}J_{FF}$ = 20.5 Hz, , $^{5}J_{FF}$ = 13.6 Hz 2F).

1-2-3-11. 3-nonyloxy-1,2,4,5-tetrafluorobenzoic acid (C9F4A)

Following the method employed for the synthesis of **C6F4A**, 25.0 g (74.3 mmol, yield=62.3 %) of **C9F4 A** was obtained as colourless crystal by using **C9F4** as the starting material. ^{1}H-NMR ($CDCl_3$, TMS, 500.0 MHz) δ 0.89 (t, *J* = 6.8 Hz, 3H), 1.28–1.35 (m, 10H), 1.46 (quintet, *J* = 7.5 Hz, 2H), 1.80 (quintet, *J* = 7.1 Hz, 2H), 4.37 (t, *J* = 6.7 Hz, 2H), 11.4 (s, O*H*); ^{19}F-NMR ($CDCl_3$, $CFCl_3$, 470.0 MHz), δ –138.6 (d, $^{3}J_{FF}$ = 16.3 Hz, 2F), –157.1 (d, $^{3}J_{FF}$ = 13.6 Hz, 2F).

1-2-3-12. 2,3,6,7,10,11-hexakis(4-nonyloxy-2,3,5,6-tetrafluorobenzoyloxy) triphenylene (C9F4E-TP)

Following the method employed for the synthesis of **C6F4E-TP**, 1.52 g (0.68 mmol, yield=50.0 %) of C9F4E-TP was obtained as colourless crystal by using C9F4A an the starting material. ^{1}H-NMR ($CDCl_3$,

TMS, 500.0 MHz) δ 0.92 (t, *J* = 7.0 Hz, 18H), 1.33–1.41 (m, 60H), 1.52 (quintet, *J* = 7.5 Hz, 12H), 1.85 (quintet, *J* = 7.5 Hz, 12H), 4.34 (t, *J* = 6.5 Hz, 12H), 8.02 (s, 6H); ^{19}F-NMR ($CDCl_3$, $CFCl_3$, 470.0 MHz), δ –138.9 (s, 12F), –158.7 (s, 12F); FTIR (KBr, cm^{-1}) 2927, 2856, 2361, 1759, 1650, 1488, 1412, 1389, 1323, 1256, 1210, 1117, 1002, 960, 935, 890, 836, 802, 772, 722, 642; Anal. Calc. for $C_{114}H_{120}F_{24}O_{18}$: C, 61.29; H, 5.41; F, 20.41 %. Found: C, 61.36; H, 5.26; F, 20.20 %.

1-2-3-13. 3-decyloxy-1,2,4,5-tetrafluorobenzene (C10F4)

Following the method employed for the synthesis of **C6F4**, 35.8 g (116.8 mmol, yield=97.0 %) of **C10F4** was obtained as colourless liquid by using 1-bromodecane as the starting material. ^{1}H-NMR ($CDCl_3$, TMS, 500.0 MHz) δ 0.89 (t, *J* = 7.0 Hz, 3H), 1.28–1.37 (m, 12H), 1.46 (quintet, *J* = 8.0 Hz, 2H), 1.78 (quintet, *J* = 7.0 Hz, 2H), 4.22 (t, *J* = 6.0 Hz, 2H), 6.74 (tt, $^3J_{HF}$ = 10.0 Hz, $^4J_{HF}$ = 4.5 Hz 1H); ^{19}F-NMR ($CDCl_3$, $CFCl_3$, 470.0 MHz), δ –140.9 (dd, $^3J_{FF}$ = 18.8 Hz, $^3J_{HF}$ = 14.1 Hz, 2F), –157.7 (dd, $^3J_{FF}$ = 23.5 Hz, $^3J_{HF}$ = 14.1 Hz, 2F).

1-2-3-14. 3-decylloxy-1,2,4,5-tetrafluorobenzoic acid (C10F4A)

Following the method employed for the synthesis of **C6F4A**, 26.5 g (75.7 mmol, yield=64.8 %) of **C10F4A** was obtained as colourless crystal by using **C10F4** as the starting material. ^{1}H-NMR ($CDCl_3$, TMS, 500.0 MHz) δ 0.88 (t, *J* = 10 Hz, 3H), 1.24–1.38 (m, 12H), 1.46 (quintet, *J* = 10.0 Hz, 2H), 1.80 (quintet, *J* = 10.0 Hz, 2H), 4.30 (t, *J* = 10.0 Hz, 2H), 11.3 (s, O*H*); ^{19}F-NMR ($CDCl_3$, $CFCl_3$, 470.0 MHz), δ –138.7 (d, $^3J_{FF}$ = 14.1 Hz, 2F), –157.2 (d, $^3J_{FF}$ = 14.1 Hz, 2F).

1-2-3-15. 2,3,6,7,10,11-hexakis(4-decyloxy-2,3,5,6-tetrafluorobenzoyloxy) triphenylene (C10F4E-TP)

Following the method employed for the synthesis of **C6F4E-TP**, 1.00 g (0.43 mmol, yield=31.6 %) of **C10F4E-TP** was obtained as colourless crystal by using **C10F4A** as the starting material. ^{1}H-NMR ($CDCl_3$, TMS, 500.0 MHz) δ 0.91 (t, *J* = 6.5Hz, 18H), 1.31–1.40 (m, 72H), 1.51 (quintet, *J* = 7.5Hz, 12H), 1.84 (quintet, *J* = 7.0Hz, 12H), 4.34 (t, *J* = 6.5Hz, 12H), 8.07 (s, 6H); 19F ($CDCl_3$, $CFCl_3$, 470.0 MHz), δ –138.8 (s, 12F), –158.4 (s, 12F), MS *m/z* = 2318.0 (Calc. 2318.3 for $C_{120}H_{132}F_{24}O_{18}$); FTIR (KBr, cm^{-1}) 2951, 2926, 2861, 2361, 2342, 1759, 1650, 1489, 1412, 1389, 1323, 1256, 1210, 1117, 1006, 939, 890, 835, 800;

Anal. Calc. for $C_{120}H_{132}F_{24}O_{18}$: C, 62.17; H, 5.74; F, 19.67%. Found: C, 62.22; H, 5.69; F, 19.77%.

1-2-3-16. 3-dodecyloxy-1,2,4,5-tetrafluorobenzene (C12F4)

Following the method employed for the synthesis of **C6F4**, 39.7 g (118.8 mmol, yield=98.7 %) of **C12F4** was obtained as colourless liquid by using 1-bromododecane as the starting material. ^{1}H-NMR ($CDCl_3$, TMS, 500.0 MHz) δ 0.88 (t, J = 7.0 Hz, 3H), 1.27–1.36 (m, 18H), 1.46 (quintet, J = 7.6 Hz, 2H), 1.77 (quintet, J = 7.1 Hz, 2H), 4.21 (t, J = 6.6 Hz, 2H), 6.73 (tt, $^3J_{HF}$ = 10.1 Hz, $^4J_{HF}$ = 3.1 Hz 1H); ^{19}F-NMR ($CDCl_3$, $CFCl_3$, 470.0 MHz), δ –140.9 (dd, $^3J_{FF}$ = 21.8 Hz, $^3J_{HF}$ = 10.9 Hz, 2F), –157.7 (dd, $^3J_{FF}$ = 21.8 Hz, $^3J_{HF}$ = 13.6 Hz, 2F).

1-2-3-17. 3-dodecylloxy-1,2,4,5-tetrafluorobenzoic acid (C12F4A)

Following the method employed for the synthesis of **C6F4A**, 37.5 g (99.1 mmol, yield=83.4 %) of **C12F4A** was obtained as colourless crystal by using **C12F4** as the starting material. ^{1}H-NMR ($CDCl_3$, TMS, 500.0 MHz) δ 0.88 (t, J = 6.7 Hz, 3H), 1.27–1.33 (m, 16H), 1.46 (quintet, J = 7.5 Hz, 2H), 1.80 (quintet, J = 7.1 Hz, 2H), 4.37 (t, J = 6.6 Hz, 2H), 10.4 (s, O*H*); ^{19}F-NMR ($CDCl_3$, $CFCl_3$, 470.0 MHz), δ –138.7 (d, $^3J_{FF}$ = 12.2 Hz, 2F), –157.1 (d, $^3J_{FF}$ = 16.3 Hz, 2F).

1-2-3-18. 2,3,6,7,10,11-hexakis(4-dodecyloxy-2,3,5,6-tetrafluorobenzoyloxy) triphenylene (C12F4E-TP)

Following the method employed for the synthesis of **C6F4E-TP**, 1.63 g (0.66 mmol, yield=48.5 %) of **C12F4E-TP** was obtained as colourless crystal by using **C12F4A** as the starting material. ^{1}H-NMR ($CDCl_3$, TMS, 500.0 MHz) δ 0.90 (t, J = 6.7 Hz, 18H), 1.30–1.40 (m, 96H), 1.51 (quintet, J = 7.8 Hz, 12H), 1.84 (quintet, J =7.9 Hz, 12H), 4.34 (t, J =6.4 Hz, 12H), 8.06 (s, 6H); ^{19}F ($CDCl_3$, $CFCl_3$, 470.0 MHz), δ –138.9 (s, 12F), –158.6 (s, 12F); Anal. Calc. for $C_{132}H_{156}F_{24}O_{18}$: C, 63.76; H, 6.32; F, 18.34 %. Found: C, 63.80; H, 6.26; F, 18.32%.

1-2-3-19. 3-tetradecyloxy-1,2,4,5-tetrafluorobenzene (C14F4)

Following the method employed for the synthesis of **C6F4**, 43.3 g (119.4 mmol, yield=99.2 %) of **C14F4** was obtained as colourless liquid by using 1-bromotetradecane as the starting material. ^{1}H-NMR

($CDCl_3$, TMS, 500.0 MHz) δ 0.88 (t, J = 6.8 Hz, 3H), 1.26–1.36 (m, 20H), 1.46 (quintet, J = 6.8 Hz, 2H), 1.77 (quintet, J = 6.6 Hz, 2H), 4.21 (t, J = 6.5 Hz, 2H), 6.73 (tt, $^3J_{HF}$ = 10.3 Hz, $^4J_{HF}$ = 3.2 Hz 1H); ^{19}F-NMR ($CDCl_3$, $CFCl_3$, 470.0 MHz), δ –140.8 (dd, $^3J_{FF}$ = 25.9 Hz, $^3J_{HF}$ = 10.9 Hz, 2F), –157.7 (dd, $^3J_{FF}$ = 21.8 Hz, $^3J_{HF}$ = 10.9 Hz, 2F).

1-2-3-20. 3-tetradecylloxy-1,2,4,5-tetrafluorobenzoic acid (C14F4A)

Following the method employed for the synthesis of **C6F4A**, 39.9 g (98.2 mmol, yield=82.2 %) of **C14F4A** was obtained as colourless crystal by using **C14F4** as the starting material. ^{1}H-NMR ($CDCl_3$, TMS, 500.0 MHz) δ 0.88 (t, J = 6.8 Hz, 3H), 1.26–1.36 (m, 20H), 1.46 (quintet, J = 7.9 Hz, 2H), 1.80 (quintet, J = 8.0 Hz, 2H), 4.37 (t, J = 6.8 Hz, 2H), 11.2 (s, O*H*); ^{19}F-NMR ($CDCl_3$, $CFCl_3$, 470.0 MHz), δ –138.6 (d, $^3J_{FF}$ = 17.7 Hz, 2F), –157.1 (d, $^3J_{FF}$ = 16.3 Hz, 2F).

1-2-3-21. 2,3,6,7,10,11-hexakis(4-tetradecyloxy-2,3,5,6-tetrafluorobenzoyloxy) triphenylene (C14F4E-TP)

Following the method employed for the synthesis of **C6F4E-TP**, 2.42 g (0.91 mmol, yield=67.1 %) of **C14F4E-TP** was obtained as colourless crystal by using **C14F4A** as the starting material. ^{1}H-NMR ($CDCl_3$, TMS, 500.0 MHz) δ 0.90 (t, J = 6.6 Hz, 18H), 1.30–1.42 (m, 120H), 1.52 (quintet, J = 7.7 Hz, 12H), 1.85 (quintet, J =6.7 Hz, 12H), 4.33 (t, J =6.3 Hz, 12H), 7.99 (s, 6H); ^{19}F ($CDCl_3$, $CFCl_3$, 470.0 MHz), δ –138.9 (s, 12F), –158.8 (s, 12F); Anal. Calc. for $C_{144}H_{180}F_{24}O_{18}$: C, 65.14; H, 6.83; F, 17.17 %. Found: C, 65.03; H, 6.77; F, 17.18 %.

1-2-3-22. 3-hexadecyloxy-1,2,4,5-tetrafluorobenzene (C16F4)

Following the method employed for the synthesis of **C6F4**, 44.8 g (114.7 mmol, yield=95.3 %) of **C16F4** was obtained as colourless liquid by using 1-bromohexadecane as the starting material. ^{1}H-NMR ($CDCl_3$, TMS, 500.0 MHz) δ 0.88 (t, J = 6.8 Hz, 3H), 1.26–1.36 (m, 24H), 1.46 (quintet, J = 7.8 Hz, 2H), 1.77 (quintet, J = 8.0 Hz, 2H), 4.21 (t, J = 6.6 Hz, 2H), 6.73 (tt, $^3J_{HF}$ = 10.0 Hz, $^4J_{HF}$ = 3.0 Hz 1H); ^{19}F-NMR ($CDCl_3$, $CFCl_3$, 470.0 MHz), δ –140.8 (td, $^3J_{FF}$ = 21.8 Hz, $^3J_{HF}$ = 10.9 Hz, 2F), –157.6 (dd, $^3J_{FF}$ = 21.8 Hz, $^3J_{HF}$ = 10.9 Hz, 2F).

1-2-3-23. 3-hexadecylloxy-1,2,4,5-tetrafluorobenzoic acid (C16F4A)

Following the method employed for the synthesis of **C6F4A**, 39.9 g (98.2 mmol, yield=84.1 %) of **C16F4A** was obtained as colourless crystal by using **C16F4** as the starting material. ^{1}H-NMR ($CDCl_3$, TMS, 500.0 MHz) δ 0.88 (t, J = 6.6 Hz, 3H), 1.26–1.36 (m, 24H), 1.46 (quintet, J = 7.7 Hz, 2H), 1.80 (quintet, J = 8.0 Hz, 2H), 4.37 (t, J = 6.4 Hz, 2H), 11.6 (s, O*H*); ^{19}F-NMR ($CDCl_3$, $CFCl_3$, 470.0 MHz), δ –138.6 (d, $^{3}J_{FF}$ = 10.9 Hz, 2F), –157.1 (d, $^{3}J_{FF}$ = 12.3 Hz, 2F).

1-2-3-24. 2,3,6,7,10,11-hexakis(4-hexadecyloxy-2,3,5,6-tetrafluorobenzoyloxy) triphenylene (C16F4E-TP)

Following the method employed for the synthesis of **C6F4E-TP**, 2.78 g (0.99 mmol, yield=72.4 %) of **C16F4E-TP** was obtained as colourless crystal by using **C16F4A** as the starting material. ^{1}H-NMR ($CDCl_3$, TMS, 500.0 MHz) δ 0.89 (t, J = 7.2 Hz, 18H), 1.28–1.42 (m, 144H), 1.51 (quintet, J = 7.7 Hz, 12H), 1.84 (quintet, J =7.8 Hz, 12H), 4.33 (t, J =6.4 Hz, 12H), 8.03 (s, 6H); ^{19}F ($CDCl_3$, $CFCl_3$, 470.0 MHz), δ –138.8 (s, 12F), –158.6 (s, 12F); Anal. Calc. for $C_{156}H_{204}F_{24}O_{18}$: C, 66.37; H, 7.28; F, 16.15 %. Found: C, 66.32; H, 7.14; F, 16.02 %.

1-2-3-25. 3-(2-octyloxy)-1,2,4,5-tetrafluorobenzene (C7(1C1)F4)

A solution of diethyl azodicarboxylate in toluene (2.2 molL^{-1}) 45.1 mL was added slowly to mixture of 2,3,5,6-tetrafluorophenol (**1**) 14.5 g (87.4 mmol), 2-octanol 11.9 g (91.4 mmol) and triphenylphosphine 26.1 g (99.3 mmol) in THF (135 mL) at 0 C in Ar atmosphere, and reaction mixture was stirred overnight at rt. The solution removed under reduced pressure and the residue was purified by column chromatography on silica gel (300 g), eluting with hexane to yield 23.9 g (85.9 mmol) of **C7(1C1)F4** as colourless liquid, yield 98.3 %. ^{1}H-NMR ($CDCl_3$, TMS, 500.0 MHz) δ 0.89 (t, J = 6.6 Hz, 3H), 1.27–1.35 (m, 9H), 1.39-1.49 (m, 2H), 1.57-1.64 (m, 1H), 1.74-1.81 (m, 1H), 4.40 (sextet, J = 6.2 Hz, 1H), 6.75 (tt, $^{3}J_{HF}$ = 10.1 Hz, $^{4}J_{HF}$ = 3.0 Hz 1H); ^{19}F-NMR ($CDCl_3$, $CFCl_3$, 470.0 MHz), δ –140.9 (td, $^{3}J_{FF}$ = 21.8 Hz, $^{5}J_{FF}$ = 10.9 Hz, 2F), –156.5 (dd, $^{3}J_{FF}$ =23.2 Hz, $^{5}J_{FF}$ = 12.3 Hz 2F).

1-2-3-26. 3-(2-octyloxy)-1,2,4,5-tetrafluorobenzoic acid (C7(1C1)F4A)

Following the method employed for the synthesis of **C6F4A**, 19.3 g (59.9 mmol, yield=65.9 %) of **C7(1C1)F4A** was obtained as colourless crystal by using **C7(1C1)F4** as the starting material. ^{1}H-NMR ($CDCl_3$, TMS, 500.0 MHz) δ 0.90 (t, J = 7.0 Hz, 3H), 1.27–1.38 (m, 6H), 1.36 (d, J = 8.9 Hz, 3H), 1.39-1.48 (m, 2H), 1.60-1.67 (m, 1H), 1.76-1.83 (m, 1H), 4.61 (sextet, J = 6.1 Hz, 1H), 10.9 (s, O*H*); ^{19}F-NMR ($CDCl_3$, $CFCl_3$, 470.0 MHz), δ –138.8 (d, $^{3}J_{FF}$ = 12.3 Hz, 2F), –155.9 (d, $^{3}J_{FF}$ = 10.9 Hz, 2F).

1-2-3-27. 2,3,6,7,10,11-hexakis(4-(2-octyloxy)-2,3,5,6-tetrafluorobenzoyloxy) triphenylene (C7(1C1)F4E-TP)

Following the method employed for the synthesis of **C6F4E-TP**, 2.16 g (1.00 mmol, yield=73.5 %) of **C7(1C1)F4E-TP** was obtained as colourless crystal by using **C7(1C1)F4A** as the starting material. ^{1}H-NMR ($CDCl_3$, TMS, 500.0 MHz) δ 0.92 (t, J = 6.6 Hz, 18H), 1.34 (d, J = 5.8 Hz, 18H), 1.29–1.41 (m, 36H), 1.44-1.52 (m, 12H), 1.62-1.69 (m, 6H), 1.79-1.86 (m, 6H), 4.56 (sextet, J = 5.8 Hz, 6H), 8.17 (s, 6H); ^{19}F ($CDCl_3$, $CFCl_3$, 470.0 MHz), δ –139.0 (s, 12F), –156.9 (s, 12F); FTIR (KBr, cm^{-1}) 2951, 2926, 2861, 2361, 2342, 1759, 1650, 1489, 1412, 1389, 1323, 1256, 1210, 1117, 1006, 939, 890, 835, 800; Anal. Calc. for $C_{108}H_{108}F_{24}O_{18}$: C, 60.33; H, 5.06; F, 21.21 %. Found: C, 60.43; H, 5.14; F, 21.08 %.

1-2-3-28. 3-(2-ethylhexyloxy)-1,2,4,5-tetrafluorobenzene (C6(2C2)F4)

Following the method employed for the synthesis of **C6F4**, 24.8 g (89.1 mmol, yield=74.0 %) of **C6(2C2)F4** was obtained as colourless liquid by using 2-ethyl-1-bromohexane as the starting material. ^{1}H-NMR ($CDCl_3$, TMS, 500.0 MHz) δ 0.89 (t, J = 7.5 Hz, 3H), 0.94 (t, J = 7.5 Hz, 3H), 1.24–1.43 (m, 8H), 1.70 (quintet, J = 6.2 Hz, 1H), 4.21 (d, J = 5.6 Hz, 2H), 6.73 (tt, $^{3}J_{HF}$ = 10.2 Hz, $^{4}J_{HF}$ = 3.2 Hz 1H); ^{19}F-NMR ($CDCl_3$, $CFCl_3$, 470.0 MHz), δ –140.8 (td, $^{3}J_{FF}$ = 21.8 Hz, $^{3}J_{HF}$ = 10.9 Hz, 2F), –157.6 (dd, $^{3}J_{FF}$ = 21.8 Hz, $^{3}J_{HF}$ = 10.9 Hz, 2F).

1-2-3-29. 4-(2-ethylhexyloxy)--2,3,5,6-tetrafluorobenzoic acid (C6(2C2)F4A)

Following the method employed for the synthesis of **C6F4A**, 12.5 g (38.8 mmol, yield=43.5 %) of **C6(2C2)F4A** was obtained as colourless crystal by using **C6(2C2)F4** as the starting material. ^{1}H-NMR ($CDCl_3$, TMS, 500.0 MHz) δ 0.91 (t, J = 7.0 Hz, 3H), 0.94 (t, J = 7.5 Hz, 3H), 1.31–1.57 (m, 8H), 1.73

(quintet, J = 6.0 Hz, 1H), 4.27 (d, J = 5.4 Hz, 2H), 11.7 (s, *OH*); ^{19}F-NMR ($CDCl_3$, $CFCl_3$, 470.0 MHz), δ –138.6 (dd, $^3J_{FF}$ = 25.9 Hz, $^3J_{HF}$ = 10.9 Hz, 2F), –157.0 (dd, $^3J_{FF}$ = 25.9 Hz, $^3J_{HF}$ = 9.5 Hz, 2F).

1-2-3-30. 2,3,6,7,10,11-hexakis(4-(2-ethylhexyloxy)-2,3,5,6-tetrafluorobenzoyloxy) triphenylene (C6(2C2)F4E-TP)

Following the method employed for the synthesis of **C6F4E-TP**, 2.20 g (1.02 mmol, yield=75.0 %) of **C6(2C2)F4E-TP** was obtained as colourless crystal by using **C6(2C2)F4A** as the starting material. ^{1}H-NMR ($CDCl_3$, TMS, 500.0 MHz) δ 0.94 (t, J = 6.9 Hz, 18H), 0.98 (t, J = 7.5 Hz, 18H), 1.35–1.38 (m, 24H), 1.42–1.59 (m, 24H), 1.75 (quintet, J = 6.0 Hz, 12H), 4.24 (quintet, J =4.2 Hz, 12H), 8.10 (s, 6H); ^{19}F ($CDCl_3$, $CFCl_3$, 470.0 MHz), δ –138.9 (s, 12F), –158.2 (s, 12F); FTIR (KBr, cm^{-1}) 2951, 2926, 2861, 2361, 2342, 1759, 1650, 1489, 1412, 1389, 1323, 1256, 1210, 1117, 1006, 939, 890, 835, 800; Anal. Calc. for $C_{108}H_{108}F_{24}O_{18}$: C, 60.33; H, 5.06; F, 21.21 %. Found: C, 60.55; H, 4.84; F, 21.12 %.

1-2-3-31. 3-(3, 7-dimethyloctyloxy)-1,2,4,5-tetrafluorobenzene (C8(3, 7C1)F4)

Following the method employed for the synthesis of **C6F4**, 31.8 g (103.8 mmol, yield=86.2 %) of **C8(3, 7C1)F4** was obtained as colourless liquid by using 3,7-dimethlbromooctane as the starting material. ^{1}H-NMR ($CDCl_3$, TMS, 500.0 MHz) δ 0.87 (d, J = 6.5 Hz, 6H), 0.94 (d, J = 6.7 Hz, 3H), 1.14–1.21 (m, 3H), 1.24–1.39 (m, 3H), 1.49-1.61 (m, 2H), 1.70 (m, J = 6.7 Hz, 1H), 1.82 (sextet, J = 5.8 Hz, 1H), 4.26 (sextet, J = 6.6 Hz, 2H), 6.74 (tt, $^3J_{HF}$ = 9.9 Hz, $^4J_{HF}$ = 3.0 Hz 1H); ^{19}F-NMR ($CDCl_3$, $CFCl_3$, 470.0 MHz), δ –140.8 (dd, $^3J_{FF}$ = 21.8 Hz, $^3J_{HF}$ = 10.9 Hz, 2F), –157.6 (dd, $^3J_{FF}$ = 21.8 Hz, $^3J_{HF}$ = 10.9 Hz, 2F).

1-2-3-32. 4-(3, 7-dimethyloctyloxy)-2,3,5,6-tetrafluorobenzoic acid (C8(3, 7C1)F4A)

Following the method employed for the synthesis of **C6F4A**, 14.0 g (40.0 mmol, yield=38.5 %) of **C8(3, 7C1)F4A** was obtained as colourless crystal by using **C8(3, 7C1)F4** as the starting material. ^{1}H-NMR ($CDCl_3$, TMS, 500.0 MHz) δ 0.87 (d, J = 6.8 Hz, 6H), 0.95 (d, J = 6.4 Hz, 3H), 1.13–1.17 (m, 3H), 1.24–1.34 (m, 3H), 1.49-1.64 (m, 2H), 1.69 (m, J = 5.4 Hz, 1H), 1.86 (sextet, J = 7.9 Hz, 1H), 4.42 (sextet, J = 6.8 Hz, 2H), 11.7 (s, *OH*); ^{19}F-NMR ($CDCl_3$, $CFCl_3$, 470.0 MHz), δ –138.6 (dd, $^3J_{FF}$ = 25.9 Hz, $^3J_{HF}$ = 13.6 Hz, 2F), –157.0 (dd, $^3J_{FF}$ = 25.9 Hz, $^3J_{HF}$ = 9.6 Hz, 2F).

1-2-3-33. 2,3,6,7,10,11-hexakis(4-(3, 7-dimethyloctyloxy)-2,3,5,6-tetrafluorobenzoyloxy) triphenylene (C8(3, 7C1)F4E-TP)

Following the method employed for the synthesis of **C6F4E-TP**, 1.65 g (0.71 mmol, yield=52.2 %) of **C8(3, 7C1)F4E-TP** was obtained as colourless crystal by using **C8(3, 7C1)F4A** as the starting material. ^{1}H-NMR ($CDCl_3$, TMS, 500.0 MHz) δ 0.90 (d, *J* = 6.5 Hz, 36H), 0.92 (d, *J* = 6.5 Hz, 18H), 1.19–1.1.25 (m, 18H), 1.29–1.40 (m, 18H), 1.52-1.66 (m, 12H), 1.71 (m, *J* = 6.5 Hz, 6H), 1.89 (sextet, *J* =7.6 Hz, 6H), 4.40 (sextet, *J* =5.3 Hz, 12H), 8.20 (s, 6H); ^{19}F ($CDCl_3$, $CFCl_3$, 470.0 MHz), δ –138.7 (s, 12F), –158.0 (s, 12F); Anal. Calc. for $C_{120}H_{132}F_{24}O_{18}$: C, 62.17; H, 5.74; F, 19.67 %. Found: C, 62.34; H, 5.63; F, 19.71 %.

1-3. Results and discussion

1-3-1. DSC measurement

The DSC curves of all compounds, expect for the branched derivatives are shown in Figure 1-2~1-9. In the DSC curve of **C16F4E-TP** (Figure 1-9), two endothermic peaks were observed at 49.0 °C and 273 °C with the phase transition enthalpies (*ΔH*) of 136 and 19.2 kJmol^{-1} on the first heating run, respectively. On the first cooling run, two exothermic peaks were observed at 267 °C and 41 °C (*ΔH*: 13.4 and 134 kJmol^{-1}, respectively), and two endothermic peaks were observed at 48 °C and 267 °C with the phase transition enthalpies (*ΔH*) of 130 and 15.3 kJmol^{-1} on the second heating run. The difference of the transition temperatures and enthalpies for the peaks around 300 °C between the first and second heating runs were probably due to a thermal decomposition. **C6F4E-TP**, **C12F4E-TP** and **C14F4E-TP** (see Figure 1-2, Figure 1-7 and Figure 1-8) also shown the similar behaviour.

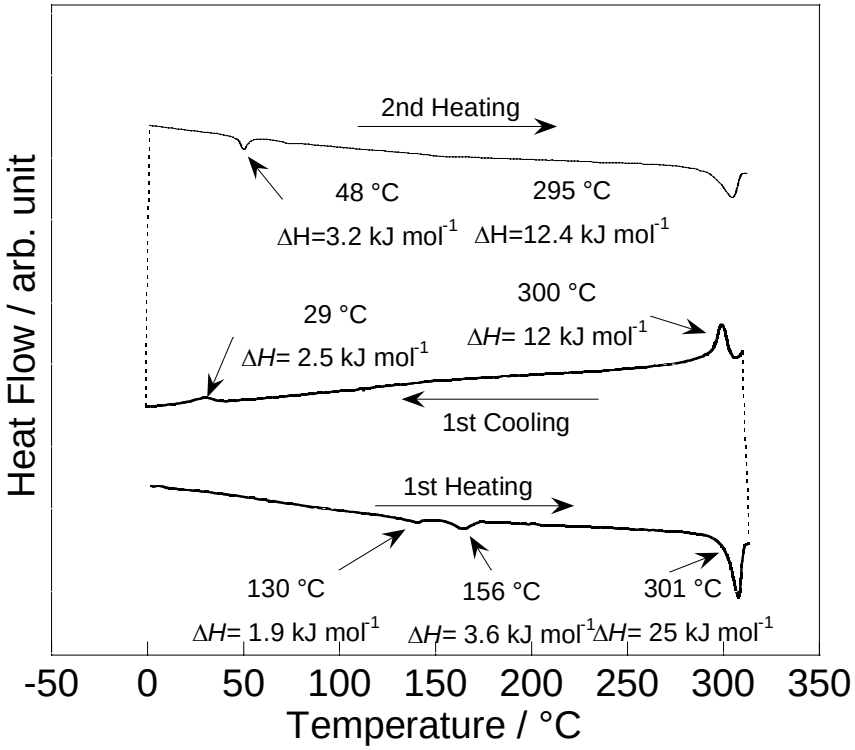

Figure 1-2 DSC curve of **C6F4E-TP** (Rate: 5 °Cmin^{-1})

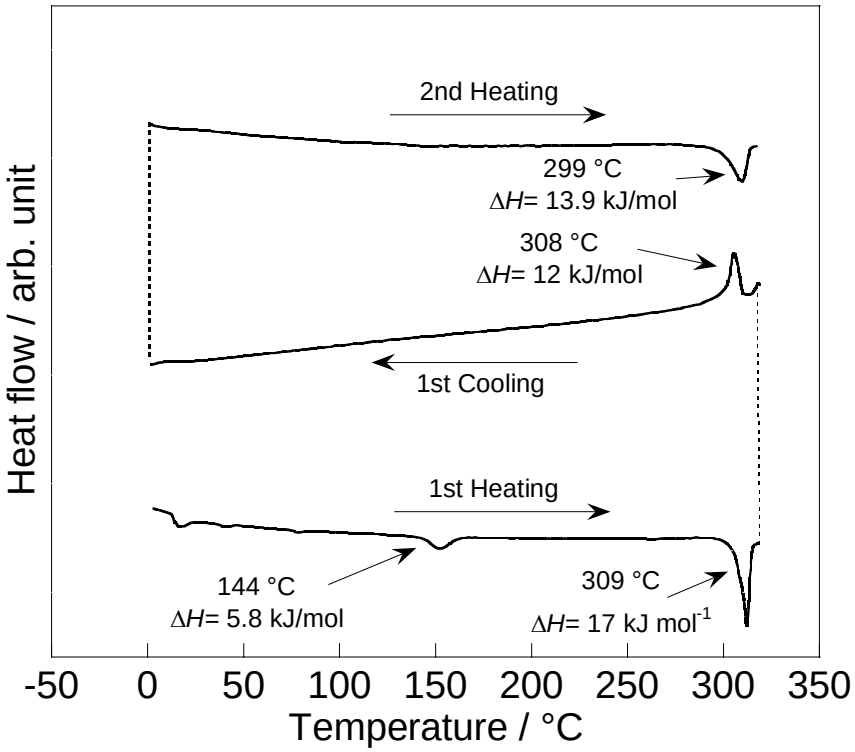

Figure 1-3 DSC curve of **C7F4E-TP** (Rate: 5 °Cmin^{-1})

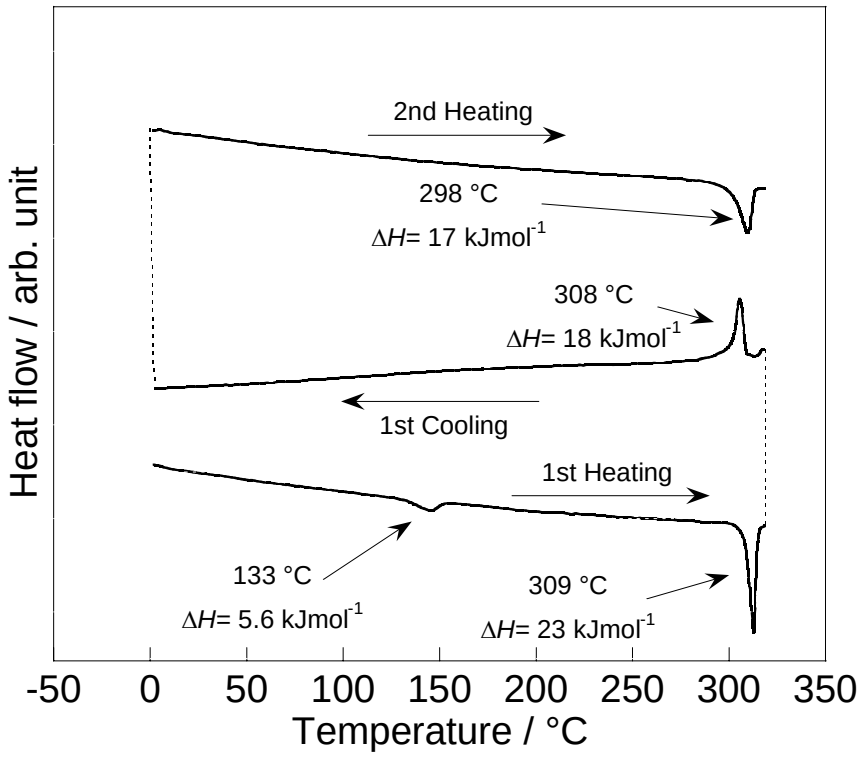

Figure 1-4 DSC curve of **C8F4E-TP** (Rate: 5 °Cmin^{-1})

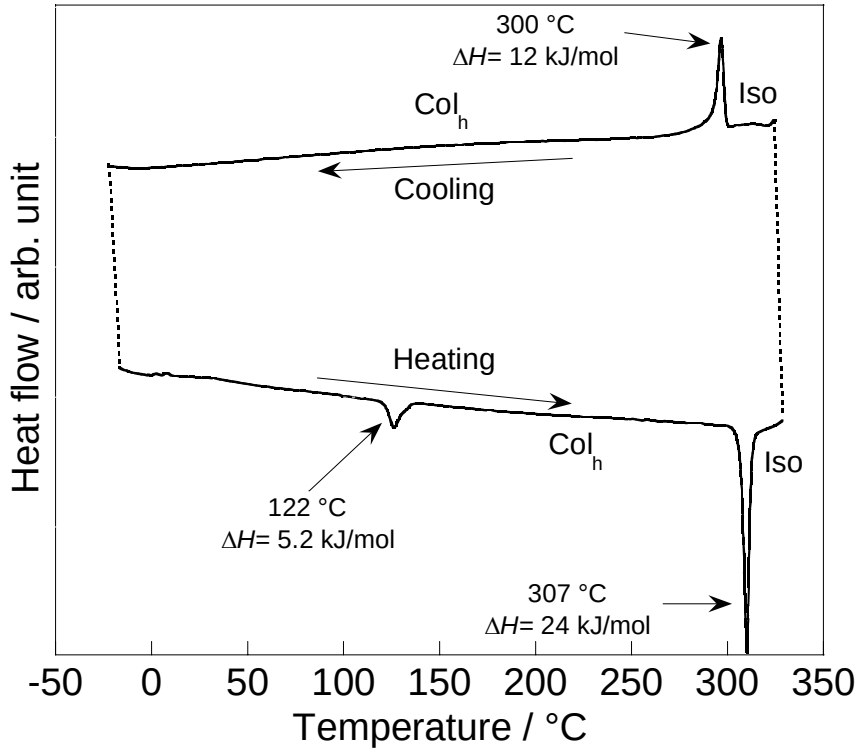

Figure 1-5 DSC curve of **C9F4E-TP** (Rate: 5 °Cmin^{-1})

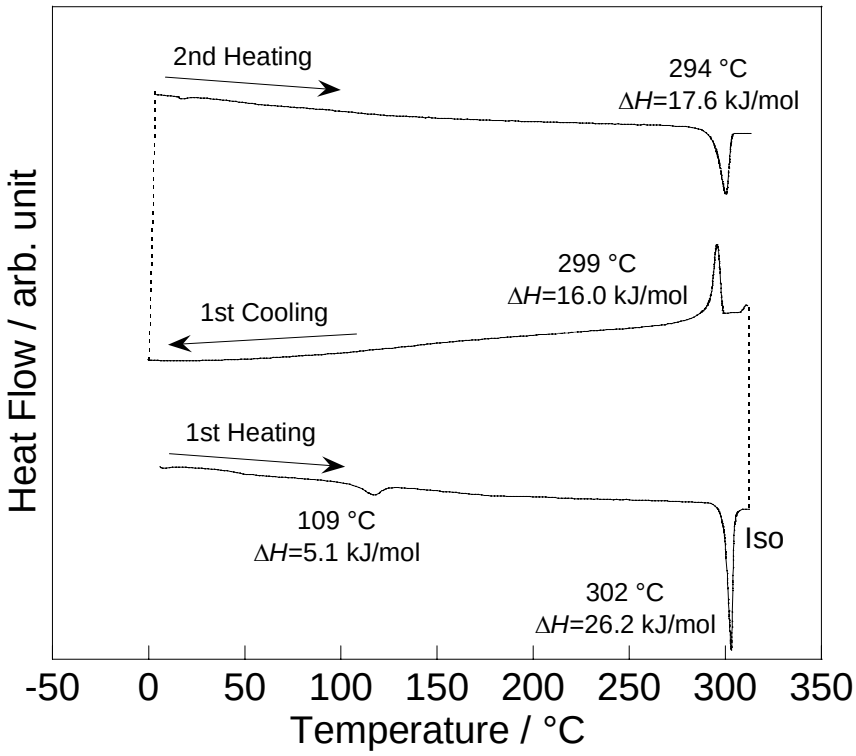

Figure 1-6 DSC curve of **C10F4E-TP** (Rate: 5 °Cmin^{-1})

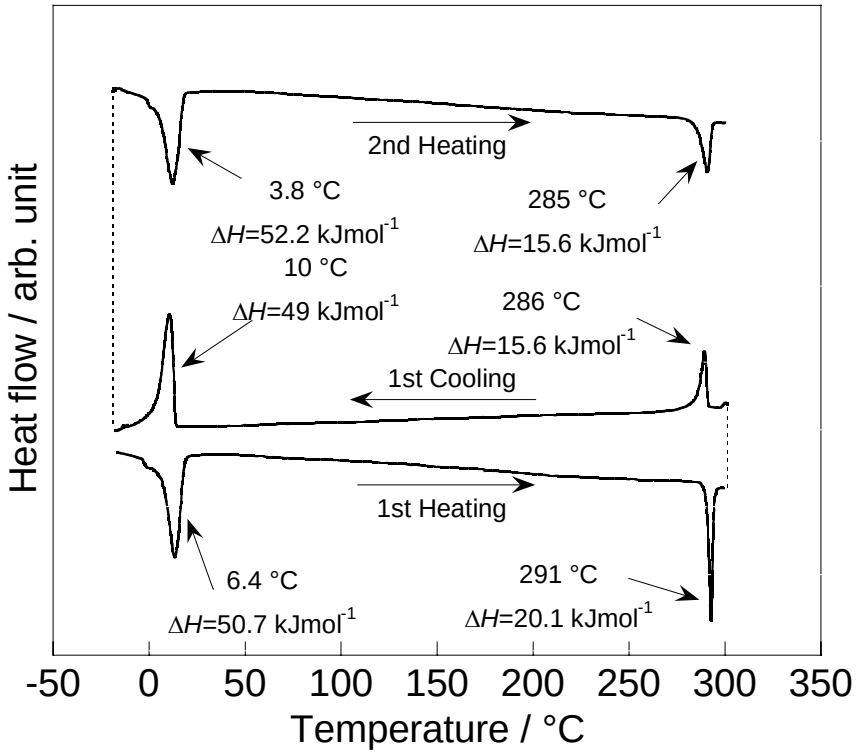

Figure 1-7 DSC curve of **C12F4E-TP** (Rate: 5 °Cmin^{-1})

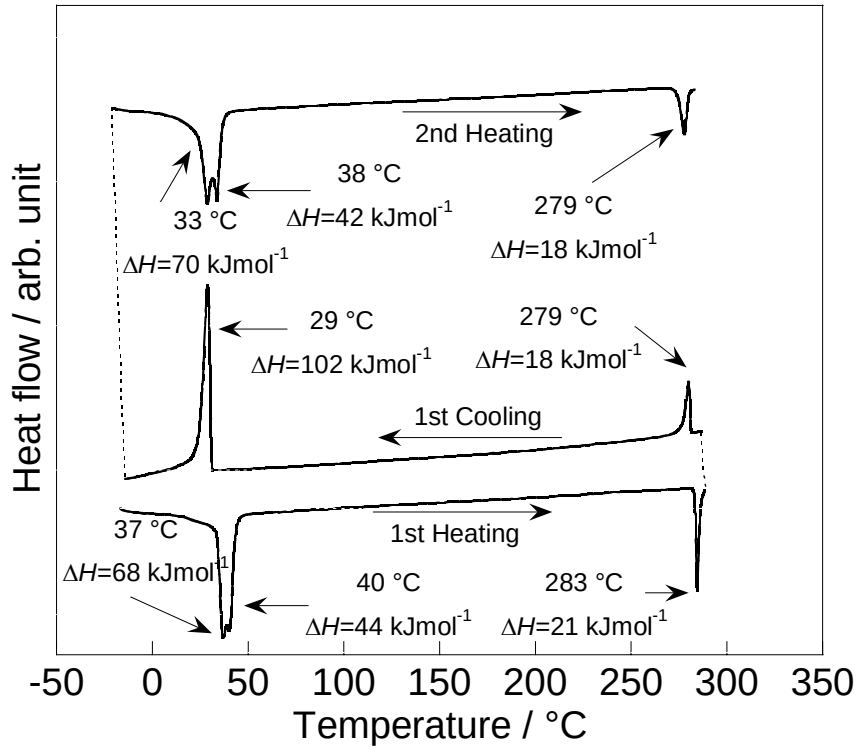

Figure 1-8 DSC curve of **C14F4E-TP** (Rate: 5 °Cmin^{-1})

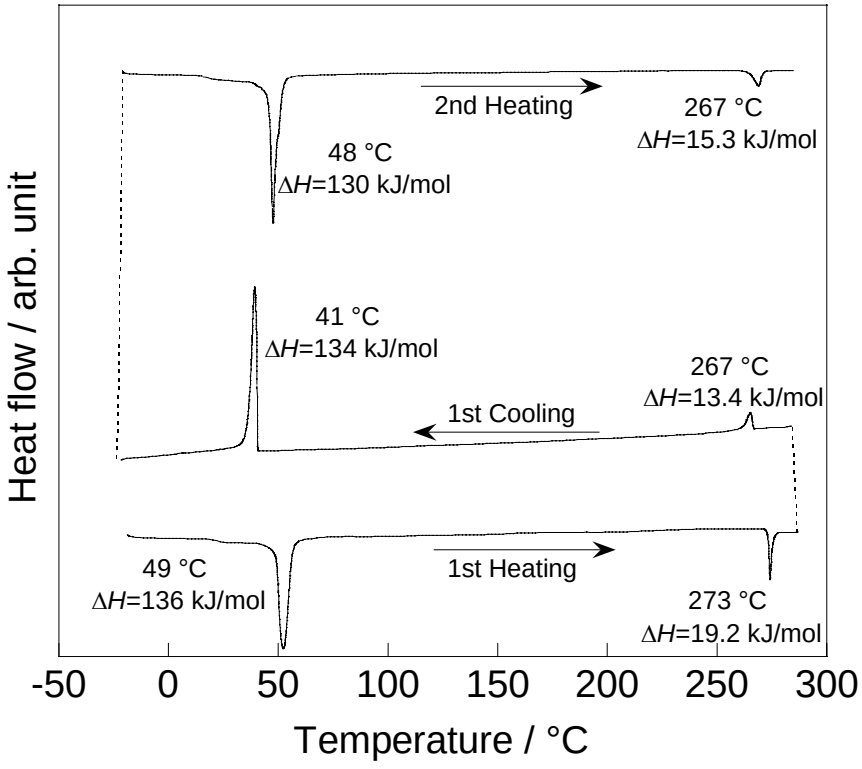

Figure 1-9 DSC curve of **C16F4E-TP** (Rate: 5 °Cmin^{-1})

On the other hand, in the DSC curves of **C10F4E-TP**, two peaks were observed at 109 °C and 309 °C with ΔH of 5.1 and 26.2 kJmol^{-1} on the first heating runs, respectively. However on first cooling, there was only one peak at 299 °C (ΔH: 16.0 kJmol^{-1}), and a peak corresponding the recrystallization point disappeared. On second heating process, it is same situation that only one peak was observed around 294 °C with the transition enthalpy of 16.0 kJmol^{-1}. Additionally, on the cooling run after the first heating runs to 150 °C there is no peak and this is the same situation to that seen on the 2nd heating run. POM observations of the optical texture indicated the mesophase is frozen to be a glassy solid on cooling though the T_g could not be detected on the DSC curves. **C7F4E-TP**, **C8F4E-TP** and **C9F4E-TP** (see Figure 1-3 Figure 1-4 and Figure 1-5) also shows the similar behaviour. There results indicate that in these homologues, the crystallization tends to take place with the longer chain derivatives. This may indicate that the benzoyloxytriphenylen moiety could be bulky for the packing to each and the shorter chains could not occupy their space in a way of crystalline solid on cooling. It is also indicative that tetrafluorophenyl groups peripherally attached to a triphenylene core intrinsically extend the central rigid core area due to the strong interaction.

The DSC curves of all compounds, which have peripheral branched alkyl chains are shown in Figure 1-10~1-12.

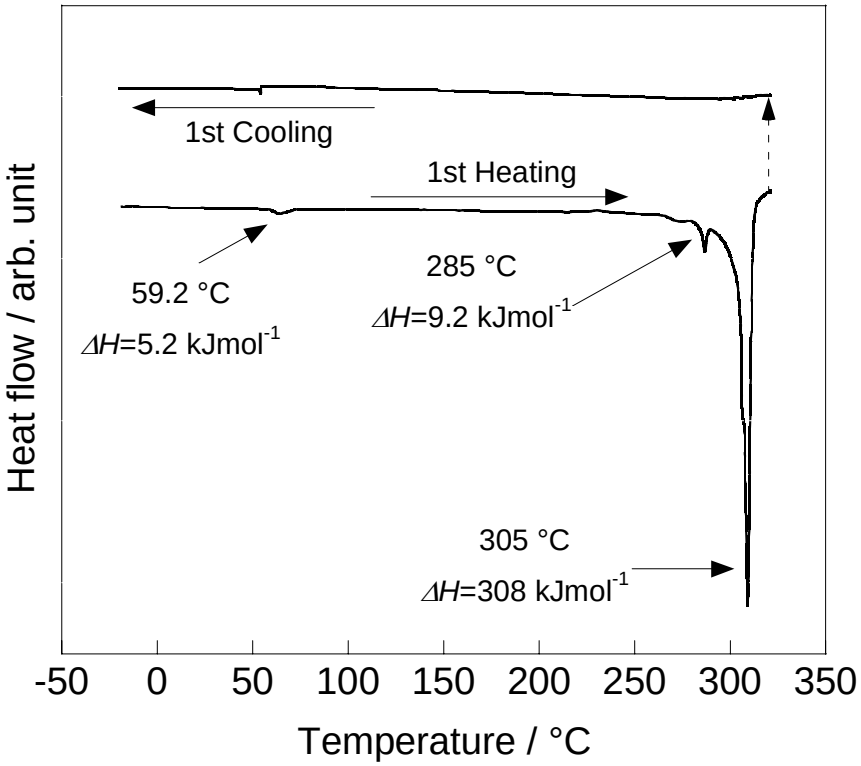

Figure 1-10 DSC curve of **C7(1C1)F4E-TP** (Rate: 5 °Cmin^{-1})

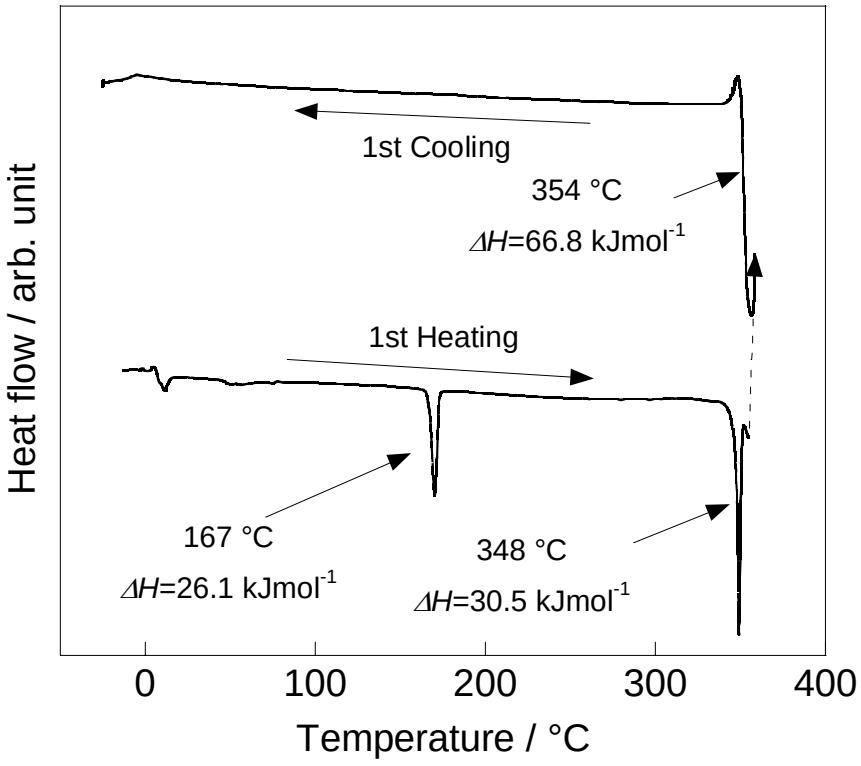

Figure 1-11 DSC curve of **C6(2C2)F4E-TP** (Rate: 5 °Cmin^{-1})

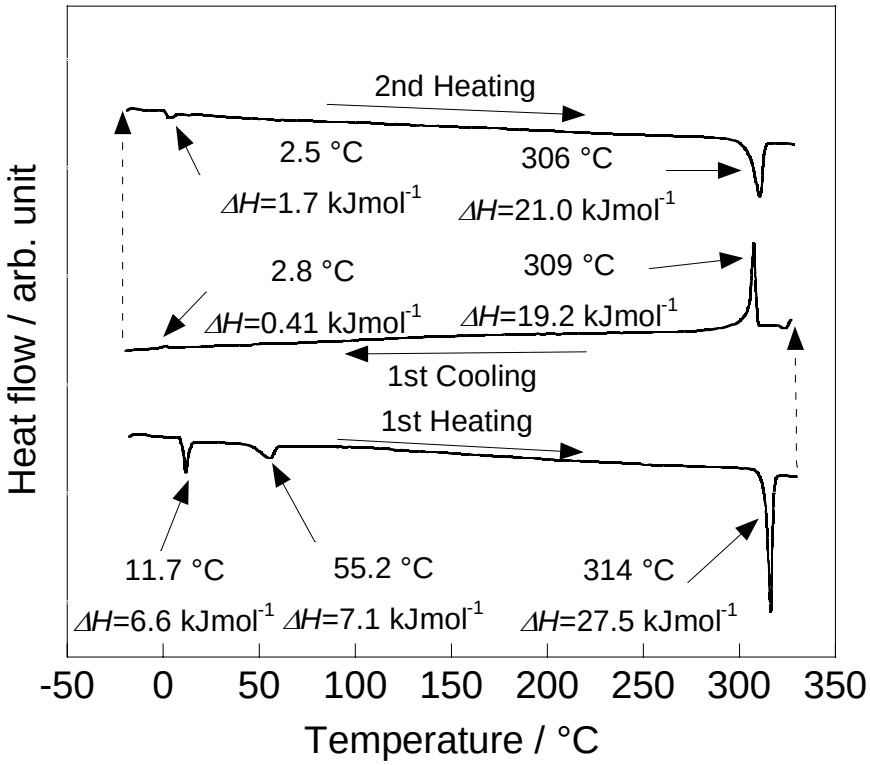

Figure 1-12 DSC curves of **C8(3,7C1)F4E-TP** (Rate: 5 °Cmin^{-1})

In the DSC curve of **C7(1C1)F4E-TP** (Figure 1-10), three endothermic peaks were observed at 11.7 °C, 55.2 °C and 273 °C with 6.6, 7.1 and 27.5 kJmol^{-1} of the phase transition enthalpies (ΔH) on the first heating run, respectively. On the first cooling run, two exothermic peaks were observed at 309 °C and 2.8 °C (ΔH: 19.2 and 0.4 kJmol^{-1}, respectively), and two endothermic peaks were observed at 48 °C and 267 °C with 130 and 15.3 kJmol^{-1} of the phase transition enthalpies (ΔH) on the second heating run. The difference of the transition temperature and enthalpies for the peaks around 300 °C between the first and second heating runs were probably due to a thermal decomposition, and the transition behaviors on the low temperature region were different between 1st and 2nd heating runs.

On the other hand in **C6(2C2)F4E-TP** and **C8(3,7C1)F4E-TP** (Figure 1-11 and Figure 1-12), the endothermic peak with a large transition enthalpy (>50 kJmol^{-1}) was observed after the isotropic liquid transition on the 1st heating, and their peaks are probably derived from the thermal decomposition.

1-3-2. Polarized optical microscope observation

The polarized optical microscopic images of **C10F4E-TP** and **C16F4E-TP** are shown in Figure 1-13 Both compounds exhibit dendric textures containing in part with dark domains, indicating these mesophases are of optical uniaxiality.

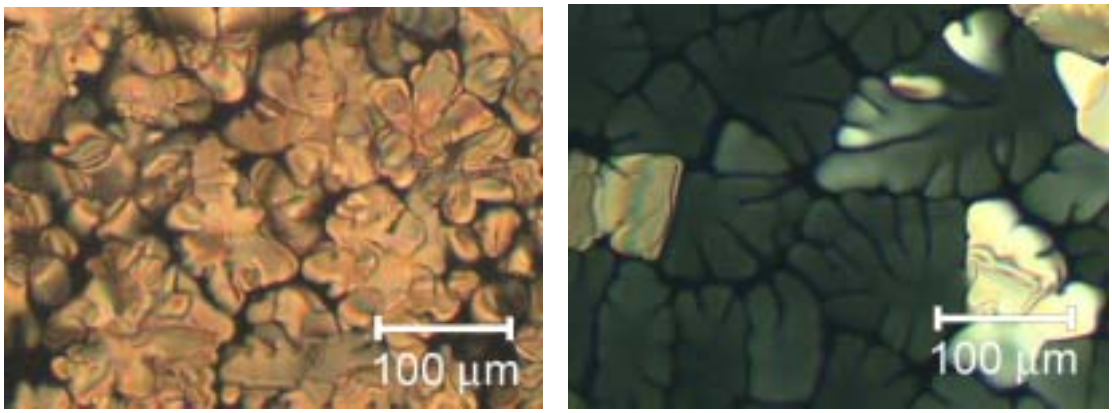

Figure 1-13 Optical textures of mesophases for **C10F4E-TP** (left; at 280 °C) and **C16F4E-TP** (right; at 238 °C).

1-3-3. X-ray diffraction patterns

X-ray diffraction patterns of the mesophase for all compounds (for a non-aligned sample), having the peripheral *n*-alkyl chains are shown in Figure 1-14~1-21. The XRD of **C16F4E-TP** at 160 °C shows several reflection peaks having spacings of 32.7, 18.9, 16.4, 12.4, 11.0, 9.1, 8.2, 7.5 and 7.1 Å (Figure 1-21), corresponding to a set of the spacing ratio, 1 : 1/√3 : 1/2 : 1/√7 : 1/3 : 1/√13 : 1/4 : 1/√19 : 1/ √21, which are an evidence of a hexagonal arrangement of molecularly stacking columns. Futhermore, two halos at 4.7 and 3.5 Å were observed in the wide angle region and the former is just comparative the molecular width of a tetrafluorophenylene moiety (the molecular width ca. 5Å), and the latter is assigned to be of the π-π stacking distance of triphenylene cores in a column. These halos at 4.7 Å and 3.5 Å are overlapped on the broad halo originated from the molten alkyl chains which comes up around 4.2 Å,[14] indicated in Figure 1-21.

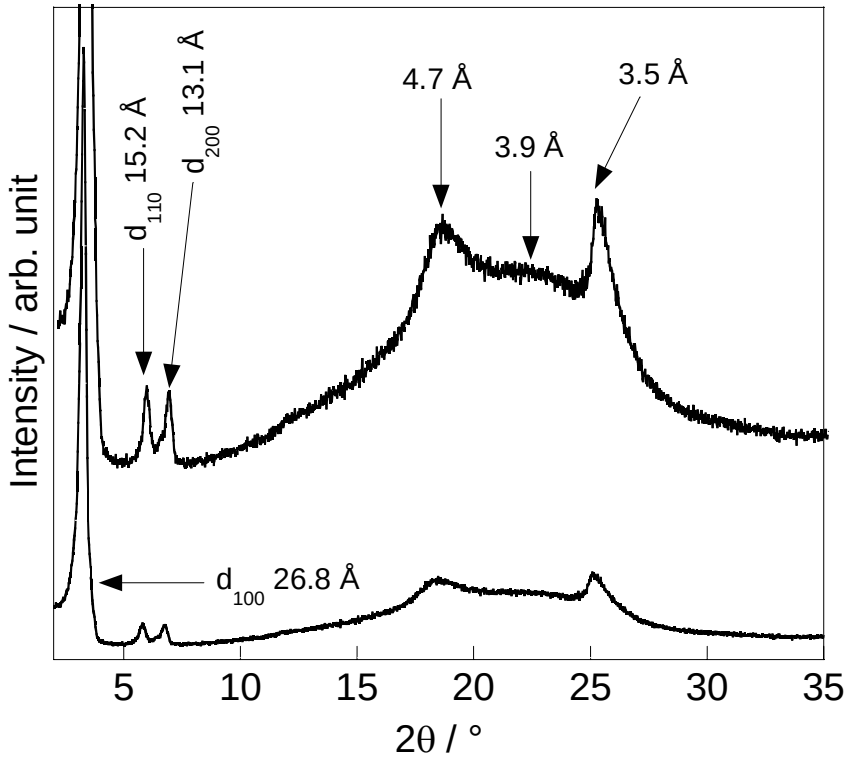

Figure 1-14 X-ray diffraction patterns of **C6F4E-TP** at 180 ºC.

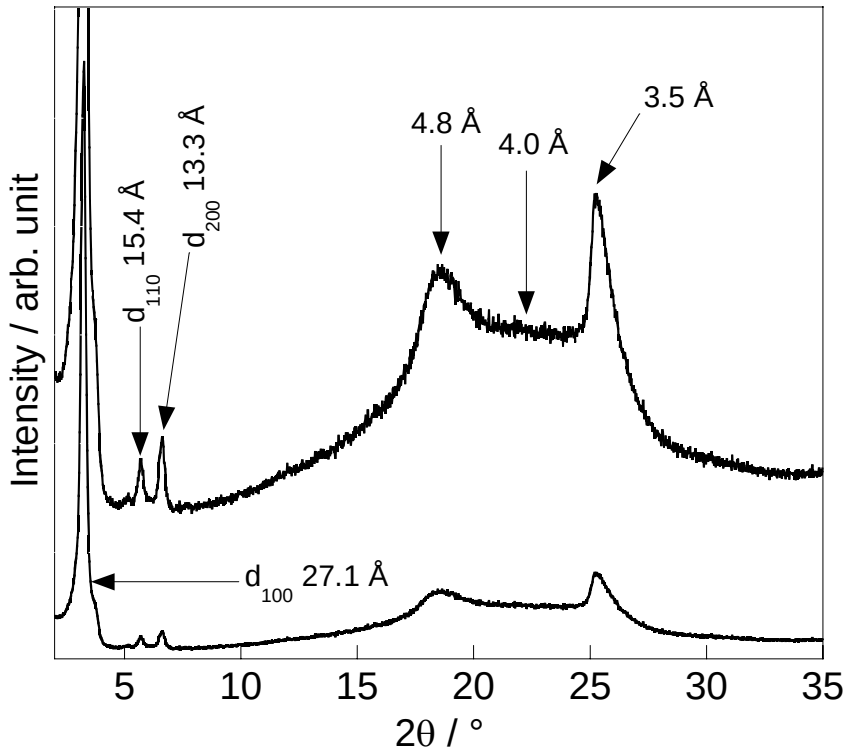

Figure 1-15 X-ray diffraction patterns of **C7F4E-TP** at 180 ºC.

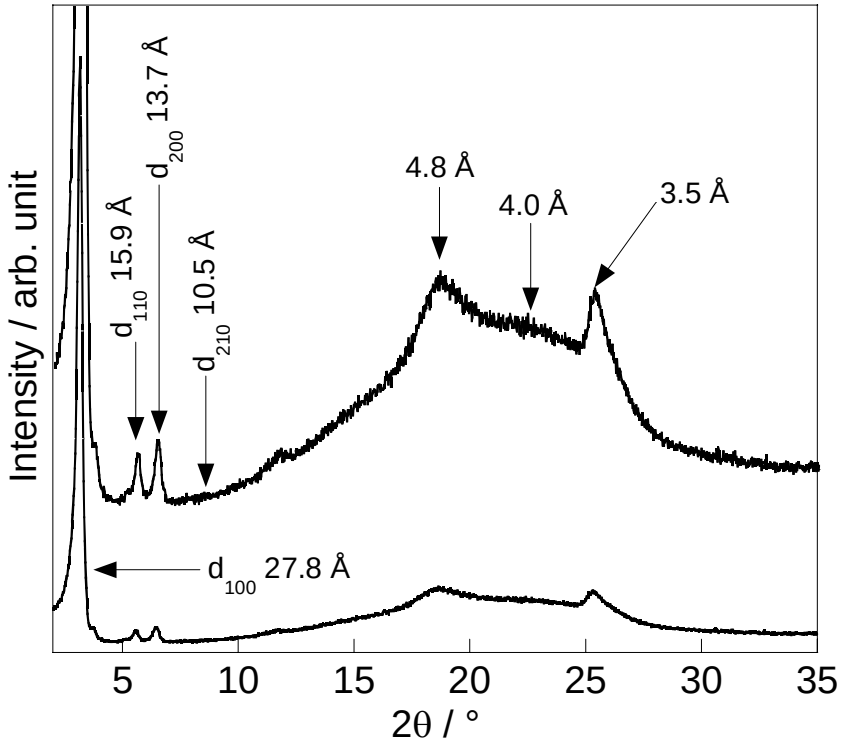

Figure 1-16 X-ray diffraction patterns of **C8F4E-TP** at 180 ºC.

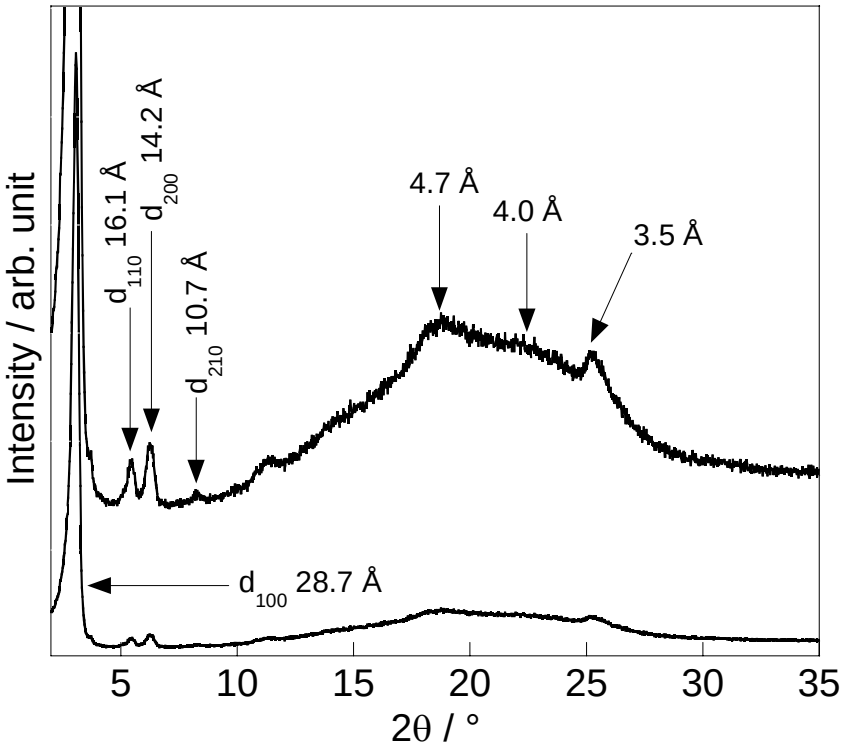

Figure 1-17 X-ray diffraction patterns of **C9F4E-TP** at 180 ºC.

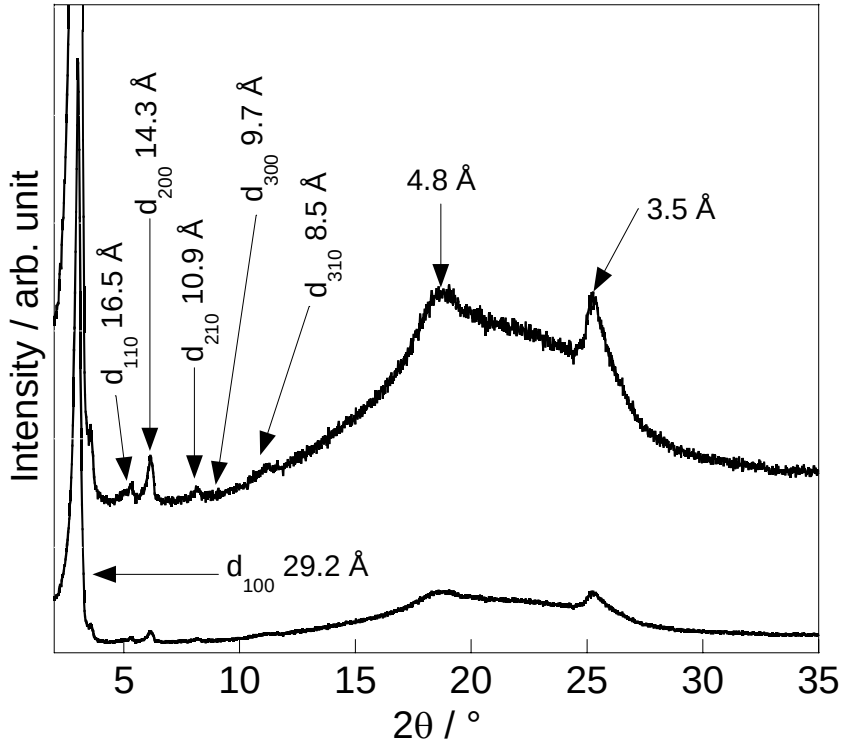

Figure 1-18 X-ray diffraction patterns of **C10F4E-TP** at 180 ºC.

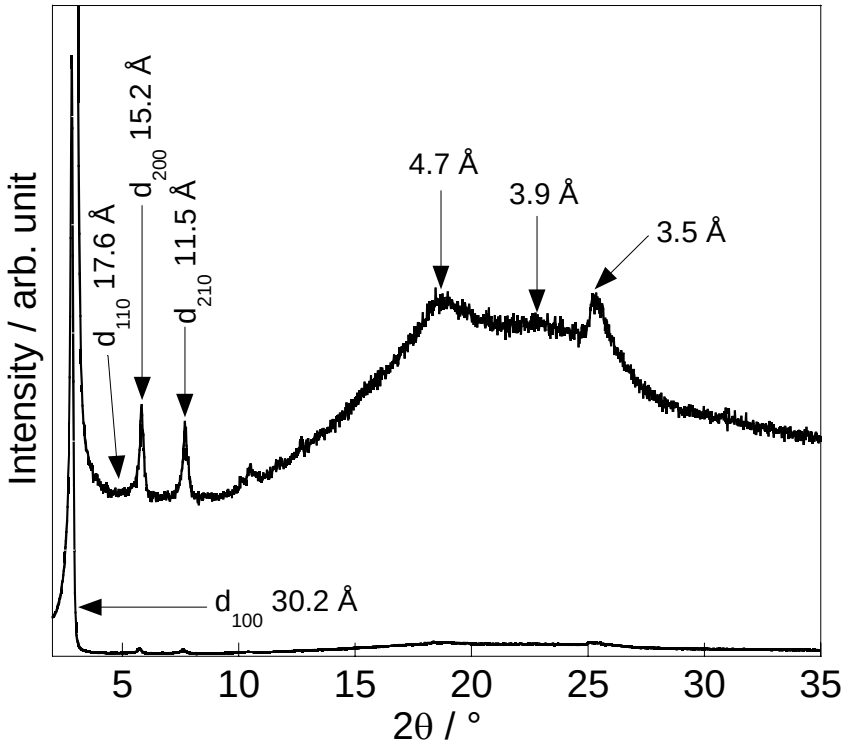

Figure 1-19 X-ray diffraction patterns of **C12F4E-TP** at 180 ºC.

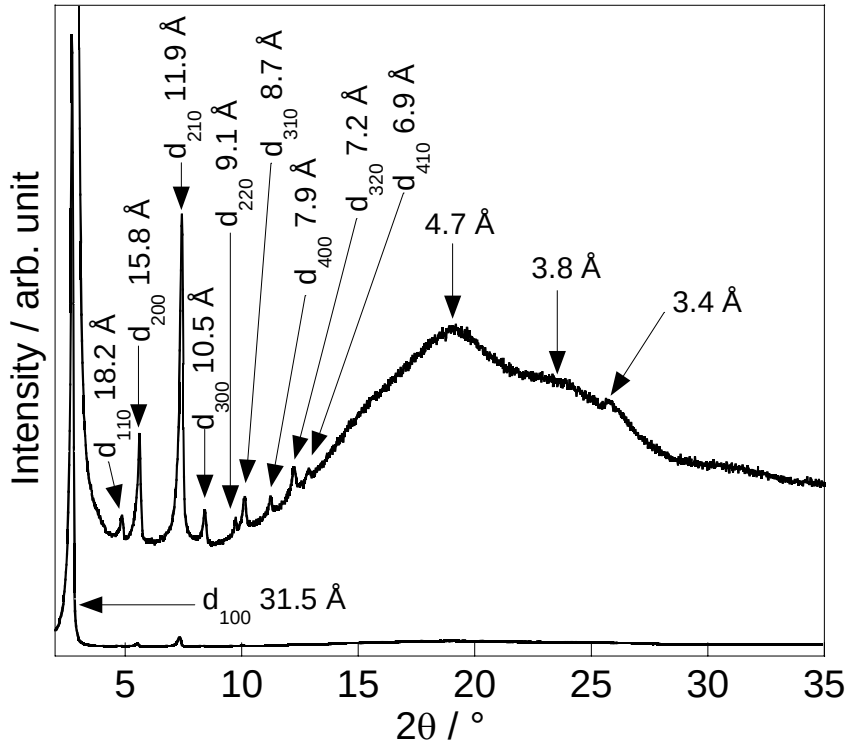

Figure 1-20 X-ray diffraction patterns of **C14F4E-TP** at 120 ºC.

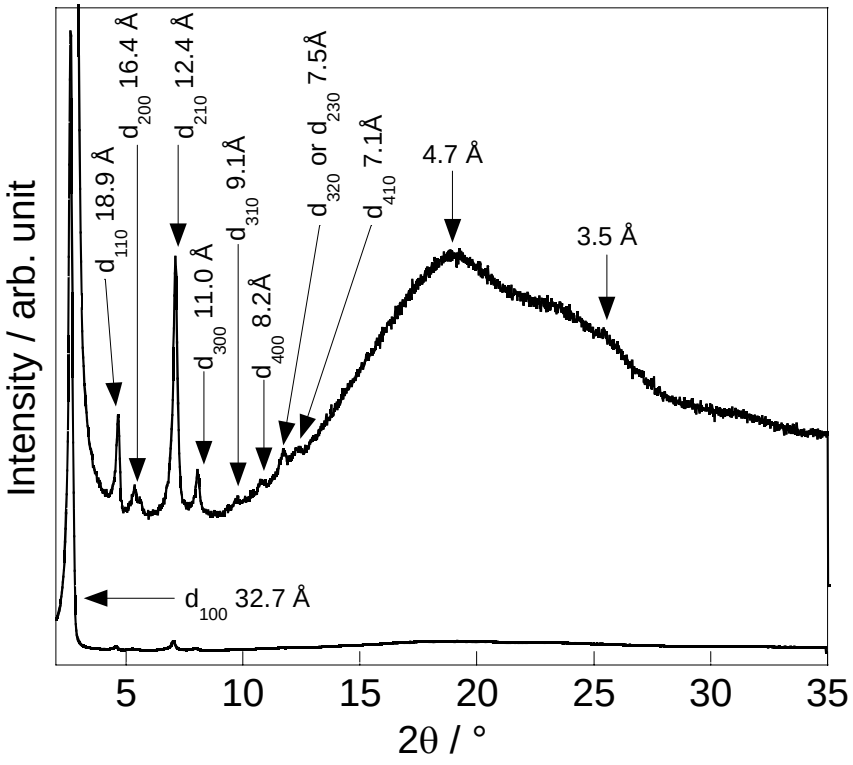

Figure 1-21 X-ray diffraction patterns of **C16F4E-TP** at 160 ºC.

In a X-ray diffraction pattern of the mesophase at 180 °C for **C10F4E-TP**, one can see the reflections in the small angle region having same set of spacing ratio of 1 : 1/√3 : 1/2 : 1/√7 : 1/3 : 1/√13, meaning the mesophase has a hexagonal arrangement of columns Two halos at 4.7 and 3.5 Å were also observed. It was clearly shown that the π-π stacking of **C10F4E-TP** in the Col_h mesophase is more ordered as compared with that of **C16F4E-TP**, probably correlating to the peripheral chain length. The X-ray reflection patterns in the Col_h mesophase for the homologues with n-alkyl chains also show the several reflection peaks corresponding to a set of spacing ratio, which is an evidence of a hexagonal packing of columns.

X-ray diffraction patterns of the mesophase for compounds having branched alkyl chain (for a non-aligned sample) are shown in Figure 1-22~1-24. A X-ray diffraction of the mesophase at 180 °C for **C6(2C2)F4E-TP** revealed the several reflections in the small angle region have the similar set of spacing ratio of 1 : 1/√3 : 1/2 : 1/√7 : 1/3 : 1/√13 : 1/4 : 1/√19, indicating the mesophase is a hexagonal arrangement of columns, and two halos at 4.8 and 3.5 Å were also observed. In X-ray reflection of the other compound having branched alkyl chains, the several reflection patterns, corresponding to a set of spacing ratio meaning an evidence of a hexagonal packing were also observed.

The results of X-ray diffractions of the non-branched and branched alkyl chain compound are summarized in Table 1-1~Table 1-4. In the compounds having non-branched alkyl chains their hexagonal lattice constant ($a_{hex.}$) slightly increases with the elongation of the peripheral chains, and show the similar correlation to those of other triphenylene hexagonal columnar mesogens that the observed a $a_{hex.}$ is almost 60-80 % of the molecular diameters evaluated by the molecular model using AM-1.

On the other hand, a_{hex} of the branched alkyl chain derivatives indicate almost similar values of the corresponding non-branched peripheral chain homologues.

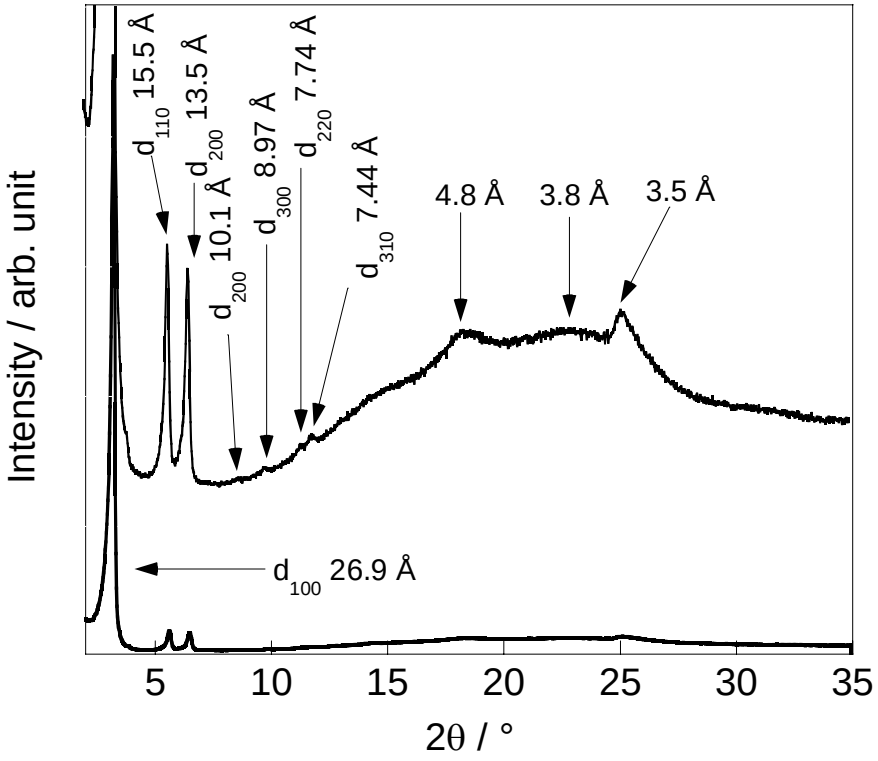

Figure 1-22 X-ray diffraction patterns of **C7(1C1)F4E-TP** at 180 °C.

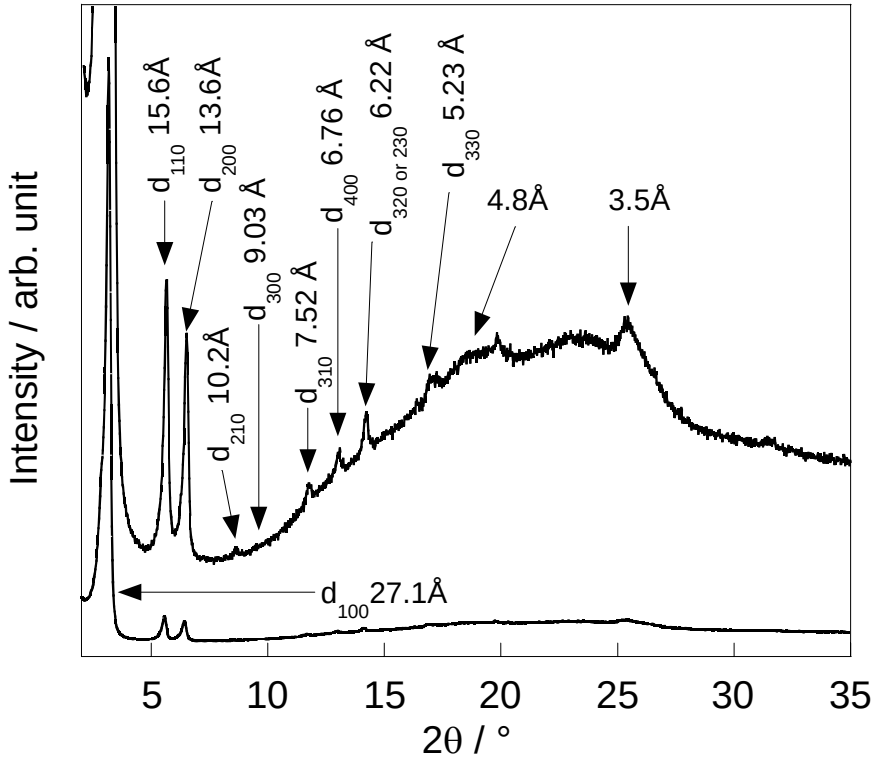

Figure 1-23 X-ray diffraction patterns of **C6(2C2)F4E-TP** at 180 °C.

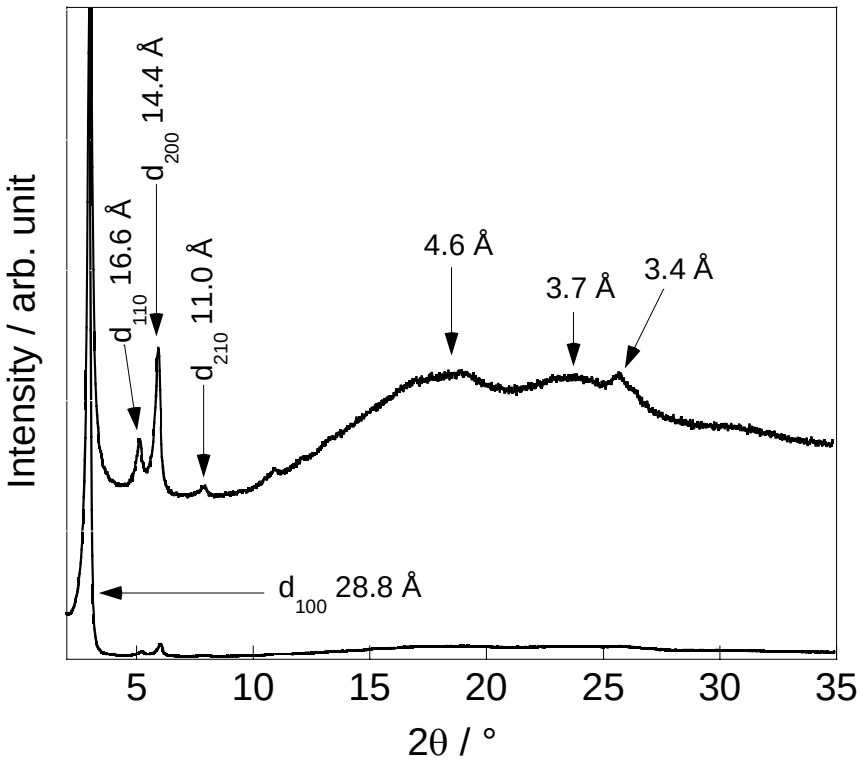

Figure 1-24 X-ray diffraction patterns of **C8(3,7C1)F4E-TP** at 120 °C.

Table 1-1 X-ray diffraction parameters for the mesophase of **C6F4E-TP**~**C9F4E-TP**.

Compound	Lattice constant / Å	Molecular Diameters[††] /Å	*hlk*	d_{hkl}/Å	
				Observed	Calculated
C6F4E-TP	Col_h	37.5	100	26.8	26.8
(180 ºC)	30.9		110	15.2	15.5
	Z=0.5[†]		200	13.1	13.4
				4.7 (br)[†††]	
				3.9 (br)	
				3.5 (br)	
C7F4E-TP	Col_h	39.6	100	27.1	27.1
(180 ºC)	31.3		110	15.4	15.6
	Z=0.5[†]		200	13.3	13.6
				4.8 (br)	
				4.1 (br)	
				3.5 (br)	
C8F4E-TP	Col_h	41.5	100	27.8	27.8
(180 ºC)	32.1		110	15.9	16.1
	Z=0.5[†]		200	13.7	13.9
			210	10.5	10.5
				4.8 (br)	
				4.0 (br)	
				3.5 (br)	
C9F4E-TP	Col_h	43.9	100	28.7	28.7
(180 ºC)	33.1		110	16.1	16.6
	Z=0.5[†]		200	14.2	14.4
			210	10.7	10.8
				4.7 (br)	
				4.0 (br)	
				3.5 (br)	

[†]: Calculated from the lattice constants *a*, correlation length along the *c*-axis (3.5 Å) and the postulated density ρ (1.0 g cm^{-3});[††]: calculated by AM-1; [†††]: br=Broad.

Table 1-2 X-ray diffraction parameters for the mesophase of **C10F4E-TP**~**C14F4E-TP**.

Compound	Lattice constant / Å	Molecular diameters[†]/Å	*hlk*	d_{hkl}/Å	
				Observed	Calculated
C10F4E-TP	Col_h	46.0	100	29.2	29.2
(180 ºC)	33.7		110	16.5	16.9
	Z=0.5[†]		200	14.3	14.6
			210	10.9	11.0
			300	9.7	9.7
			310	8.5	8.4
				4.8 (br)[†††]	
				4.1 (br)	
				3.5 (br)	
C12F4E-TP	Col_h	50.8	100	30.2	30.2
(180ºC)	34.9		110	17.6	17.4
	Z=0.5[†]		200	15.2	15.1
			210	11.5	11.4
				4.7 (br)	
				3.9 (br)	
				3.5 (br)	
C14F4E-TP	Col_h	56.3	100	31.5	31.5
(120ºC)	36.4		110	18.2	18.2
	Z=0.5[†]		200	15.8	15.8
			210	11.9	11.9
			300	10.5	10.5
			220	9.1	9.1
			310	8.7	8.7
			400	7.9	7.9
			320	7.2	7.2
			410	6.9	6.9
				4.7 (br)	
				3.8 (br)	
				3.4 (br)	

[†]: Calculated from the lattice constants *a*, correlation length along the *c*-axis (3.5 Å) and the postulated density ρ (1.0 g cm^{-3});[††]: calculated by AM-1; [†††]: br=Broad.

Table 1-3 X-ray diffraction parameters for the mesophase of **C16F4E-TP**, **C7(1C1)F4E-TP** and **C6(2C2)F4E-TP**

Compound	Lattice constant. /Å	Molecular diameters[††]/Å	*hlk*	d_{hkl}/Å	
				Observed	Calculated
C16F4E-TP	Col_h	61.2	100	32.7	32.7
(160 ºC)	37.8		110	18.9	18.9
	Z=0.5[†]		200	16.5	16.3
			210	12.4	12.4
			300	11.0	10.9
			310	9.1	9.1
			400	8.2	8.2
				4.7 (br)[†††]	
				4.0 (br)	
				3.5 (br)	
C7(1C1)F4E-TP	Col_h	40.7	100	26.9	26.9
(180 °C)	31.1		110	15.5	15.5
	Z=0.5[†]		200	13.5	13.5
			210	10.1	10.2
			300	9.0	9.0
			220	7.7	7.77
			310	7.4	7.5
				4.8 (br)	
				3.8 (br)	
				3.5 (br)	
C6(2C2)F4E-TP	Col_h	37.7	100	27.1	27.1
(180ºC)	31.3		110	15.6	15.6
	Z=0.5[†]		200	13.6	13.6
			210	10.2	10.2
			300	9.0	9.0
			310	7.5	7.5
			400	6.8	6.8
			320	6.2	6.2
			330	5.2	5.2
				4.8 (br)	
				3.5 (br)	

[†]: Calculated from the lattice constants *a*, correlation length along the *c*-axis (3.5 Å) and the postulated density ρ (1.0 g cm^{-3});[††]: calculated by AM-1; [†††]: br=Broad.

Table 1-4 X-ray diffraction parameters for the mesophase of **C8(3,7C1)F4E-TP**.

Compound	Lattice constant. /Å	Molecular diameters[††]/Å	*hlk*	d_{hkl}/Å	
				Observed	Calculated
C8(3,7C1)F4E-TP	33.3	42.5	100	28.8	28.8
(120ºC)	Z=0.5[†]		110	16.6	16.6
			200	14.4	14.4
			210	11.0	10.9
				4.6 (br)[†††]	
				3.7 (br)	
				3.4 (br)	

[†]: Calculated from the lattice constants *a*, correlation length along the *c*-axis (3.5 Å) and the postulated density ρ (1.0 g cm^{-3});[††]: calculated by AM-1; [†††]: br=Broad.

1-3-4. Comparison of the mesomorphism

The phase transition parameters of 4-alkoxy-2,3,5,6-tetrafluorobenzoyloxytriphenylenes are summarised in Table 1-5, with those of the correspounding non-fluorinated homologues.[13] All hexakis(4-alkoxytetrafluorobenzoyloxy)triphenylenes having several peripheral chains (non-branched and branched) exhibit only a Col_h mesophase, though the corresponding non-fluorinated homologue exhibit a discotic nematic (N_D) phase accompanied with a Col_r phase in the lower temperature region. And all compounds show relatively higher clearing points (over 250 °C) from those of the triphenylene discotic liquid crystal compounds. Additionally, the transition enthalpies of clearing points are much larger (over almost 20 kJ/mol) than usual ones of Col_h phase shown by other triphenylene derivatives (<10 kJ/mol).[15]

The clearing points of non-branched derivatives slightly decrease as the increase of peripheral chain length, while those of **CnH4E-TP**s decrease with the elongation of peripheral chain. This invariant thermal stability for the peripheral chain length also suppors a triphenylene plays a role of the large core part involving the peripheral tetrafluorophenyl moieties and indicate a strong interaction works among the stacking molecules.

It is difficult to think that there is a significant interaction between the tetrafluorophenyl and triphenylene

Table 1-5 Phase transition temperature of **CnF4E-TP**s (non-branched and branched) and **CnH4E-TP**s (non-fluorinated homologues).

Compound	Phase transition temperature / °C (ΔH: kJmol^{-1})
C6F4E-TP	Cr_1 130 (1.9) Cr_2 157 (3.6) Col_h 301 (25.4) Iso
C7F4E-TP	Cr 144 (5.7) Col_h 308 (26.4) Iso
C8F4E-TP	Cr 133 (6.2) Col_h 308 (28.4) Iso
C9F4E-TP	Cr 122 (5.2) Col_h 306 (24.6) Iso
C10F4E-TP	Cr 109 (5.1) Col_h 302 (26.2) Iso
C12F4E-TP	Cr 6.4 (50.7) Col_h 288 (23.7) Iso
C14F4E-TP	Cr 32.6 (93.0) Col_h 281(18.0) Iso
C16F4E-TP	Cr 48.2 (141.4) Col_h 266 (14.2) Iso
C7(1C1)F4E-TP	Cr 59.2 (5.2) Col_h 285 (9.2) Iso
C6(2C2)F4E-TP	Cr 167 (26.1) Col_h 348 (30.5) Iso
C8(3,7C1)F4E-TP	Cr_1 11.7 (6.6) Cr_2 55.2 (7.1) Col_h 314 (27.5) Iso
C6H4E-TP [12]	Cr (9.5) Col_t† 193 N_D† 274 Iso
C7H4E-TP [12]	Cr 168 (9.4) N_D† 253 Iso
C8H4E-TP [12]	Cr 152 (19.2) Col_r† 168 N_D† 244 Iso
C9H4E-TP [12]	Cr 154 (13.6) Col_r† 183 N_D† 227 Iso
C10H4E-TP [12]	Cr 142 (34.9) Col_r† 191 N_D† 212 Iso
C12H4E-TP [12]	Cr 146 (6.1) Col_r† 174 Iso

†: Col_t: tetragonal columnar phase, Col_r: rectangular columnar phase, N_D: discotic nematic phase.

moieties such as hexafluorobenzene-benzene interaction[10-12] on its column order by the XRD result. Therefore, it is reasonable to think that tetrafluorophenylene moiety could have strong interactions to each other.

In mesomorphism of **C7(1C1)F4E-TP**, **C6(2C2)F4E-TP** and **C8(3,7C1)F4E-TP** having branched peripheral chains, the introduction of branched structures into the chains give no change in the type of mesomorphism, every compound exhibit only a Col_h mesophase. In comparison with the corresponding non-branched peripheral chain homologues, the Col_h phase for **C6(2C2)F4E-TP** and **C8(3,7C1)F4E-TP**

were stabilized. Especially clearing points of **C6(2C2)F4E-TP** was about 50 °C higher than **C6F4E-TP**. For the introduction of branched structures to the peripheral chains in discotic liquid crystals, it was reported that thermal stabilities of mesomorphism in phthalocyanine mesogens having branched peripheral chains were much lower than those for the corresponding non-branched peripheral chain homologues owing to the excluded volume effect of branched chains.[16] The enthalpy changes for the clearing points of **C6(2C2)F4E-TP** and **C8(3,7C1)F4E-TP** also are much larger than those for the corresponding non-branched peripheral chain homologues. These enhancements of mesophase stability are quite new and interesting.

In branched peripheral chain systems, the peripheral tetrafluorophenyl moieties also behave as core part with triphenylene rings, and indicate a strong interaction works among the stacking molecules. Therefore, the branched peripheral chain may fill the space of intercolumns in the Col_h phase, and the thermal stabilities of mesomorphism are more stable than non-branched peripheral chain homologues.

1-4. Conclusions

A homologue series of a novel 2,3,6,7,10,11-hexakis(4-alkoxy-2,3,5,6-tetrafluorobenzoyloxy)-triphenylenes having non-branched and branched peripheral chains were synthesized and investigated on the mesomorphic behavior.

All compounds exhibit Col_h phase with higher thermal stabilities which have relatively higher clearing points (>270 °C) with large transition enthalpies, while the corresponding non-fluorinated homologue exhibit predominantly discotic nematic (N_D), and their clearing point are relatively invariable for elongation of peripheral chain.

In these homologues it was found that columnar phase is induced by introduction of tetrafluoro phenyl moiety on peripheral position exhibits extraordinaly large transition enthalpy of $T_{Colh\text{-}Iso}$. The clearing point of **CnF4E-TP**s indicate weak dependence on the peripheral chain length. Consequently, the peripheral tetrafluorinated phenyl groups thought to be involved in the rigid core part of discogen.

1-5. References

[1] *Organofluorine Chemistry Principle and Commercial Applications*, ed by R. E. Banks, B. E. Amart, J. C. Tatlow, Plenum, New York, **1994**.

[2] Y. Goto, T. Ogawa, S. Sawada, S. Sugimori, *Mol. Cryst. Liq. Cryst*., 1991, **209**, 1.

[3] Y. Sasada, K. Miyazawa and D. Demus, *Liq. Cryst.*, 2003, **30**, 1371.

[4] S. Matsui, T. Kondo, K. Sago, *Mol. Cryst. Liq. Cryst*., 2004, **411**, 127.

[5] Y. Sasada, T. Shimada, M. Ushioda and S. Matsui, *Liq. Cryst.*, 2007, **34**, 569.

[6] D. Pauluth, K. Tarumi, *J. Mater. Chem*., 2004, **14**, 1219.

[7] N. Terasawa, H. Monobe, K. Kiyohara, Y. Shimizu, *Chem. Lett*., 2003, **32**, 214.

[8] B. Alameddine, O. F. Aebischer, W. Amrein, B. Donnio, R. Deschenaux, D. Guillon, C. Savary, D. Scanu, O. Scheidegger, T. A. Jenny, *Chem. Mater.* 2005, **17**, 4798.

[9] U. Dahn, C. Erdelen, H. Ringsdorf, R. Festag, J. H. Wendof, P. A. Heiney, N. C. Maliszewskyj, *Liq. Cryst*., **1995**, *19*, 759.

[10] E. G. Cox, D. W. Cruickshank and J. A. Smith, *Proc. Royal Soc. London, Ser. A.*, 1958, **274**, 1.

[11] C. R. Patrick and G. S. Prosser, *Nature*, 1960, **187**, 1021.

[12] J. H. Williams, *Acc. Chem. Res.*, 1993, **26**, 593.

[13] N. H. Tinh, H. Gasparoux, C. Destrade, *Mol. Cryst. Liq. Cryst*., 1981, **68**, 101.

[14] A. M. Levelut, *J. Phys. Lett.*, **1979**, 81.

[15] C. Destrade, M. C. Mondon, J. Malthete, *J. Phys. (Paris), Suppl. 40*, **1979**, C3, 17.

[16] P. G. Schouten, J. F. Van Der Pol, J. W. Zwikker, W. Drenth and S. J. Picken, *Mol. Cryst. Liq. Cryst*, 1991, **195**, 291.

Chapter 2

Aromatic fluorination effect on the mesomorphic properties of discotic liquid crystals of alkoxybenzoyloxytriphenylenes

2-1. Introduction

In Chapter 1, it is reported that hexakis (4-alkoxybenzoyloxy) triphenylene derivatives having tetrafluorophenylene moieties on the peripheral positions exhibit a hexagonal columnar (Col_h) mesophase with the higher thermal stability, while the corresponding non-fluorinated homologues predominantly exhibit a discotic nematic (N_D) phase.[1]

Therefore, in chapter 2, hexakis (4-octyloxybenzoyloxy) triphenylene derivatives with mono- or di-fluorinated at the inner (2- and/or 6- [**C8(2F)E-TP**, **C8(2F6F)E-TP**]), outer (3- and/or 5- [**C8(3F)E-TP**, **C8(3F5F)E-TP**]) or inner and outer (2- and 5- [**C8(2F5F)E-TP**]) positions in the peripheral aromatic rings were synthesised (Figure 2-1), and investigated on the mesomorphic behaviour to reveal the alteration of fluorinated positions in the phenyl rings leads to a drastic change of the mesomorphism involving the thermal stability in comparison with corresponding non-fluorinated homologue (**C8H4E-TP**) and fully fluorinated homologue (**C8F4E-TP**).

The identification of these compounds was carried out by ^{1}H-NMR, ^{19}F-NMR, FT-IR, elemental analyses and, TOF-MS. And the mesomorphic behavior was investigated by polarized optical microscopy (POM), DSC measurement and X-ray diffraction technique.

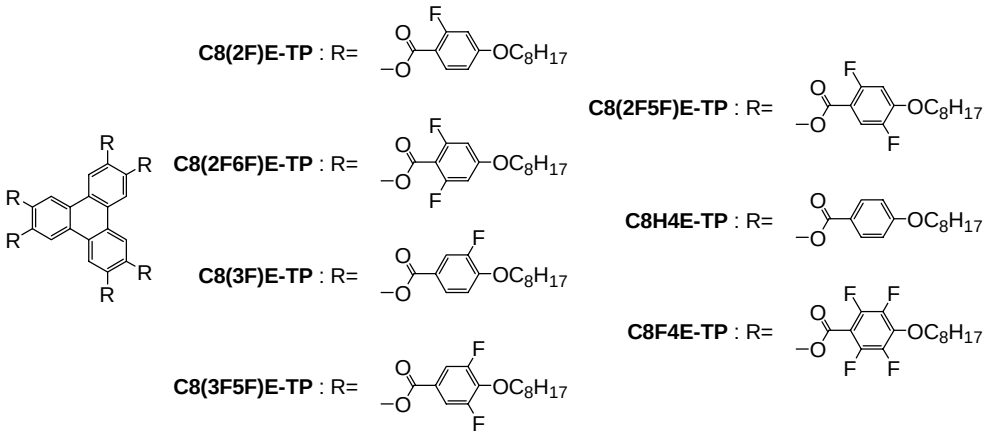

Figure 2-1 chemical structures of fluorinated hexakis (4-alkoxybenzoyloxy) triphenylene derivatives.

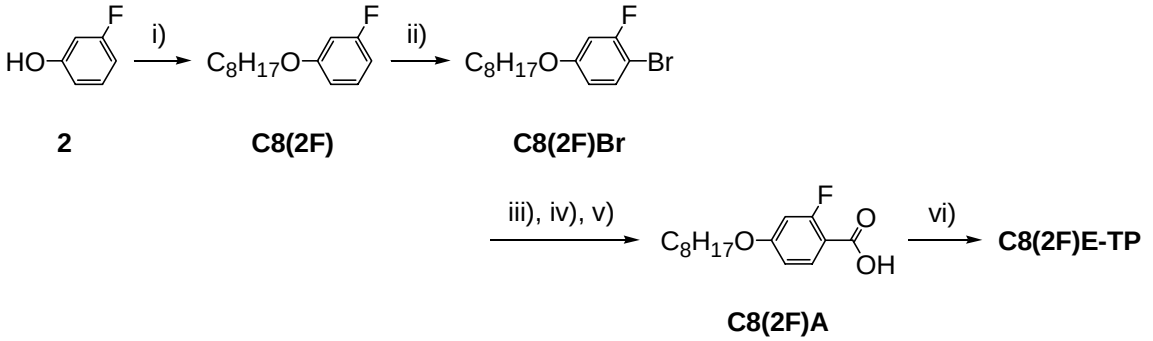

Scheme 2-1 Synthetic route of **C8(2F)E-TP**: i) $C_8H_{17}Br$, K_2CO_3, TBAB, MEK, reflux; ii) Br_2; iii) *n*-BuLi/Hexane, THF, -78 °C; iv) $CO_{2(S)}$, -78 °C; v) 3M-HCl*aq*, rt.; vi) 2,3,6,7,10,11-hexahydroxytriphenylene, DCC, DMAP, CH_2Cl_2, rt.

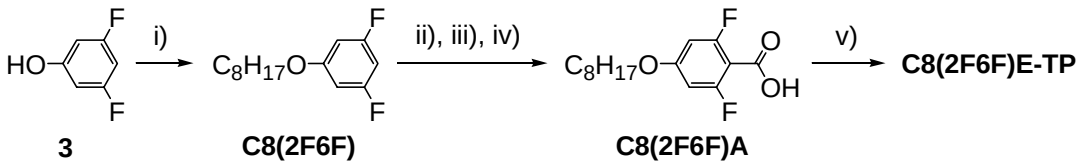

Scheme 2-2 Synthetic route of **C8(2F6F)E-TP**: i) $C_8H_{17}Br$, K_2CO_3, TBAB, MEK, reflux; ii) *n*-BuLi/Hexane, THF, -78 °C; iii) $CO_{2(S)}$, -78 °C; iv) 3M-HCl*aq*, rt.; v) 2,3,6,7,10,11-hexahydroxytriphenylene, DCC, DMAP, CH_2Cl_2, rt.

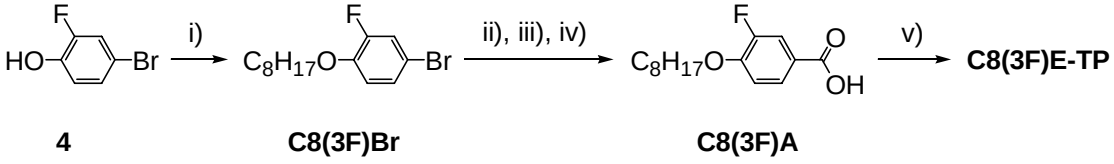

Scheme 2-3 Synthetic route of **C8(3F)E-TP**: i) $C_8H_{17}Br$, K_2CO_3, TBAB, MEK, reflux; ii) Mg, THF, reflux; iii) $CO_{2(S)}$, -78 °C; iv) 3M-HCl*aq*, rt.; v) 2,3,6,7,10,11-hexahydroxytriphenylene, DCC, DMAP, CH_2Cl_2, rt.

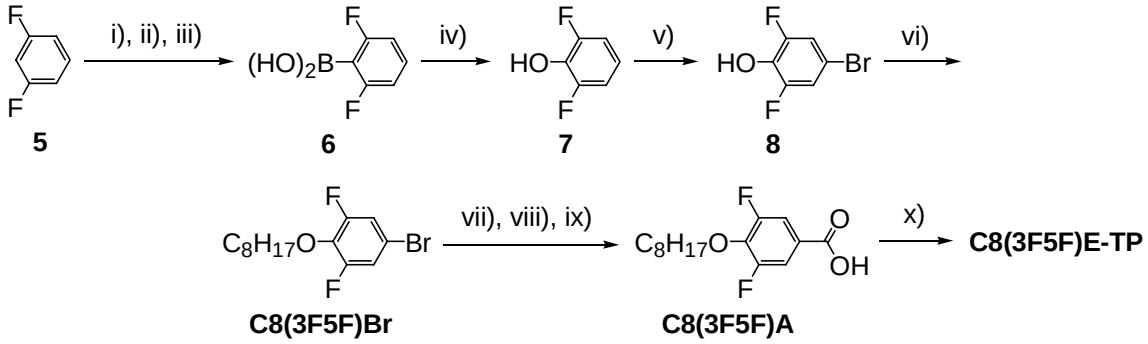

Scheme 2-4 Synthetic route of **C8(3F5F)E-TP**: i) *n*-BuLi/Hexane, THF, -78 °C; ii) $B(O^iPr)_3$, -78 °C; iii) 3M-HCl*aq*, rt.; iv) H_2O_2, THF; v) Br_2, Fe, CH_2Cl_2; vi) $C_8H_{17}Br$, K_2CO_3, TBAB, MEK, reflux; vii) Mg, THF, reflux; viii) $CO_{2(S)}$, -78 °C; ix) 3M-HCl*aq*, rt.; x) 2,3,6,7,10,11-hexahydroxytriphenylene, DCC, DMAP, CH_2Cl_2, rt.

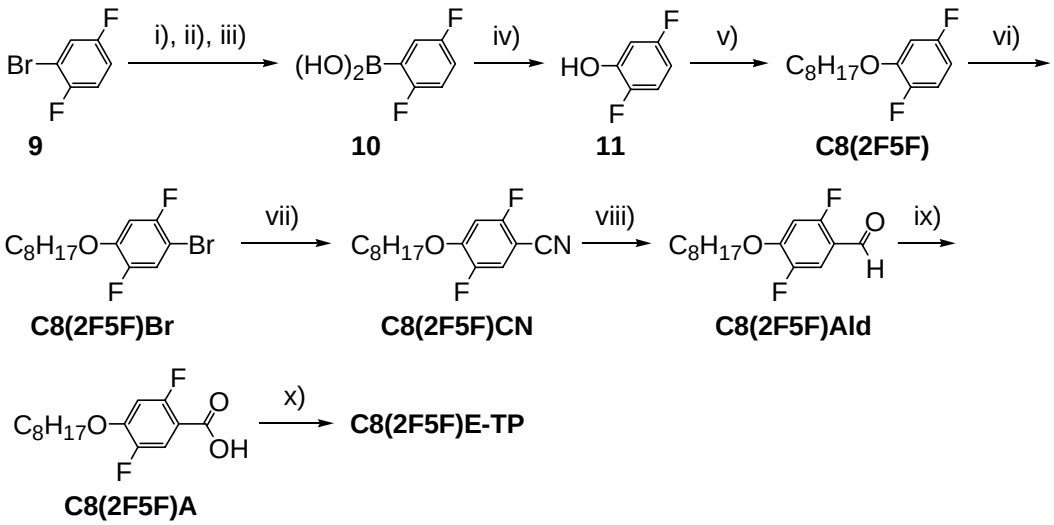

Scheme 2-5 Synthetic route of **C8(2F5F)E-TP**: i) Mg, THF, reflux; ii) $B(OCH_3)_3$, -78 °C; iii) 3M-HCl*aq*, rt.; iv) H_2O_2, THF; v) $C_8H_{17}Br$, K_2CO_3, TBAB, MEK, reflux; vi) Br_2; vii) CuCN, DMF; viii) DIBAL-H, CH_2Cl_2, -78 °C; ix) Jone's reagent, acetone, rt.; x) 2,3,6,7,10,11-hexahydroxytriphenylene, DCC, DMAP, CH_2Cl_2, rt.

2-2. Experimental

2-2-1. General measurement

^{1}H-NMR spectra were observed at 500.0 MHz on JEOL ECA500 FT-NMR spectrometer using $CDCl_3$ as solvent. Tetrametylsilane was used internal standard.^{19}F-NMR spectra were observed at 470.6 MHz on the same spectrometer, Mass spectra were obtained on JEOL Accu TOF spectrometer. IR spectra were measured on Bio-Rad FTS6000 FT-IR spectrometer for the KBr pellet.

2-2-2. Measurement of mesomorphism

The phase transition temperatures and enthalpies of the compounds were measured by differential scanning calorimetry min (DSC, TA instrument DSC2920) for 5-10 mg samples of freshly recrystallised materials at a scanning rate of 5 °Cmin^{-1} or 3 °Cmin^{-1}. Microscopic observation of the optical texture of mesophase was observed by a polarized microscope (Olympus BH2) equipped with hot stage (Mettler FP90). The mesophases were identified by X-ray diffraction (Rigaku, RINT-2000) for non-arraigned sample in the mesophase temperature ranges.

2-2-3. Synthesis

2-2-3-1. 3-fluorooctyloxybenzene (C8(2F))

K_2CO_3 22.2 g (160.6 mmol), tetrabutylammonium bromide 5.2 g (16.1 mmol) and the solution of bromooctane 31.0 g (160.6 mmol) in 2-butanone (40 mL) were added into the solution of 3-fluorophenol (**2**) 15.0 g (133.8 mmol) in 2-buanone (80 mL). The suspension mixture was refluxed for 4 h. The reaction mixture was cooled down and distilled water (100 mL) and diethyl ether were added at room temperature. The separated organic layer was washed with brine (100 mL) and dried over anhydrous $MgSO_4$. The solvent was removed under reduced pressure and the residue was purified by column chromatography on silica gel (300 g), eluting with hexane to yield 29.7 g (132.5 mmol) of **C8(2F)** as colourless liquid, yield 99.0 %. ^{1}H-NMR ($CDCl_3$, TMS, 500.0 MHz) δ 0.89 (t, J = 7.3 Hz, 3H), 1.28–1.35 (m, 8H), 1.43 (quintet, J = 7.0 Hz, 2H), 1.77 (quintet, J = 6.6 Hz, 2H), 3.90 (t, J = 6.5 Hz, 2H), 6.57-6.63 (m, 2H), 6.65 (dd, $^{3}J_{HF}$ =

8.6 Hz, ^{4}J = 2.1 Hz 1H), 7.17 (dd, J = 6.9 Hz, 1H); ^{19}F-NMR ($CDCl_3$, $CFCl_3$, 470.0 MHz), δ –112.4 (d, $^{3}J_{FH}$ = 10.9 Hz, 1F).

2-2-3-2. 4-octyloxy-2-fluorobromobenzene (C8(2F)Br)

Bromine 21.1 g (132.5 mmol) was slowly added into **C8(2F)** 29.7 g (132.5 mmol) at 0 °C under vigorous stirring, and the reaction mixture was continuously stirred for 1 h at the same temperature. Distilled water and diethyl ether were added into the mixture, and the separated organic layer was washed with saturated aqueous solution of sodium sulfite, brine (100 mL) and dried over anhydrous $MgSO_4$. The solvent was removed under reduced pressure and the residue was purified by column chromatography on silica gel (300 g), eluting with hexane to yield 36.0 g (118.8 mmol) of **C8(2F)Br** as colourless liquid, yield 89.7 %. ^{1}H-NMR ($CDCl_3$, TMS, 500.0 MHz) δ 0.89 (t, J = 6.8 Hz, 3H), 1.28–1.34 (m, 8H), 1.43 (sextet, J = 7.8 Hz, 2H), 1.76 (quintet, J = 8.1 Hz, 2H), 3.89 (t, J = 6.6 Hz, 2H), 6.58 (dd, ^{3}J = 8.7 Hz, $^{4}J_{HF}$ = 1.5 Hz 1H), 6.67 (dd, $^{3}J_{HF}$ = 10.5 Hz, ^{4}J = 2.9 Hz 1H), 7.37 (t, J = 8.5 Hz, 1H); ^{19}F-NMR ($CDCl_3$, $CFCl_3$, 470.0 MHz), δ –106.0 (t, $^{3}J_{FH}$ = 10.9 Hz, 1F).

2-2-3-3. 2-fluoro-4-octyloxybenzoic acid (C8(2F)A)

89 mL (142 mmol) of *n*-BuLi hexane solution (1.60 $molL^{-1}$) was added into the solution of 4-octyloxy-2-fluorobromobenzene (**C8(2F)Br**) 36.0 g (118.7 mmol) in dry THF (250 mL) at –78 ºC, and the reaction mixture was stirred for 2 h at –78 ºC. A solidified CO_2 (Dry Ice) was added into the reaction mixture at –78 ºC, and it was stirred for 1h at –78 ºC and further at room temperature over night. 3M-HCl*aq* (100 mL) and diethyl ether (200 mL) were added to the reaction mixture at 0 ºC, and the separated organic layer was washed with brine (100 mL) and dried over anhydrous $MgSO_4$. The solvent was removed under reduced pressure and the purified by recrystallization using n-hexane to yield 8.4 g (31.3 mmol) of **C8(2F)A** as colourless crystal (yield=26.4 %). ^{1}H-NMR ($CDCl_3$, TMS, 500.0 MHz) δ 0.89 (t, J = 6.6 Hz, 3H), 1.29–1.34 (m, 8H), 1.45 (quintet, J = 8.0 Hz, 2H), 1.80 (quintet, J = 6.9 Hz, 2H), 4.00 (t, J = 6.4 Hz, 2H), 6.64 (dd, $^{3}J_{HF}$ = 12.5 Hz, ^{4}J = 2.3 Hz 1H), 6.73 (dd, ^{3}J = 8.30 Hz, $^{4}J_{HF}$ = 2.3 Hz 1H), 8.00 (t, J = 8.3 Hz, 1H); ^{19}F-NMR ($CDCl_3$, $CFCl_3$, 470.0 MHz), δ –105.3 (t, $^{3}J_{FH}$ = 10.9 Hz, 1F).

2-2-3-4. 2,3,6,7,10,11-hexakis(4-octyloxy-2-fluorobenzoyloxy)triphenylene (C8(2F)E-TP)

4-dimethylaminopyridine 1.50 g (12.24 mmol) was added into the solution of 2-fluoro-4-octyloxybenzoic acid (**C8(2F)A**) 4.38 g (16.32 mmol) and 2,3,6,7,10,11-hexahydorxytriphenylene (0.40g, 1.36 mmol) in CH_2Cl_2 (60 mL) and stirred for 1h at rt. *N*,*N*-dicyclohexylcarbodiimide (DCC) 2.53 g (12.24 mmol) in CH_2Cl_2 (20 mL) was then added, and the reaction mixture was stirred overnight at rt. The resulting mixture was filtrated and the filtrate was poured to brine and stirred for 1 h and the separated organic layer was washed with 3M-HCl*aq*, $NaHCO_3$*aq* and brine (50 mL, for each), and dried over anhydrous $MgSO_4$. The solvent was removed under reduced pressure to give a residue which was purified by column chromatography on silica gel (300 g), with n-hexane/ ethyl acetate=3/1 as eluent. Further purification was carried out by recrystallization using toluene (50 mL) and EtOH (450 mL) solution to yield 1.41 g (0.77 mmol) of **C8(2F)E-TP** as colourless crystaline solid (yield=56.6 %). ^{1}H-NMR ($CDCl_3$, TMS, 500.0 MHz) δ 0.90 (t, J = 7.0 Hz, 18H), 1.30–1.34 (m, 48H), 1.44 (quintet, J = 7.9 Hz, 12H), 1.76 (quintet, J = 8.0 Hz, 12H), 3.89 (t, J = 6.6 Hz, 12H), 6.42 (d, $^3J_{HF}$ = 12.5 Hz, 6H), 6.49 (d, J = 9.0 Hz, 6H), 7.90 (t, J = 8.7 Hz, 6H), 8.33 (s, 6H); ^{19}F-NMR ($CDCl_3$, $CFCl_3$, 470.0 MHz), δ –104.9 (d, $^3J_{FH}$ = 10.9 Hz, 6F); MS *m/z* = 1826.3 (Calc. 1826.1 for $C_{108}H_{126}F_6O_{18}$); FTIR (KBr, cm^{-1}) 2929, 2856, 1750, 1622, 1511, 1468, 1422, 1343, 1243, 1179, 1123, 1043, 1022, 961, 905, 839 ; Anal. Calc. for $C_{108}H_{126}F_6O_{18}$: C, 71.03; H, 6.95; F, 6.24%. Found: C, 70.94; H, 6.91; F, 6.25 %.

2-2-3-5. 3,5-difluoro-1-octyloxybenzene (C8(2F6F))

Following the method employed for the synthesis of **C8(2F)**, 28.6 g (118.0 mmol, yield=99.5 %) of **C8(2F6F)** was obtained as colourless liquid by use of 3,5-difluorophenol (**2**) as the starting material. ^{1}H-NMR ($CDCl_3$, TMS, 500.0 MHz) δ 0.89 (t, J = 7.3 Hz, 3H), 1.29–1.36 (m, 8H), 1.43 (quintet, J = 7.9 Hz, 2H), 1.76 (quintet, J = 8.1 Hz, 2H), 3.90 (t, J = 6.7 Hz, 2H), 6.35-6.42 (m, 3H); ^{19}F-NMR ($CDCl_3$, $CFCl_3$, 470.0 MHz), δ –110.1 (d, $^3J_{FH}$ = 10.9 Hz, 2F).

2-2-3-6. 2,6-difluoro-4-octyloxybenzoic acid (C8(2F6F)A)

C8(2F6F)A was synthesised by following the procedure described in the synthesis of **C8(2F)A**, 17.9 g

(62.4 mmol, yield=52.9 %) of **C8(2F6F)A** was obtained as colourless crystal by using **C8(2F6F)** as the starting material. ^{1}H-NMR ($CDCl_3$, TMS, 500.0 MHz) δ 0.89 (t, J = 6.8 Hz, 3H), 1.29–1.33 (m, 8H), 1.44 (quintet, J = 6.8 Hz, 2H), 1.79 (quintet, J = 7.8 Hz, 2H), 3.97 (t, J = 6.7 Hz, 2H), 6.49 (d, $^{3}J_{HF}$ = 11.0 Hz 2H); ^{19}F-NMR ($CDCl_3$, $CFCl_3$, 470.0 MHz), δ –106.0 (d, $^{3}J_{FH}$ = 10.9 Hz, 2F).

2-2-3-7. 2,3,6,7,10,11-hexakis(2,6-difluoro-4-octyloxybenzoyloxy) triphenylene (C8(2F6F)E-TP)

C8(2F6F)E-TP was synthesised by following the method employed for the synthesis of **C8(2F)E-TP**, 1.50 g (0.78 mmol, yield=57.4 %) of **C8(2F6F)E-TP** was obtained as colourless crystal by using **C8(2F6F)A** as the starting material. ^{1}H-NMR ($CDCl_3$, TMS, 500.0 MHz) δ 0.90 (t, J = 7.2 Hz, 18H), 1.30–1.35 (m, 48H), 1.45 (quintet, J = 8.0 Hz, 12H), 1.80 (quintet, J = 7.9 Hz, 12H), 4.00 (t, J = 6.6Hz, 12H), 6.50 (d, $^{3}J_{HF}$ = 10.6 Hz, 12H), 8.52 (s, 6H); ^{19}F-NMR ($CDCl_3$, $CFCl_3$, 470.0 MHz), δ –105.5 (d, $^{3}J_{FH}$ = 10.9 Hz, 12F); MS *m/z* = 1834.4 (Calc. 1834.1for $C_{108}H_{120}F_{12}O_{18}$); FTIR (KBr, cm^{-1}) 2928, 2856, 1756, 1636, 1578, 1511, 1469, 1449, 1421, 1356, 1313, 1249, 1199, 1164, 1124, 1079, 1049, 1023, 949, 904, 839, 775; Anal. Calc. for $C_{108}H_{120}F_{12}O_{18}$: C, 67.07; H, 6.25; F, 11.79%. Found: C, 67.10; H, 6.27; F, 11.88 %.

2-2-3-8. 4-octyloxy-3-fluorobromobenzene (C8(3F)Br)

24.0 g (79.2 mmol, yield=99.6 %) of **C8(3F)Br** was obtained as colourless liquid by using 2-fluoro-4-bromophenol (**4**) as the starting material under following the procedure employed for the synthesis of **C8(2F)**. ^{1}H-NMR ($CDCl_3$, TMS, 500.0 MHz) δ 0.88 (t, J = 6.8 Hz, 3H), 1.28–1.33 (m, 8H), 1.44 (quintet, J = 7.2 Hz, 2H), 1.80 (quintet, J = 6.5 Hz, 2H), 3.90 (t, J = 6.6 Hz, 2H), 6.81 (t, J = 8.7 Hz, 1H), 7.15 (td, ^{3}J = 9.00 Hz, $^{4}J_{HF}$ = 1.3 Hz, 1H), 7.20 (dd, $^{3}J_{HF}$ = 10.6 Hz, ^{4}J = 2.3 Hz, 1H); ^{19}F-NMR ($CDCl_3$, $CFCl_3$, 470.0 MHz), δ –131.7 (d, $^{3}J_{FH}$ = 10.9 Hz, 1F).

2-2-3-9. 3-fluoro-4-octyloxybenzoic acid (C8(3F)A)

The solution of 4-octyloxy-3-fluorobromobenzene (**C8(3F)Br**) 24.0 g (79.2 mmol) in dry THF (200 mL) was added into Mg 2.31 g (95.0 mmol) dried up in Ar, and the reaction mixture refluxed for 1 hr, and the reaction mixture was cooled down to –78 ºC, and solidified CO_2 (Dry Ice) was added into the mixture at –78 ºC, and was stirred for 1h at –78 ºC followed by at room temperature over night. 3M-HCl*aq* (100 mL)

and diethyl ether (200 mL) were added to the reaction mixture at 0 ºC, and the separated organic layer was washed with brine (100 mL) and dried over anhydrous $MgSO_4$. The solvent was removed under reduced pressure and the reside was purified by recrystallization using n-hexane to yield 16.4 g (61.0 mmol) of **C8(3F)A** as colourless crystal (yield=77.0 %). ^{1}H-NMR ($CDCl_3$, TMS, 500.0 MHz) δ 0.89 (t, J = 6.9 Hz, 3H), 1.28–1.37 (m, 8H), 1.47 (quintet, J = 7.9 Hz, 2H), 1.85 (quintet, J = 7.3 Hz, 2H), 4.01 (t, J = 6.5 Hz, 2H), 6.98 (t, J = 8.5 Hz, 1H), 7.79 (dd, $^3J_{HF}$ = 11.5 Hz, ^4J = 1.8 Hz, 1H), 7.87 (td, ^3J = 8.6 Hz, $^4J_{HF}$ =1.2 Hz, 1H); ^{19}F-NMR ($CDCl_3$, $CFCl_3$, 470.0 MHz), δ –134.3 (t, $^3J_{FH}$ = 10.9 Hz, 1F).

2-2-3-10. 2,3,6,7,10,11-hexakis(2,6-difluoro-4-octyloxybenzoyloxy) triphenylene (C8(3F)E-TP)

Following the procedure described in the synthesis of **C8(2F)E-TP**, 0.64 g (0.35 mmol, yield=25.8 %) of **C8(3F)E-TP** was obtained as colourless crystal by using **C8(3F)A** as the starting material. ^{1}H-NMR ($CDCl_3$, TMS, 500.0 MHz) δ 0.89 (t, J = 7.1 Hz, 18H), 1.30–1.34 (m, 48H), 1.45 (quintet, J = 7.9 Hz, 12H), 1.81 (quintet, J = 8.0 Hz, 12H), 3.96 (t, J = 6.8 Hz, 12H), 6.65 (t, J = 8.0 Hz, 6H), 7.48 (dd, $^3J_{HF}$ 11.5 Hz, ^4J = 1.8 Hz, 6H), 7.65 (d, ^3J = 8.8 Hz, 6H), 8.21 (s, 6H); ^{19}F ($CDCl_3$, $CFCl_3$, 470.0 MHz) δ –134.5 (d, J = 8.1 Hz 6F); MS m/z = 1826.4 (Calc. 1826.1 for $C_{108}H_{126}F_6O_{18}$); FTIR (KBr, cm^{-1}) 2955, 2927, 2857, 1741, 1617, 1519, 1469, 1437, 1425, 1286, 1253, 1193, 1141, 1123, 1071, 931, 893, 750 ; Anal. Calc. for $C_{108}H_{126}F_6O_{18}$: C, 71.03; H, 6.95; F, 6.24%. Found: C, 71.09; H, 6.93; F, 6.31%.

2-2-3-11. 2,6-difluorophenylboronic acid (10)

123.3 mL (197.3 mmol) of *n*-BuLi hexane solution (1.60 $molL^{-1}$) was added into the solution of 1,3-difluorobenzene (**9**) 25.0 g (164.4 mmol) in dry THF (250 mL) at –78 ºC, and the reaction mixture was stirred for 2 h at –78 ºC, and a solution of 2-propyl borate 61.8 g (328.8 mmol) in dry THF 60 mL was added into the reaction mixture at –78 ºC, and it was stirred for 1h at –78 ºC and further at room temperature over night. 3M-HCl*aq* (100 mL) and diethyl ether (200 mL) were added into the reaction mixture at 0 ºC, and the separated organic layer was washed with brine (100 mL) and dried over anhydrous $MgSO_4$. The solvent was removed under reduced pressure to yield 31.9 g of **10** as colourless liquid, which was used without further purification.

2-2-3-12. 2,6-difluorophenol (11)

Hydrogen peroxide (30 %, aqueous solution) 37.3 g (328.8 mmol) was slowly added into the solution of 2,6-difluorophenylboronic acid (**10**) 31.9 g in THF (150 mL) under 30 ºC, and the reaction mixture was stirred for 2 h at rt. A saturated aqueous solution of sodium sulfite (100 mL) and diethyl ether (200 mL) were added to the reaction mixture at 0 ºC, and the separated organic layer was washed with a saturated aqueous solution of sodium sulfite and brine (100 mL) and dried over anhydrous $MgSO_4$. The solvent was removed under reduced pressure and the residue was purified by distillation under reduced pressure, b. p. 65 °C at 11.3 kPa to yield 18.4 g (141.7 mmol) of **11** as colourless liquid (yield=86.2% from **9**). ^{1}H-NMR ($CDCl_3$, TMS, 500.0 MHz) δ 6.76 (tt, $^3J_{HF}$ =6.9 Hz, ^4J =1.8 Hz, 1H), 6.85 (td, $^3J_{HF}$ =7.1 Hz, ^4J =1.1 Hz, 2H); ^{19}F-NMR ($CDCl_3$, $CFCl_3$, 470.0 MHz), δ –135.9 (s, 2F).

2-2-3-13. 4-bromo-2,6-difluorophenol (12)

Bromine 23.7 g (148.5 mmol) was slowly added into a suspension mixture of 2,6-difluorophenol (**11**) 18.4 g (141.4 mmol) and Fe (powdered) 1.0 g, and the reaction mixture was stirred at refluxed for 8 h. The reaction mixture was poured into ice water and extracted with CH_2Cl_2, and the separated organic layer was washed with a saturated aqueous solution of sodium sulfite and brine (100 mL) and dried over anhydrous $MgSO_4$. The solvent was removed under reduced pressure to yield 27.6 g (132.2 mmol) of **12** as colourless liquid (yield=93.5%), which was used without further purification. ^{1}H-NMR ($CDCl_3$, TMS, 500.0 MHz) δ 7.04 (d, $^3J_{HF}$ =6.9 Hz, 2H); ^{19}F-NMR ($CDCl_3$, $CFCl_3$, 470.0 MHz), δ –132.9 (s, 2F).

2-2-3-14. 4-octyloxy-3,5-difluorobromobenzene (C8(3F5F)Br)

Following the method described in the synthesis of **C8(2F)** 25.3 g (79.0 mmol, yield=82.5 %) of **C8(3F5F)Br** was obtained as colourless liquid by using 4-bromo-2,6-difluorophenol (**8**) as the starting material. ^{1}H-NMR ($CDCl_3$, TMS, 500.0 MHz) δ 0.92 (t, J = 6.7 Hz, 3H), 1.32–1.35 (m, 8H), 1.46 (quintet, J = 5.4 Hz, 2H), 1.77 (quintet, J = 8.1 Hz, 2H), 4.13 (t, J = 6.7 Hz, 2H), 7.08 (d, $^3J_{HF}$ = 7.4 Hz, 2H); ^{19}F-NMR ($CDCl_3$, $CFCl_3$, 470.0 MHz), δ –126.4 (d, $^3J_{FH}$ = 10.9 Hz, 1F).

2-2-3-15. 2,6-difluoro-4-octyloxybenzoic acid (C8(3F5F)A)

Following the method showed in the synthesis of **C8(3F)A**, 9.0g (31.4 mmol, yield=40.4 %) of **C8(3F5F)A** was obtained as colourless crystal by using **C8(3F5F)Br** as the starting material. ^{1}H-NMR ($CDCl_3$, TMS, 500.0 MHz) δ 0.89 (t, J = 6.7 Hz, 3H), 1.29–1.33 (m, 8H), 1.46 (quintet, J = 7.2 Hz, 2H), 1.78 (quintet, J = 7.1 Hz, 2H), 4.27 (t, J = 6.6 Hz, 2H), 7.63 (d, $^{3}J_{HF}$ =8.2 Hz 2H); ^{19}F-NMR ($CDCl_3$, $CFCl_3$, 470.0 MHz), δ –127.1 (d, $^{3}J_{FH}$ = 10.9 Hz, 2F).

2-2-3-16. 2,3,6,7,10,11-hexakis(3,5-difluoro-4-octyloxybenzoyloxy) triphenylene (C8(3F5F)E-TP)

1.75 g (0.91 mmol, yield=66.5 %) of **C8(3F5F)E-TP** was obtained as colourless crystal on following the procedure employed for the synthesis of **C8(2F)E-TP**, by using **C8(3F5F)A** as the starting material. ^{1}H-NMR ($CDCl_3$, TMS, 500.0 MHz) δ 0.90 (t, J = 7.0 Hz, 18H), 1.30–1.34 (m, 48H), 1.46 (quintet, J = 8.0 Hz, 12H), 1.76 (quintet, J = 8.0 Hz, 12H), 4.19 (t, J = 6.6Hz, 12H), 7.38 (d, $^{3}J_{HF}$ = 7.8 Hz, 12H), 8.06 (s, 6H); ^{19}F ($CDCl_3$, $CFCl_3$, 470.0 MHz), δ –127.0 (s, 12F), MS *m/z* = 1934.4 (Calc. 1934.1 for $C_{108}H_{120}F_{12}O_{18}$); FTIR (KBr, cm^{-1}) 2957, 2928, 2857, 1744, 1622, 1583, 1516, 1436, 1350, 1254, 1205, 1123, 1035, 1002, 947, 890, 751 ; Anal. Calc. for $C_{108}H_{120}F_{12}O_{18}$: C, 67.07; H, 6.25; F, 11.79%. Found: C, 67.15; H, 6.34; F, 11.87 %.

2-2-3-17. 2,5-difluorophenylboronic acid (10)

19.6g of **10** was obtained as colourless liquid by following the method employed for the synthesis of 2,6-difluorophenylboronic acid (**6**) with 2,5-difluorobromobenzene (**9**) as the starting material. 2,5-difluorophenylboronic acid (**10**) was used without further purification.

2-2-3-18. 2, 5-difluorophenol (11)

On following the method employed for the synthesis of 2,6-difluorophenol (**7**), 11.3 g (86.9 mmol, yield=66.8 %) of 2,5-difluorophenol (**11**) was obtained as colourless liquid by using 2,5-difluorophenylboronic acid (**10**) as the starting material. ^{1}H-NMR ($CDCl_3$, TMS, 500.0 MHz) δ 6.51 (tt, $^{3}J_{HF}$ = 8.3 Hz, $^{4}J_{HF}$ = 3.3 Hz, 1H), 6.70 (ddd, $^{3}J_{HF}$ = 7.3 Hz, ^{3}J = 5.3 Hz, $^{4}J_{HF}$ = 3.3 Hz, 1H), 7.00 (dt, $^{3}J_{HF}$ = 9.6 Hz, ^{3}J = 5.2 Hz 1H); ^{19}F-NMR ($CDCl_3$, $CFCl_3$, 470.0 MHz), δ –117.7 (d, $^{3}J_{FH}$ = 9.5 Hz, 1F), –146.0 (s, 1F).

2-2-3-19. 2,5-difluoro-1-octyloxybenzene (C8(2F5F))

Following the way employed for the synthesis of **C8(2F)**, 14.4 g (59.2 mmol, yield=68.1 %) of **C8(2F5F)** was obtained as colourless liquid by using 2,5-difluorophenol (**11**) as the starting material. ^{1}H-NMR ($CDCl_3$, TMS, 500.0 MHz) δ 0.89 (t, J = 7.5 Hz, 3H), 1.29–1.37 (m, 8H), 1.46 (quintet, J = 7.5 Hz, 2H), 1.80 (quintet, J = 6.4 Hz, 2H), 3.98 (t, J = 6.7 Hz, 2H), 6.54 (tt, $^{3}J_{HF}$ = 7.7 Hz, $^{4}J_{HF}$ = 3.3 Hz, 1H), 6.67 (ddd, $^{3}J_{HF}$ = 6.8 Hz, ^{3}J = 6.2 Hz, $^{4}J_{HF}$ = 2.9 Hz, 1H), 6.98 (dt, $^{3}J_{HF}$ = 9.9 Hz, ^{3}J = 5.6 Hz 1H); ^{19}F-NMR ($CDCl_3$, $CFCl_3$, 470.0 MHz), δ –117.4 (t, $^{3}J_{FH}$ = 16.3 Hz, 1F), –141.0 (s, 1F).

2-2-3-20. 2,5-difluoro-4-octyloxybromobenzene (C8(2F5F)Br)

Following the way described in the synthesis of **C8(2F)Br**, 17.0 g (52.9 mmol, yield=89.4 %) of **C8(2F5F)Br** was obtained as colourless liquid by using 2,5-difluoro-1-octyloxybenzene (**C8(2F5F)**) as the starting material. ^{1}H-NMR ($CDCl_3$, TMS, 500.0 MHz) δ 0.92 (t, J = 6.2 Hz, 3H), 1.32–1.36 (m, 8H), 1.48 (quintet, J = 7.6 Hz, 2H), 1.84 (quintet, J = 7.4 Hz, 2H), 4.00 (t, J = 6.4 Hz, 2H), 6.78 (t, $^{3}J_{HF}$ = 7.7 Hz, 1H), 7.26 (dd, $^{3}J_{HF}$ = 10.2 Hz, ^{3}J = 6.9 Hz 1H); ^{19}F-NMR ($CDCl_3$, $CFCl_3$, 470.0 MHz), δ –111.3 (t, $^{3}J_{FH}$ = 13.1 Hz, 1F), –138.0 (dd, $^{3}J_{FH}$ = 20.7 Hz, $^{4}J_{FH}$ = 12.2 Hz 1F).

2-2-3-21. 2,5-difluoro-4-octyloxybenzonitryl (C8(2F5F)CN)

5.8g (65.0 mmol) of Copper cyanide (I) was added into the solution of 2,5-difluoro-4-octyloxybenzene (**C8(2F5F)Br**) 17.4 g (54.2 mmol) in DMF (50 mL). The reaction mixture was refluxed for 4h. The reaction mixture was poured into an aqueous ammonia (100 mL) and diethyl ether, and the separated organic layer was washed with brine (100 mL) and dried over anhydrous $MgSO_4$. The solvent was removed under reduced pressure and the residue was purified by column chromatography on silica gel (300 g), eluting with the mixture of CH_2Cl_2 and *n*-hexane (1:1) to yield 10.3 g (38.5 mmol) of **C8(2F5F)CN** as colourless liquid, yield 71.0 %. ^{1}H-NMR ($CDCl_3$, TMS, 500.0 MHz) δ 0.92 (t, J = 6.8 Hz, 3H), 1.31–1.40 (m, 8H), 1.50 (quintet, J = 7.8 Hz, 2H), 1.88 (quintet, J = 7.9 Hz, 2H), 4.09 (t, J = 6.8 Hz, 2H), 6.81 (dd, $^{3}J_{HF}$ = 10.3 Hz, ^{3}J = 6.8 Hz, 1H), 7.30 (dd, $^{3}J_{HF}$ = 9.8 Hz, ^{3}J = 6.1 Hz, 1H); ^{19}F-NMR ($CDCl_3$, $CFCl_3$, 470.0 MHz), δ –108.7 (t, $^{3}J_{FH}$ = 13.6 Hz, 1F), –137.2 (t, $^{3}J_{FH}$ = 13.6 Hz, 1F).

2-2-3-22. 2,5-difluoro-4-octyloxybenzaldehyde (C8(2F5F)Ald)

38.5 mL (57.8 mmol) of diidobutylalminium hydride (DIBAL-H) toluene solution (1.5 $molL^{-1}$) was added into a solution of 2,5-difluoro-4-octyloxybenonitryl (**C8(2F5F)CN**) 10.3 g (38.5 mmol) in CH_2Cl_2 (150 mL) at 0 °C. After stirring for 1h at rt., the reaction mixture was poured into 3M-HCl *aq* (200 mL), and extracted with diethyl ether. The separated organic layer was washed with brine (100 mL) and dried over anhydrous $MgSO_4$. The solvent was removed under reduced pressure to yield 9.83 g (38.5 mmol) of **C8(2F5F)Ald** as colourless liquid, yield 82.8 %. 2,5-difluoro-4-octyloxybenzaldehyde (**C8(2F5F)Ald**) was used for the next reaction without further purification.

2-2-3-23. 2,5-difluoro-4-octyloxybenzoic acid (C8(2F5F)A)

Jones reagent (Chromic oxide (IV) sulfuric acid solution) 20 mL was added into a solution of 2,5-difluoro-4-octyloxybenzaldehyde (**C8(2F5F)Ald**) 9.8 g (36.4 mmol) in acetone (30 mL) at 0 °C, and reaction mixture was stirred over night at rt. A saturated aqueous sodium sulfite was poured into the reaction mixture and extracted with diethyl ether. The separated organic layer was washed with brine (100 mL) and dried over anhydrous $MgSO_4$. The solvent was removed under reduced pressure and the residue was purified by recrystallization using n-hexane to yield 5.9 g (20.7 mmol) of **C8(2F5F)A** as colourless crystal (yield=57.0 %). ^{1}H-NMR ($CDCl_3$, TMS, 500.0 MHz) δ 0.89 (t, J = 6.7 Hz, 3H), 1.29–1.38 (m, 8H), 1.47 (quintet, J = 7.9 Hz, 2H), 1.86 (quintet, J = 8.0 Hz, 2H), 4.06 (t, J = 6.5 Hz, 2H), 6.71 (dd, $^3J_{HF}$ = 11.6 Hz, ^3J = 6.5 Hz, 1H), 7.71 (dd, $^3J_{HF}$ = 11.2 Hz, ^3J = 6.8 Hz, 1H); ^{19}F-NMR ($CDCl_3$, $CFCl_3$, 470.0 MHz), δ –109.1 (s, 1F), –139.4 (t, $^3J_{FH}$ = 16.4 Hz, 1F).

2-2-3-24. 2,3,6,7,10,11-hexakis(2,5-difluoro-4-octyloxybenzoyloxy) triphenylene (C8(2F5F)E-TP)

Following the procedure showed in the synthesis of **C8(2F)E-TP**, 1.24 g (0.64 mmol, yield=47.1 %) of **C8(2F5F)E-TP** was obtained as colourless crystal by using **C8(2F5F)A** as the starting material. ^{1}H-NMR ($CDCl_3$, TMS, 500.0 MHz) δ 0.90 (t, J = 6.8 Hz, 18H), 1.30–1.35 (m, 48H), 1.47 (quintet, J = 7.9 Hz, 12H), 1.83 (quintet, J = 7.9 Hz, 12H), 3.96 (t, J = 6.7 Hz, 12H), 6.50 (dd, $^3J_{HF}$ = 11.6 Hz, ^3J = 6.7 Hz, 6H), 7.56 (dd, $^3J_{HF}$ = 11.3 Hz, ^3J = 6.8 Hz, 6H), 8.23 (s, 6H); ^{19}F-NMR ($CDCl_3$, $CFCl_3$, 470.0 MHz), δ –108.2 (s, 6F),

–139.7 (s, 6F); Anal. Calc. for $C_{108}H_{120}F_{12}O_{18}$: C, 67.07; H, 6.25; F, 11.79%. Found: C, 66.98; H, 6.23; F, 11.78 %.

2-3. Results and discussion

2-3-1. Mesomorphic properties

The DSC curves on heating of the **C8(2F)E-TP** and **C8(2F6F)E-TP** for which the peripheral phenylene groups are fluorinated at the inner position are shown in Figure 2-2 and 2-3. These exhibit enantiotropic mesomorphism. For **C8(2F)E-TP**, four endothermic peaks were observed at 82.3, 120, 150 and 213 ºC on the first heating run with the phase transition enthalpies (ΔH), 12.5, 27.3, 28.3 and 0.83 kJmol^{-1}, respectively. On the first cooling run, however five exothermic peaks were observed at 212, 139, 141, 55.9 and 30.2 ºC (ΔH: 0.97, 17.6, 9.7, 7.9 and 5.5 kJmol^{-1}, respectively). On the first heating run, **C8(2F6F)E-TP** shows three peaks at 53.2, 116 and 176 ºC (ΔH: 18.1, 60.9 and 23.0 kJ/mol, respectively). On the first cooling run, three peaks were observed at 173, 103 and 65.2 ºC with 20.8, 26.5 and 12.7 kJ/mol of ΔH, respectively. The microscopic texture observation of **C8(2F)E-TP** revealed the former two on the first heating runs are crystal-crystal transitions, and the latter two are the melting and clearing points, respectively. A typical Schlieren texture was observed for the mesophase of **C8(2F)E-TP** (as show in Figure 2-4), and thus it could be identified to be a discotic nematic (N_D) mesophase, also supported by the DSC results.

C8(2F6F)E-TP shows a solid-like texture in the mesophase (see in Figure 2-4), and it is a highly viscous state to indicate this phase is a highly ordered mesophase. This is also supported by the X-ray diffraction results (as shown in Figure 2-5).

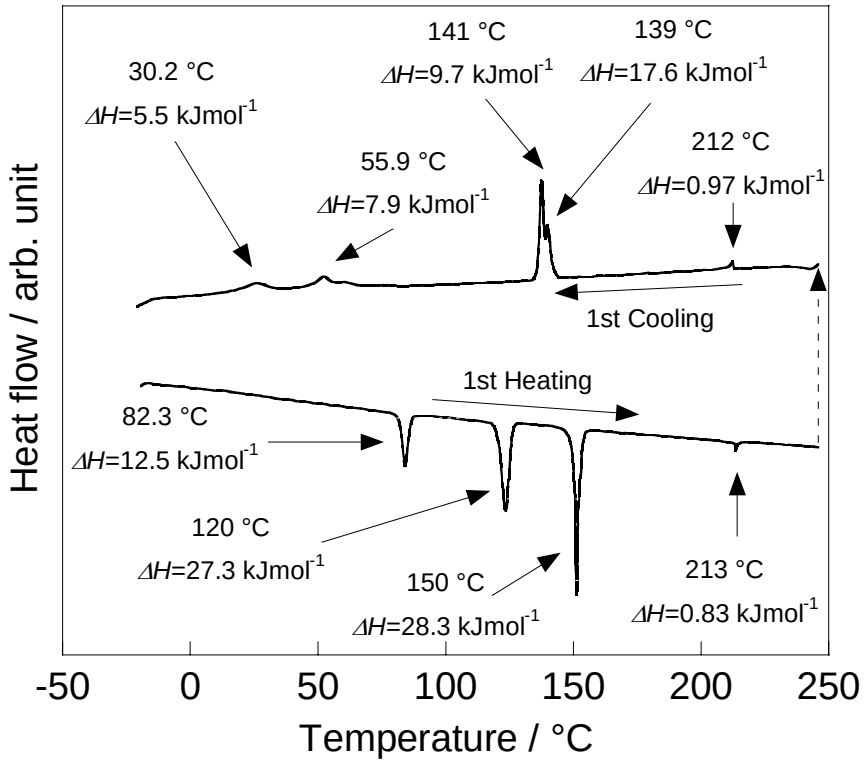

Figure 2-2 DSC curves of **C8(2F)E-TP** (rate: 5 °C min^{-1}).

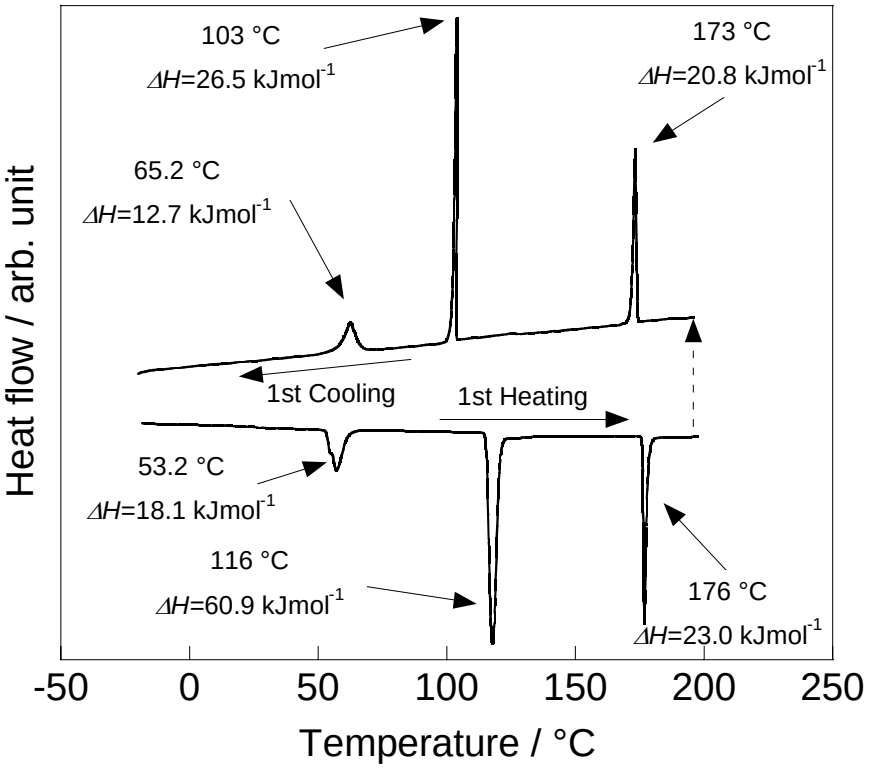

Figure 2-3 DSC curves of **C8(2F6F)E-TP** (rate: 5 °C min^{-1}).

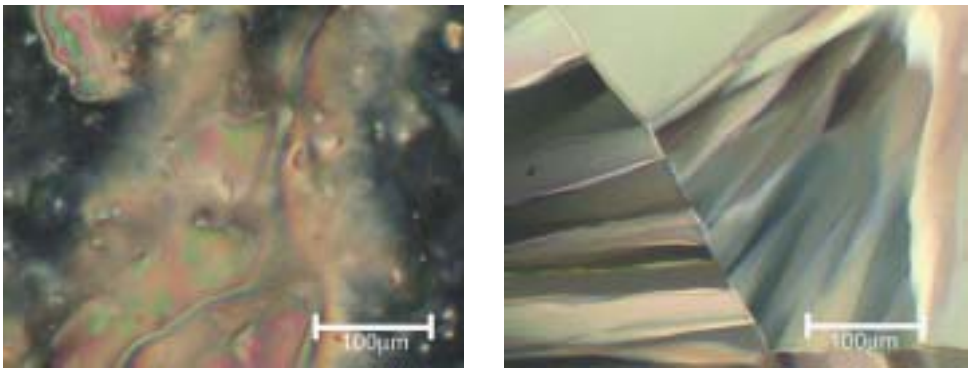

Figure 2-4 Optical textures of mesophases for **C8(2F)E-TP** (left: at 200 ºC) and **C8(2F6F)E-TP** (right: at 155 ºC).

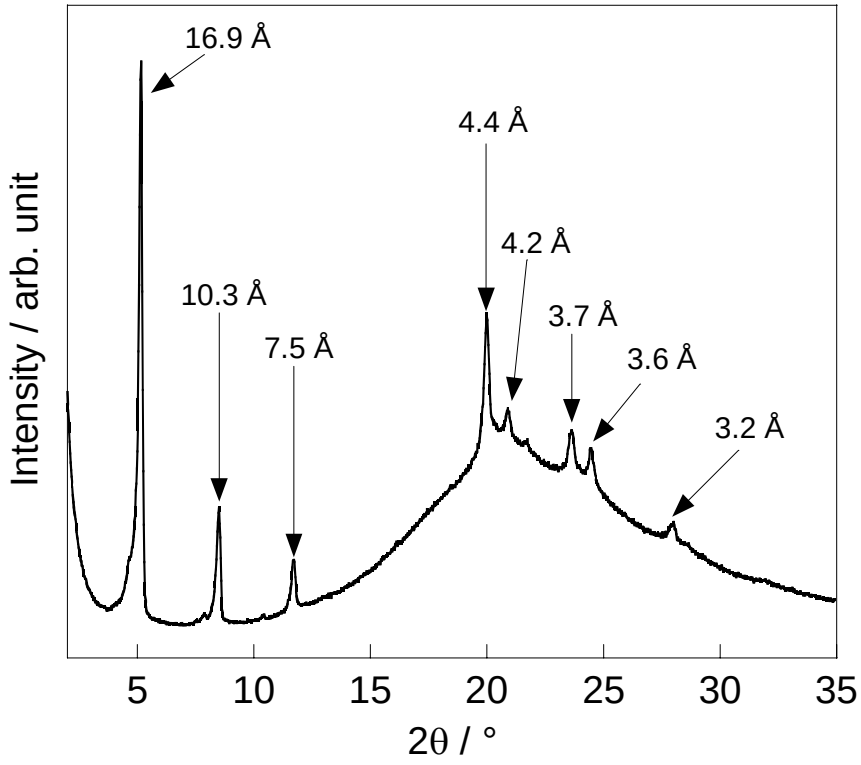

Figure 2-5 X-ray diffraction pattern of **C8(2F6F)E-TP** at 140 °C.

On the other hand, the DSC curves of **C8(3F)E-TP** and **C8(3F5F)E-TP**, in which the outer positions (3/ 3 and 5 sites) of the phenyl rings are fluorinated are shown in Figure 2-6 and 2-7. These also exhibit enantiotropic mesomorphism. For **C8(3F)E-TP** four endothermic peaks were observed at 56.1, 196, 210 and 237 ºC with the phase transition enthalpies (ΔH), 3.6, 3.1, 0.61 and 0.67 kJmol^{-1}, respectively. **C8(3F5F)E-TP** shows only two peaks at 14.7 ºC and 140 ºC (ΔH: 5.3 kJ/mol and 11.1 kJmol^{-1}, respectively).

In the microscopic texture observation up to 420 ºC, the clearing points of **C8(3F)E-TP** and **C8(3F5F)E-TP** could not definitively be detected. Both compounds only show thermal decomposition below the isotropisation temperature. For example, thermal stability of mesomorphism for **C8(3F)E-TP** is much larger than one of corresponding positional isomer **C8(2F)E-TP**. These drastic enhancements of mesomorphism induced by the only difference of the position for fluorination are quite new and interesting. It is noteworthy that fluorination at the outer positions of the peripheral groups (semi-flexible/ semi-rigid core part) drastically enhance the thermal stability of columnar mesophase.

In the X-ray diffraction patterns of the mesophase of **C8(3F)E-TP** at 205 ºC (for the non-aligned samples), several reflection peaks were detected, which have the spacing of 26.4 Å, 24.5 Å, 15.6 Å, 13.3 Å and 9.9 Å (Figure 2-8), and this mesophase was assigned to be a Col_r phase with *C*2/m symmetry. Almost invariable situation of the diffraction patterns was observed for the three mesophases above 196 ºC, indicating these mesophases are classified to be Col_r phases with a tiny change of the molecular order to each (as shown in Figure 2-8). Between 205 °C and 220 °C, only the lattice constant was slightly changed and symmetry of molecular order (C2/m) was kept. However, molecular formation was changed from *C*2/m to $P2_1/a$ between 220 °C and 250 °C.

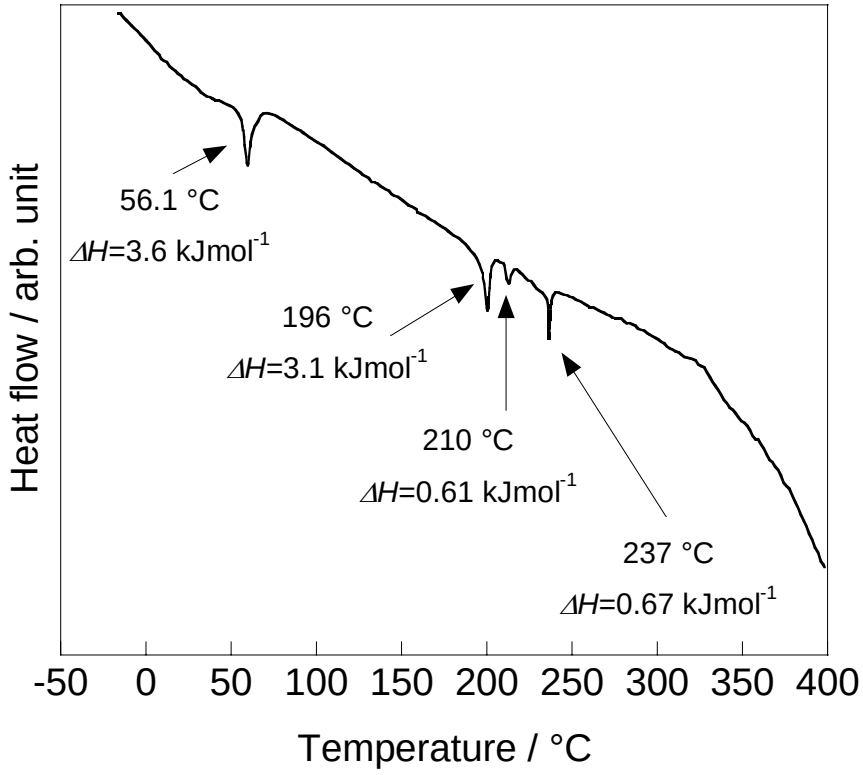

Figure 2-6 DSC curve of **C8(3F)E-TP** (Heating rate 5 °C min^{-1}).

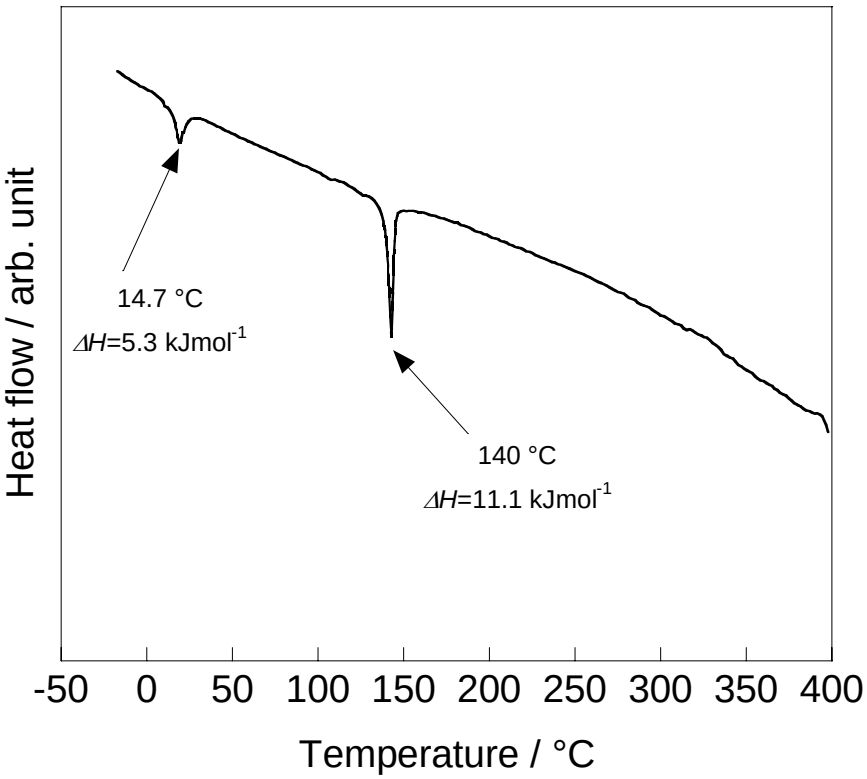

Figure 2-7 DSC curve of **C8(3F5F)E-TP** (Heating rate: 5 °Cmin^{-1}).

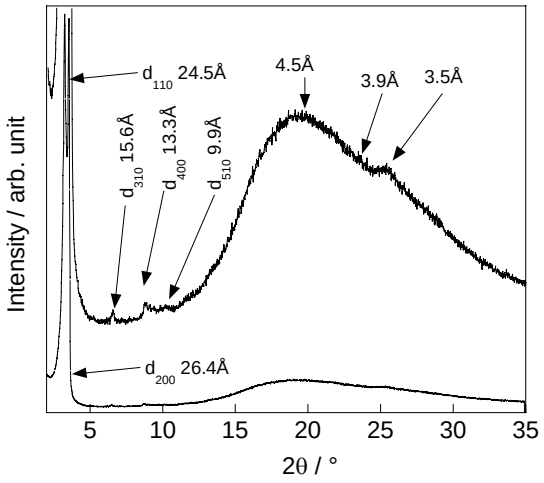

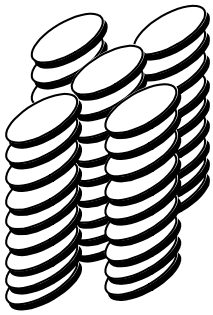

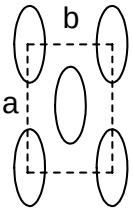

*C*2/m

at 205 °C

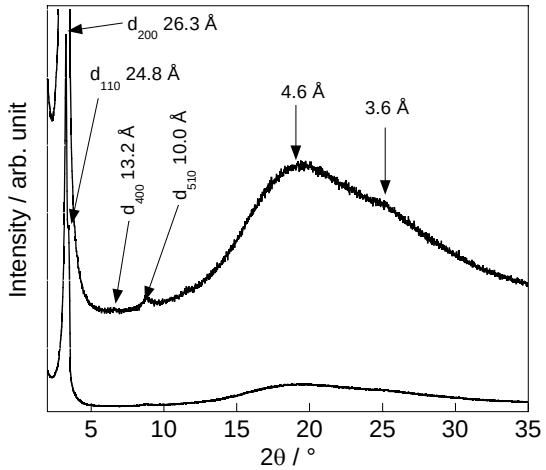

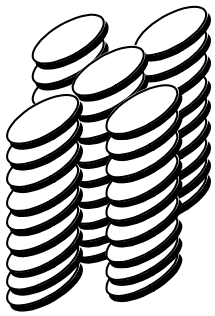

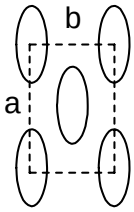

*C*2/m

at 220 °C

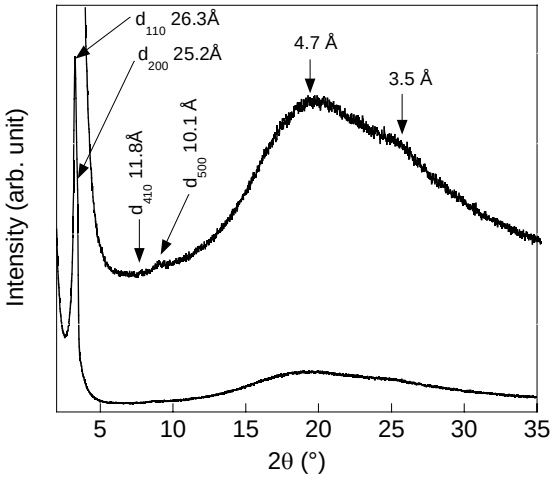

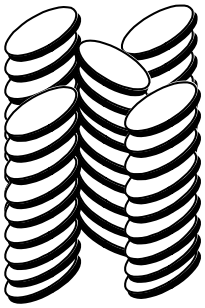

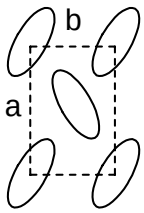

$P2_1/a$

at 250 °C

Figure 2-8 XRD patterns and molecular positions of **C8(3F)E-TP** at each temperature.

Table 2-1 X-ray diffraction parameters for the mesophase of **C8(3F)E-TP** (205 °C, 220 °C and 250 °C) and **C8(3F5F)E-TP**.

Compound	Temperature	Lattice constant / Å	hkl	d_{hkl} / Å	
				Observed	Calculated
C8(3F)E-TP	205 °C	Col_r	200	26.4	26.4
		(*C2/m*)	110	24.5	24.5
		a=52.9	310	15.6	14.9
		b=27.7	400	13.3	13.2
		Z=2[†]	510	9.9	9.9
				4.5 (br)[††]	
				3.5 (br)	
	220 °C	Col_r	200	26.3	26.3
		(*C2/m*)	110	24.8	24.8
		a=52.6	400	13.2	13.1
		b=28.1	510	10.0	9.8
		Z=2[†]		4.6 (br)	
				3.6 (br)	
	250 °C	Col_r	200	26.3	26.3
		($P2_1/a$)	110	25.2	25.2
		a=52.6	310	15.2	15.0
		b=28.7	410	11.8	12.0
		Z=2[†]	510	10.1	9.9
				4.7 (br)	
				3.5 (br)	
C8(3F5F)E-TP	160 °C	Col_h	100	26.9	26.9
		a=31.1	110	15.5	15.5
		Z=0.5[†]	200	13.6	13.5
			210	10.1	10.2
			300	9.1	9.0
			220	7.8	7.8
				4.5 (br)	
				3.5 (br)	

[†]: Calculated from the lattice constants *a* and *b*, correlation length along the *c*-axis (3.5 Å) and the postulated density ρ (1.0 g cm^{-3}); [††]: br = Broad.

The X-ray diffraction pattern of **C8(3F5F)E-TP** at 160 ºC (for the non-aligned samples) shows the small number of reflections as shown in Figure 2-9. The reflections in the small angle region have a spacing ratio of 1:1/√3:1/2, which is an evidence of a hexagonal arrangement of molecularly stacked columns. Furthermore, three halos of which spacing are 4.5 and 3.5 Å were observed in the wide-angle region. The halo centered at 4.5 Å could be assigned to the averaged diameter of molten alkyl chain[2] and the π–π staking distance of triphenylene cores in a column gives a reflection at 3.5 Å. The X-ray diffraction parameters of **C8(3F)E-TP** and **C8(3F5F)E-TP** are summarised in Table 2-1.

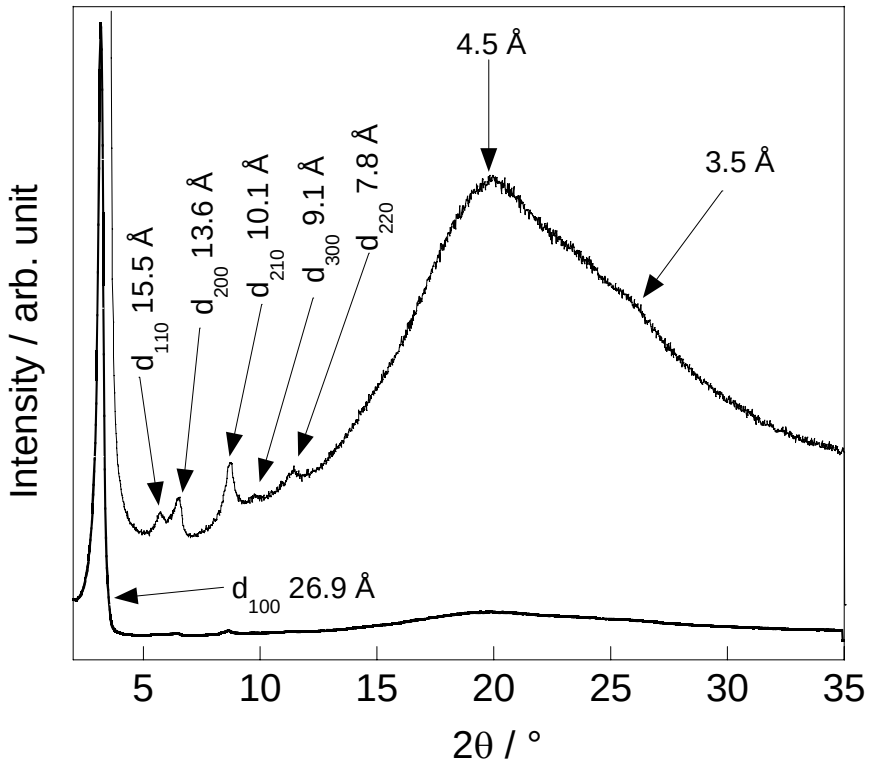

Figure 2-9 X-ray diffraction pattern of **C8(3F5F)E-TP** at 160 °C.

Furthermore, the DSC curve of **C8(2F5F)E-TP**, in which the inner and outer positions (2 and 5 sites) of the phenyl rings are fluorinated is shown in Figure 2-10. **C8(2F5F)E-TP** also exhibits enantiotropic mesomorphism. Two endothermic peaks were observed for **C8(2F5F)E-TP** at 90.0 ºC and 157 ºC on first heating run with the phase transition enthalpies (ΔH), 21.8 and 10.2 kJmol^{-1}, respectively. On the first cooling run, **C8(2F5F)E-TP** shows two peaks at 252 ºC and 63.3 ºC (ΔH: 8.1 kJmol^{-1} and 20.2 kJmol^{-1}, respectively).

The X-ray diffraction pattern of **C8(2F5F)E-TP** at 160 ºC (for the non-aligned samples) shows several reflection peaks having the spacing of 25.8 Å, 22.5 Å, 16.4 Å, 13.4 Å, 10.1 Å and 9.3 Å (Figure 2-11), and this mesophase was assigned to be a Col_r phase of which packing of columns is *C*2/m. Furthermore, three halo spacing of 4.5 Å observed in the wide-angle region. The halo centered at 4.5 Å could be assigned to the averaged diameter of molten alkyl chain.[2] The X-ray diffraction parameters of **C8(2F5F)E-TP** is summarised in Table 2-2.

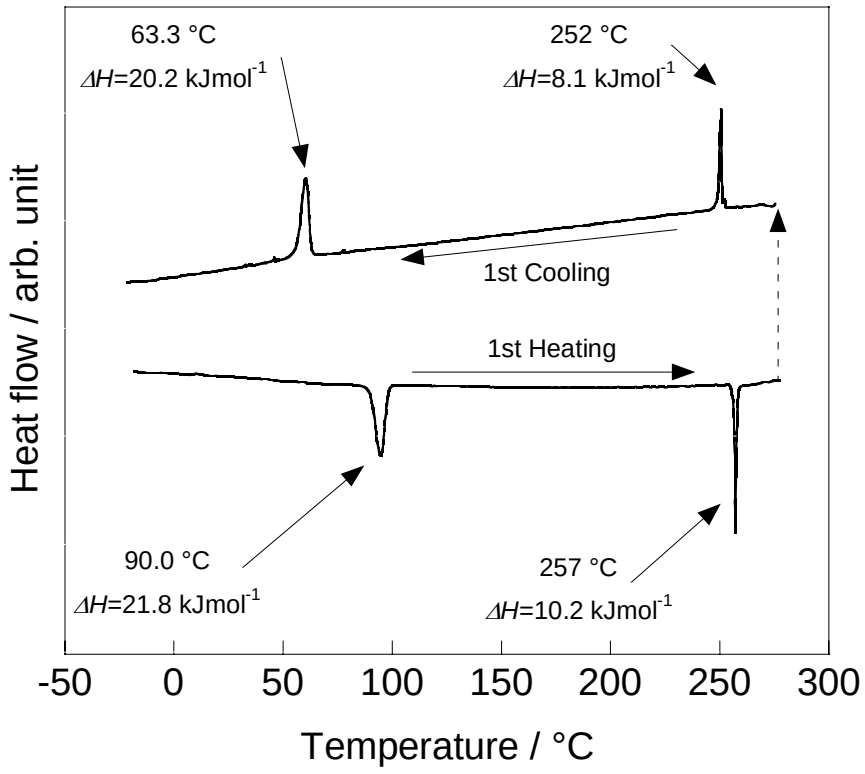

Figure 2-10 DSC curve of **C8(2F5F)E-TP** (rate: 3 °C min^{-1}).

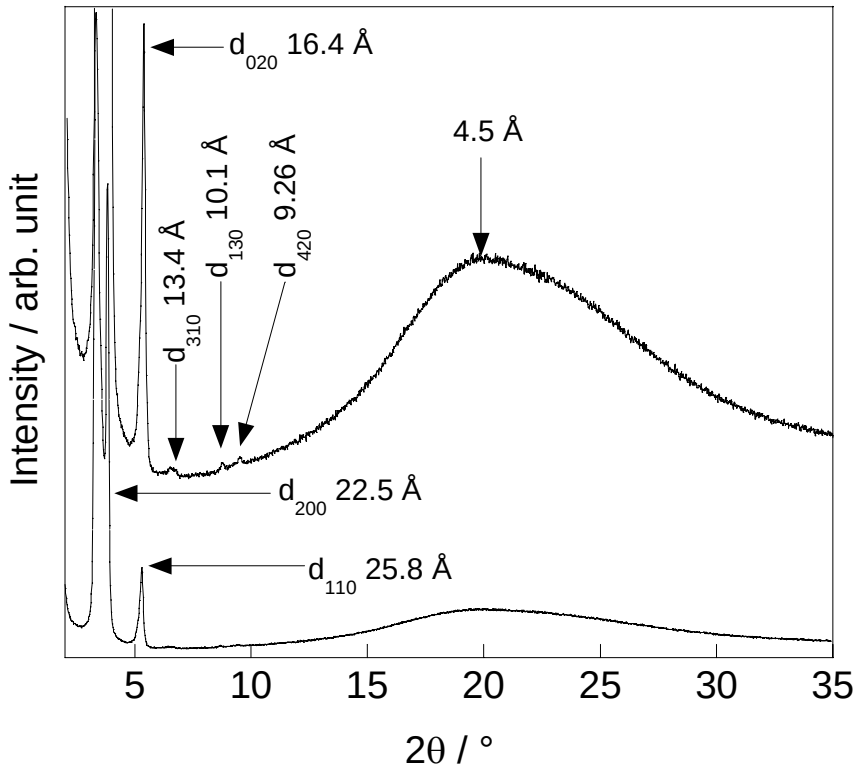

Figure 2-11 X-ray diffraction pattern of **C8(2F5F)E-TP** at 140 °C.

Table 2-2 X-ray diffraction parameters for the mesophase of **C8(2F5F)E-TP**.

Compound	Lattice const. / Å	hkl	d_{hkl} / Å	
			Observed	Calculated
C8(2F5F)E-TP	Col_r	110	25.8	26.5
(140 °C)	(*C2/m*)	200	22.5	22.5
	a=45.0	020	16.4	16.4
	b=32.8	310	13.4	13.7
	Z=2[†]	130	10.9	10.6
		420	9.3	9.2
			4.4 (br) [††]	

[†]: Calculated from the lattice constants *a* and *b*, correlation length along the *c*-axis (3.5 Å) and the postulated density ρ (1.0 g cm^{-3}); [††]: br = Broad.

2-3-2. Comparison of the mesomorphic behaviours

The phase transition parameters of **C8(2F)E-TP**, **C8(2F6F)E-TP**, **C8(3F)E-TP**, **C8(3F5F)E-TP** and **C8(2F5F)E-TP** are summarized in Table 2-3 and Figure 2-12, with those of **C8H4E-TP**[1] and **C8F4E-TP** as the control. These results show the variation of the position and the number of fluorine atoms on the peripheral phenyl rings leads to a drastic change of mesomorphism. Especially, the thermal stability of the columnar mesophase are extremely stabilized over 400 ºC in **C8(3F)E-TP** and **C8(3F5F)E-TP**, for which peripheral phenylene groups are fluorinated at the outer positions, while the corresponding inner fluorinated homologues exhibit relatively low thermal stability of mesomorphism. It is quite interesting that mesomorphic properties are drastically change by the tiny difference of the position in fluorination on peripheral aromatic rings. Those results strongly indicate that a certain attractive force works around the fluorinated phenylene moieties. However, it is difficult to think that there is significant interactions between intra-columnar by XRD result of **C8(3F)E-TP** and **C8(3F5F)E-TP**. Therefore, it is reasonable to think that these highly stability of mesomorphism for **C8(3F)E-TP** and **C8(3F5F)E-TP** were induced by very strong inter-columnar interaction owing to fluorination at outer position on peripheral phenyl moieties.

Thermal stability of mesophase over 400 ºC has been reported only for the compounds having a large π-conjugation systems, such as hexabenzocolonenes,[3-4] carbonatious mesophase,[5-12] and metarophtalocyanines.[13] However, in calamitic liquid crystals, no report has been seen such that fluorination of aromatic rings so drastically enhances the mesomorphic thermal stability.[14-19] Therefore, these results indicate other factors affected by such fluorination should be considered rather than the change of electronic state.

Table 2-3 Phase transition properties of **C8(2F)E-TP**, **C8(2F6F)E-TP**, **C8(3F)E-TP**, **C8(3F5F)E-TP**, **C8(2F5F)E-TP**, **C8H4E-TP** and **C8F4E-TP**.

Compound	Phase transition temperature / °C (ΔH / kJmol^{-1})
C8(2F)E-TP	Cr_1 82.3 (12.6) Cr_2 120 (15.0) Cr_3 150 (28.3) N_D 213 (0.8) Iso
C8(2F6F)E-TP	Cr_1 53.2 (18.1) Cr_2 116 (60.9) M 176 (23.0) Iso
C8(3F)E-TP	Cr_1 56.1 (3.6) Cr_2 196 (3.1) Col_{r1} 210 (0.6) Col_{r2} 237 (0.7) Col_{r3} 400< Dec[†]
C8(3F5F)E-TP	Cr_1 14.7 (5.3) Cr_2 140 (11.1) Col_h 400< Dec[†]
C8(2F5F)E-TP	Cr 90.0 (21.8) Col_r 25.7 (10.2) Iso
C8H4E-TP	Cr 149 (21.7) Col_r 170 (7.2) N_D 242 (0.3) Iso
C8F4E-TP	Cr 133 (6.2) Col_h 308 (28.4) Iso

[†]: Dec: Decomposition.

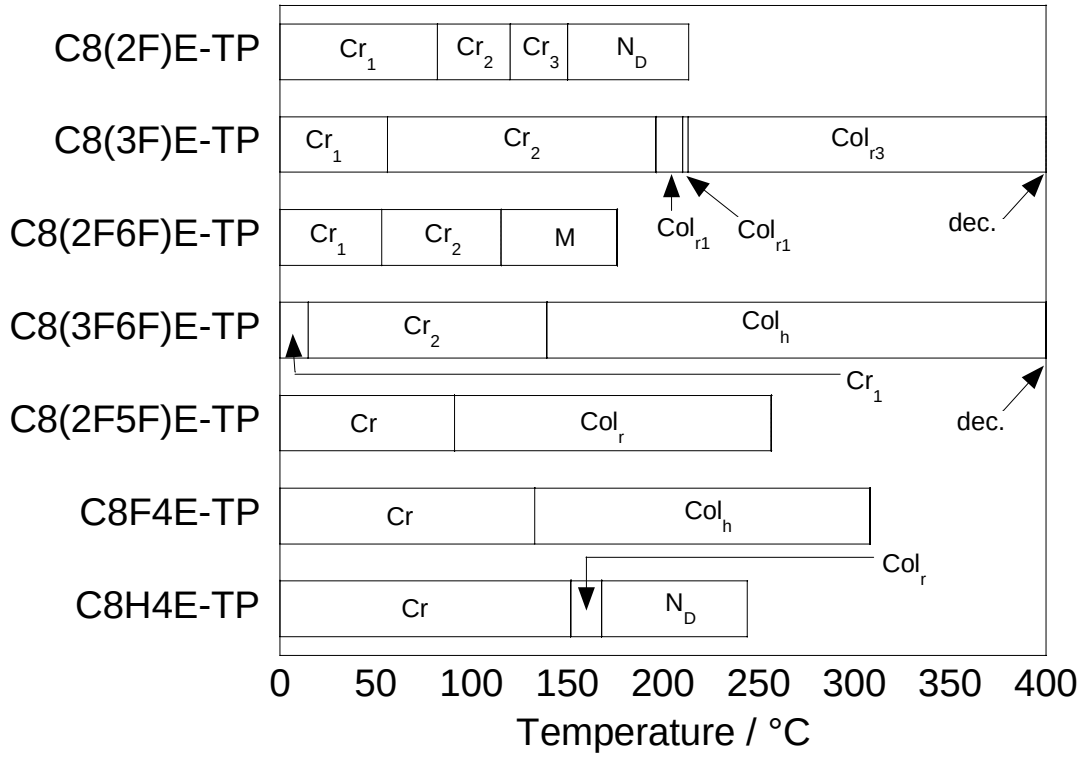

Figure 2-12 The mesomorphic behavior of **C8(2F)E-TP**, **C8(2F6F)E-TP**, **C8(3F)E-TP**, **C8(3F5F)E-TP**, **C8(2F5F)E-TP**, **C8H4E-TP** and **C8F4E-TP**.

On the other hand, the thermal stabilities of the mesophases for **C8(2F)E-TP** and **C8(2F6F)E-TP**, for which peripheral phenylene groups are fluorinated at the inner positions are decreased in comparison with **C8H4E-TP** and **C8F4E-TP**, which are non-fluorinated or fully-fluorinated homologues. This lower thermal stability may be due to the non-coplanarity of the phenyl ring to the carbonyl sp^2 plane probably derived from an electrostatic repulsive force between the strongly electro-negative fluorine and carbonyl oxygen atoms. However, **C8(2F6F)E-TP** exhibits a highly ordered mesophase from XRD measurement. These results indicate that a certain interaction is brought by di-fluorinated phenyl moiety at inner position. The thermal stability of the mesophase for **C8(2F5F)E-TP**, for which peripheral phenylene groups are fluorinated at the inner and the outer positions locate between the inner (**C8(2F)E-TP** and **C8(2F6F)E-TP**) and outer (**C8(3F)E-TP** and **C8(3F5F)E-TP**) derivatives.

Mesomorphic summaries indicate that the fluorination at peripheral phenylene rings of 2,3,6,7,10,11-hexakis(4-alkoxybenzoyloxy)triphenylenes induce columnar mesophase or highly ordered mesophase, without **C8(2F)E-TP**, while the corresponding non-fluorinated homologue (**C8H4E-TP**) shows a strong tendency to form a N_D phase accompanied with a Colr phase. These results of mesomorphism strongly indicate that there is a certain attractive interaction between intra- or inter-columns owing to fluorination on peripheral aromatic rings.

2-4. Conclusion

Hexakis (4-octyloxybenzoyloxy) triphenylene derivatives with mono- or di-fluorinated at the inner (2- and/or 6- [**C8(2F)E-TP**, **C8(2F6F)E-TP**]), outer (3- and/or 5- [**C8(3F)E-TP**, **C8(3F5F)E-TP**]) or inner and outer (2- and 5- [**C8(2F5F)E-TP**] positions in the peripheral aromatic rings were synthesised and investigated on the mesomorphic behaviour to reveal the alteration of fluorinated positions in the phenyl rings leads to a drastic change of the mesomorphism involving the thermal stability.

Their mesomorphism show the variation of the position and the number of fluorine atoms on the

peripheral phenyl rings leads to a drastic change of mesomorphism. Especially, the thermal stability of the columnar mesophase are extremely stabilized over 400 ºC in **C8(3F)E-TP** and **C8(3F5F)E-TP**, for which peripheral phenylene groups are fluorinated at the outer positions. On the other hand, the thermal stabilities of the mesophases for **C8(2F)E-TP** and **C8(2F6F)E-TP**, for which peripheral phenylene groups are fluorinated at the inner positions are decreased in comparison with **C8H4E-TP** and **C8F4E-TP**, which are non-fluorinated or fully-fluorinated homologues.

2-5. References

[1] N. H. Tinh, H. Gasparoux, C. Destrade, *Mol. Cryst. Liq. Cryst.*, 1981, **68**, 101.

[2] A. M. Levelut, *J. Phys. Lett.*, **1979**, 81.

[3] P. Herwig, C. W. Kayser, K. Müllen, H. W. Spiess, *Adv. Mater*. **1996**, 8, 510.

[4] S. Ito, M. Wehmeier, J. D. Brand, C. Kübel, R. Epsch, J. P. Rabe, and K. Müllen, *Chem. Eur. J*., **2000**, 6, 4327.

[5] J. D. Brooks and G. H. Taylor, *Carbon*, **1965**, 3, 185.

[6] J. L. White, G. L. Guthrie and J. O. Gardner, *Carbon*, **1967**, 5, 517.

[7] H. Honda, K. Kimura, Y. Sanada, S. Sugiwara and T. Furuta, *Carbon*, **1970**, 8, 151.

[8] T. Imamura, M. Nakamoto, and H. Honda, *Carbon*, **1978**, 16, 487.

[9] T. Imamura, Y. Yamada, S. Oi, and H. Honda, *Carbon*, **1978**, 16, 481.

[10] C. A. Kovac and I. C. Lewis, *Carbon*, **1978**, 16, 433.

[11] T. Imamura and M. Nakamoto, *Carbon*, **1979**, 17, 507.

[12] K. J. Huttinger, *Bitumen Teele Asphatlte*, 1973, **24**, 255.

[13] M. K. Engel, P. Bassoul, L. Bosio, H. Lehmann, M. Hanack and J. Simon, *Liq. Cryst*., **1993**, 15, 709.

[14] A. S. Matharu, S. J. Cowling and G. Wright, *Liq. Cryst*., **2007**, 34, 489.

[15] S. J. Cowling, K. J. Toyne and J. W. Goodby, *J. Mater. Chem.*, **2001**, 11, 1590.

[16] P. Balkwill, D. Bishop, A. Pearson and I. Sage, *Mol. Cryst. Liq. Cryst.*, 1985, **123**, 1.

[17] G. W. Gray and S. M. Kelly, *Mol. Cryst. Liq. Cryst.*, 1981, **75**, 109.

[18] M. Chambers, R. Clemitson, D. Coates, S. Greenfield, J. A. Jenner and I. C. Sage, *Liq. Cryst.*, 1989, **5**, 153.

[19] G. W. Gray, M. Hird and K. J. Toyne, *Mol. Cryst. Liq. Cryst.*, 1991, **195**, 221.

Chapter 3

Mesomorphic properties of

4-alkoxy-2,3,5,6-tetrafluorobenyloxytriphenylens

3-1. Introduction

In Chapter 1, it is reported that the fluorination on the peripheral phenyl groups for hexakis (4-alkoxybenzoyloxy) triphenylene derivatives induces a remarkable change of mesomorphism, for example inducement of columnar mesophase, drastic enhancement of thermal stability and so on, while the corresponding non-fluorinated homologues predominately exhibit a discotic nematic (N_D) phase.[1]

For the further studies of fluorination effect for discotic liquid crystals, hexakis (4-alkoxybenzyloxy) triphenylene derivatives (**CnF41O-TP**s, as shown Figure 3-1), of which the methyleneoxy linkage is less bulky and more flexible in comparison to the ester one, were synthesised (as shown Scheme 3-1) and investigated on the mesomorphic behaviour to reveal the alteration of molecular structure leads to a change of the mesomorphism and thus the corresponding ester homologues were compared in mesomorphism. The identification of these compounds was carried out by ^{1}H-NMR, ^{19}F-NMR, FT-IR and elemental analyses. And the mesomorphic behaviour was investigated by texture observations with a polarized optical microscopy (POM), DSC measurements and a X-ray diffraction technique.

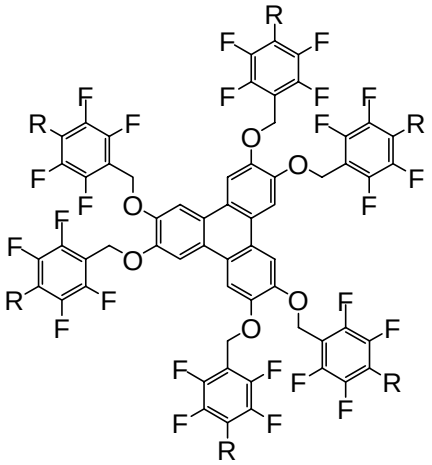

C6F41O-TP: R=-OC_6H_{13}

C8F41O-TP: R=-OC_8H_{17}

C10F41O-TP: R=-$OC_{10}H_{21}$

Figure 3-1 Chemical structure of **CnF41O-TP**.

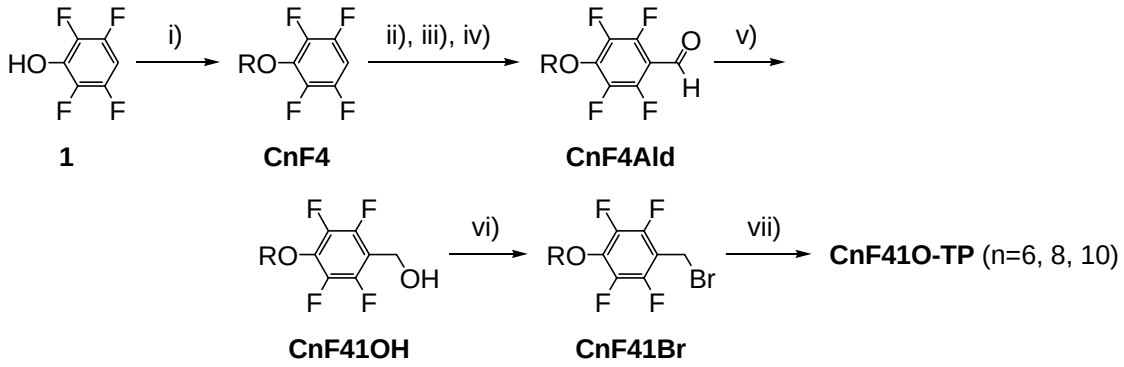

Scheme 3-1 Synthetic route of **CnF41O-TP** (n= 6, 8, 10): i) RBr, K_2CO_3, TBAB, MEK, reflux; ii) *n*-BuLi/Hex., THF, -78 °C; iii) EtOCHO, -78 °C; iv) Na_2CO_3*aq*, rt.; v) Me_2NH-BH_3, AcOH, rt.; vi) PBr_3, Et_2O; vii) 2,3,6,7,10,11-hexahydroxytriphenylene, K_2CO_3, TBAB, MEK, reflux.

3-2. Experimental

3-2-1. General measurement

^{1}H-NMR spectra were observed at 500.0 MHz on JEOL ECA500 FT-NMR spectrometer using $CDCl_3$ as solvent. Tetrametylsilane was used internal standard.^{19}F-NMR spectra were observed at 470.6 MHz on the same spectrometer.

3-2-2. Measurement of mesomorphism

The phase transition temperatures and enthalpies of the compounds were measured by differential scanning calorimetry (DSC, TA instrument DSC2920) for 5-10 mg samples of the freshly recrystallised materials at a scanning rate of 5 °Cmin^{-1}. Microscopic observations of the optical texture of mesophase were observed by a polarized microscope (Olympus BH2) equipped with hot stage (Mettler FP90). The mesophases were identified by a X-ray diffraction (Rigaku, RINT-2000) for the non-arraigned sample in the mesophase temperature ranges.

3-2-3. Synthesis

3-2-3-1. 2,3,5,6-tetrafluorohexyloxybenzene (C6F4)

A solution of bromohexane 14.9 g (90.3 mmol) in 2-butanone (40 mL) was added into the suspension mixture of K_2CO_3 12.5 g (90.3 mmol), 2,3,5,6-tetrafluorophenol (**1**) 15.0 g (90.3 mmol) and

tetrabutylammonium bromide 2.9 g (9.0 mmol) in 2-buanone (80 mL), and it was stirred and at refluxed for 4 h. Distillated water (100 mL) and diethyl ether were added to the reaction mixture at room temperature, and the separated organic layer was washed with brine (100 mL) and dried over anhydrous $MgSO_4$. The solution removed under reduced pressure and the residue was purified by column chromatography on silica gel (eluate: hexane) to yield 21.6 g (86.3 mmol) of **C6F4** as colourless liquid, yield 95.6 %. ^{1}H-NMR ($CDCl_3$, TMS, 500.0 MHz) δ 0.92 (t, J = 7.0 Hz, 3H), 1.27–1.36 (m, 4H), 1.47 (quintet, J = 7.5 Hz, 2H), 1.78 (quintet, J = 8.0 Hz, 2H), 4.22 (t, J = 6.5 Hz, 2H), 6.74 (tt, $^3J_{HF}$ = 10.0 Hz, $^4J_{HF}$ = 3.0 Hz 1H); ^{19}F-NMR ($CDCl_3$, $CFCl_3$, 470.0 MHz), δ –140.8 (dd, $^3J_{FF}$ = 14.8 Hz, $^4J_{FF}$ = 8.9 Hz, 2F), –157.6 (td, $^3J_{FF}$ = 13.6 Hz, $^4J_{FF}$ = 7.1 Hz 2F).

3-2-3-2. 4-hexyloxy-2,3,5,6-tetrafluorobenzaldehyde (C6F4Ald)

90 mL (144 mmol) of *n*-BuLi hexane solution (1.60 molL^{-1}) was added into the solution of 3-hexyloxy-1,2,4,5-tetrafluorobenzene (**C6F4**) 30.0 g (120.0 mmol) in dry THF (120 mL) at –78 ºC, and the reaction mixture was stirred for 2 h at –78 ºC. Ethyl formate 17.8 g (240 mmol) was added into reaction mixture and it was warmed up to room temperature. A saturated aqueous solution of sodium carbonate (100 mL) and diethyl ether (100 mL) were added into the reaction mixture, and the separated organic layer was washed with brine (100 mL) and dried over anhydrous $MgSO_4$. The solvent was removed under reduced pressure to yield 36.9 g of residue containing **C6F4Ald** as colourless liquid, which was used without further purification. ^{1}H-NMR ($CDCl_3$, TMS, 500.0 MHz) δ 0.88 (t, J = 7.0 Hz, 3H), 1.28–1.36 (m, 4H), 1.46 (quintet, J = 7.6 Hz, 2H), 1.81 (quintet, J = 7.9 Hz, 2H), 4.41 (t, J = 6.6 Hz, 2H), 10.2 (s, 1H); ^{19}F-NMR ($CDCl_3$, $CFCl_3$, 470.0 MHz), δ –146.8 (dd, $^3J_{FF}$ = 25.8 Hz, $^4J_{FF}$ = 10.9 Hz, 2F), –157.7 (dd, $^3J_{FF}$ = 23.2 Hz, $^4J_{FF}$ = 10.9 Hz 2F).

3-2-3-3. 4-hexyloxy-2,3,5,6-tetrafluorophenylmethanol (C6F41OH)

Borane dimethylamine complex 8.5 g (144 mmol) was added into a solution of 36.9 g of the residue containing **C6F4Ald** in acetic acid (300 mL) at room temperature, and the reaction mixture was stirred for 2 h at room temperature. The solvent was removed under reduced pressure, and $CHCl_3$ (100 mL) was

added into the residue. The organic layer was washed with saturated aqueous solution of sodium bicarbonate (100 mL) brine (100 mL) and dried over anhydrous $MgSO_4$. The solvent was removed under reduced pressure to yield 42.5 g of residue containing **C6F41OH** as colourless liquid, which was used without further purification. ^{1}H-NMR ($CDCl_3$, TMS, 500.0 MHz) δ 0.91 (t, J = 7.3 Hz, 3H), 1.32–1.36 (m, 4H), 1.46 (quintet, J = 7.9 Hz, 2H), 1.77 (quintet, J = 8.0 Hz, 2H), 2.33 (s, *OH*), 4.22 (t, J = 6.8 Hz, 2H), 4.76 (s, 2H); ^{19}F-NMR ($CDCl_3$, $CFCl_3$, 470.0 MHz), δ –146.5 (dd, $^3J_{FF}$ = 21.8 Hz, $^4J_{FF}$ = 10.9 Hz, 2F), –157.8 (dd, $^3J_{FF}$ = 21.8 Hz, $^4J_{FF}$ = 10.9 Hz 2F).

3-2-3-4. 4-hexyloxy-2,3,5,6-tetrafluorophenylbromomethane (C6F41Br)

A solution of phosphorus tribromide 32.5 g (120 mmol) in diethyl ether 25 mL was added into a solution of 42.5 g of the residue containing **C6F41OH** in diethyl ether (100 mL) at 0 °C, and the reaction mixture was stirred for 1 h at room temperature. The reaction mixture was poured into an ice water, and the separated organic layer was washed with saturated aqueous solution of sodium bicarbonate (100 mL) brine (100 mL) and dried over anhydrous $MgSO_4$. The solution removed under reduced pressure and the residue was purified by column chromatography on silica-gel (eluate; hexane:CH_2Cl_2=1:1) to yield 25.9 g (75.5 mmol) of **C6F41Br** as colourless liquid, yield 62.9 % (from **C6F4**). ^{1}H-NMR ($CDCl_3$, TMS, 500.0 MHz) δ 0.91 (t, J = 6.3 Hz, 3H), 1.32–1.35 (m, 4H), 1.47 (quintet, J = 8.0 Hz, 2H), 1.78 (quintet, J = 7.9 Hz, 2H), 4.24 (t, J = 6.3 Hz, 2H), 4.50 (s, 2H); ^{19}F-NMR ($CDCl_3$, $CFCl_3$, 470.0 MHz), δ –144.9 (dd, $^3J_{FF}$ = 23.2 Hz, $^4J_{FF}$ = 8.2 Hz, 2F), –157.4 (dd, $^3J_{FF}$ = 21.8 Hz, $^4J_{FF}$ = 10.9 Hz 2F).

3-2-3-5. 2,3,6,7,10,11-hexakis(4-hexyloxy-2,3,5,6-tetrafluorobenzyloxy)triphenylene (C6F41O-TP)

A solution of 4-hexyloxy-2,3,5,6-tetrafluorophenylbromomethane (**C6F41Br**) 10.3 g (30.0 mmol) was added into a suspension mixture of 2,3,6,7,10,11-hexahydorxytriphenylene (1.0g, 3.0 mmol), K_2CO_3 8.3 g (60.0 mmol) and tetrabutylammonium bromide 0.97 g (3.0 mmol) in 2-buanone (100 mL) and it was stirred at refluxed for 24 h. Distillated water (100 mL) and diethyl ether were added to the reaction mixture at room temperature, and the separated organic layer was washed with brine (100 mL) and dried over

anhydrous $MgSO_4$. The solution removed under reduced pressure and the residue was purified by column chromatography on silica gel (eluate: $CHCl_3$ followed by recrystallization using toluene (200 mL) and 2-propanol (800 mL) to yield 2.5 g (1.32 mmol) of **C6F41O-TP** as colourless crystaline solid (yield=43.9 %). ^{1}H-NMR ($CDCl_3$, TMS, 500.0 MHz) δ 0.89 (t, J = 6.8 Hz, 18H), 1.31–1.35 (m, 24H), 1.45 (quintet, J = 8.0 Hz, 12H), 1.77 (quintet, J = 8.1 Hz, 12H), 4.23 (t, J = 6.5 Hz, 12H), 5.40 (s, 12H), 7.97 (s, 6H); ^{19}F-NMR ($CDCl_3$, $CFCl_3$, 470.0 MHz), δ –144.7 (dd, $^3J_{FF}$ = 20.4 Hz, $^5J_{FF}$ = 6.8 Hz, 12F), –157.7 (td, $^3J_{FF}$ = 21.8 Hz, $^5J_{FF}$ = 9.6 Hz, 12F); Anal. Calc. for $C_{96}H_{96}F_{24}O_{12}$: C, 60.76; H, 5.10; F, 24.03 %. Found: C, 60.99; H, 5.09; F, 23.80 %.

3-2-3-6. 3-octyloxy-1,2,4,5-tetrafluorobenzene (C8F4)

Following the method employed for the synthesis of **C6F4**, 32.9 g (118.5 mmol, yield=98.4 %) of **C8F4** was obtained as colourless liquid by using 1-bromooctane as the starting material. ^{1}H-NMR ($CDCl_3$, TMS, 500.0 MHz) δ 0.80 (t, J = 6.8 Hz, 3H), 1.26–1.38 (m, 8H), 1.46 (quintet, J = 7.5 Hz, 2H), 1.78 (quintet, J = 6.6 Hz, 2H), 4.21 (t, J = 6.4 Hz, 2H), 6.74 (tt, $^3J_{HF}$ = 10.2 Hz, $^4J_{HF}$ = 2.9 Hz 1H); ^{19}F-NMR ($CDCl_3$, $CFCl_3$, 470.0 MHz), δ –140.9 (dd, $^3J_{FF}$ = 24.6Hz, $^5J_{FF}$ = 13.6 Hz, 2F), –157.7 (td, $^3J_{FF}$ = 30.0 Hz, , $^5J_{FF}$ = 19.1 Hz 2F).

3-2-3-7. 4-octyloxy-2,3,5,6-tetrafluorobenzaldehyde (C8F4Ald)

C8F4Ald was synthesised by following the method described in the synthesis of **C6F4Ald**, 37.1 g of residue containing **C8F4Ald** was obtained as colourless liquid by using 3-octyloxy-1,2,4,5-tetrafluorobenzene (**C8F4**) as the starting material. It was used without further purification. ^{1}H-NMR ($CDCl_3$, TMS, 500.0 MHz) δ 0.89 (t, J = 7.3 Hz, 3H), 1.26–1.34 (m, 8H), 1.46 (quintet, J = 7.9 Hz, 2H), 1.81 (quintet, J = 6.6 Hz, 2H), 4.41 (t, J = 6.4 Hz, 2H), 10.2 (s, 1H); ^{19}F-NMR ($CDCl_3$, $CFCl_3$, 470.0 MHz), δ –146.8 (dd, $^3J_{FF}$ = 21.8 Hz, $^4J_{FF}$ = 10.9 Hz, 2F), –157.7 (d, $^3J_{FF}$ = 24.5 Hz, 2F).

3-2-3-8. 4-octyloxy-2,3,5,6-tetrafluorophenylmethanol (C8F41OH)

Following the procedure employed for the synthesis of **C6F41OH**, 43.7 g of residue containing

C8F41OH was obtained as colourless liquid by using 4-octyloxy-1,2,4,5-tetrafluorobenzaldehyde (**C8F4Ald**) as the starting material. It was used without further purification. ^{1}H-NMR ($CDCl_3$, TMS, 500.0 MHz) δ 0.89 (t, J =6.8 Hz, 3H), 1.29–1.33 (m, 8H), 1.46 (quintet, J = 6.6 Hz, 2H), 1.77 (quintet, J = 7.7 Hz, 2H), 2.33 (s, *OH*), 4.21 (t, J = 6.6 Hz, 2H), 4.76 (d, J = 5.5 Hz, 2H); ^{19}F-NMR ($CDCl_3$, $CFCl_3$, 470.0 MHz), δ –146.9 (d, $^{3}J_{FF}$ = 21.8 Hz, 2F), –157.7 (dd, $^{3}J_{FF}$ = 21.8 Hz, $^{5}J_{FF}$ = 10.9 Hz 2F).

3-2-3-9. 4-octyloxy-1,2,4,5-tetrafluorophenylbromomethane (C8F41Br)

Following the method described in the synthesis of **C6F41Br**, 33.6 g (90.4 mmol, yield=76.3% from **C8F4**) of **C8F41Br** was obtained as colourless liquid by using 4-octyloxy-1,2,4,5-tetrafluorophenylmethanol (**C8F41OH)** as the starting material. ^{1}H-NMR ($CDCl_3$, TMS, 500.0 MHz) δ 0.89 (t, J = 8.2 Hz, 3H), 1.29–1.34 (m, 8H), 1.46 (quintet, J = 7.0 Hz, 2H), 1.78 (quintet, J = 8.0 Hz, 2H), 4.24 (t, J = 6.4 Hz, 2H), 4.50 (d, J = 1.10 Hz, 2H); ^{19}F-NMR ($CDCl_3$, $CFCl_3$, 470.0 MHz), δ –144.9 (dd, $^{3}J_{FF}$ = 21.8 Hz, $^{5}J_{FF}$ = 10.9 Hz, 2F), –157.4 (dd, $^{3}J_{FF}$ = 21.8 Hz, $^{5}J_{FF}$ = 10.9 Hz 2F).

3-2-3-10. 2,3,6,7,10,11-hexakis(4-octyloxy-2,3,5,6-tetrafluorobenzyloxy)triphenylene (C8F41O-TP)

Following the procedure described in the synthesis of **C6F41O-TP**, 4.01 g (1.94 mmol, yield=64.7%) of **C8F41Br** was obtained as colourless crystalline solid by using 4-octyloxy-1,2,4,5-tetrafluorophenylbromomethane (**C8F41Br)** as the starting material. ^{1}H-NMR ($CDCl_3$, TMS, 500.0 MHz) δ 0.88 (t, J = 7.4 Hz, 18H), 1.27–1.31 (m, 48H), 1.45 (quintet, J = 6.5 Hz, 12H), 1.77 (quintet, J =7.7 Hz, 12H), 4.22 (t, J = 6.5 Hz, 12H), 5.40 (s, 12H), 7.98 (s, 6H); ^{19}F-NMR ($CDCl_3$, $CFCl_3$, 470.0 MHz), δ –144.6 (dd, $^{3}J_{FF}$ = 20.4 Hz, $^{5}J_{FF}$ = 9.5 Hz, 12F), –157.7 (d, $^{3}J_{FF}$ = 20.5 Hz, 12F) ; Anal. Calc. for $C_{108}H_{120}F_{24}O_{12}$: C, 62.78; H, 5.85; F, 22.07 %. Found: C, 63.03; H, 6.04; F, 22.09 %.

3-2-3-11. 3-decyloxy-1,2,4,5-tetrafluorobenzene (C10F4)

Following the method shown in the synthesis of **C6F4**, 36.8 g (120.0 mmol, yield=99.2 %) of **C10F4** was obtained as colourless liquid by using 1-bromooctane as the starting material. ^{1}H-NMR ($CDCl_3$, TMS,

500.0 MHz) δ 0.89 (t, J = 7.0 Hz, 3H), 1.28–1.37 (m, 12H), 1.46 (quintet, J = 8.0 Hz, 2H), 1.78 (quintet, J = 7.0 Hz, 2H), 4.22 (t, J = 6.0 Hz, 2H), 6.74 (tt, $^3J_{HF}$ = 10.0 Hz, $^4J_{HF}$ = 4.5 Hz 1H); ^{19}F-NMR ($CDCl_3$, $CFCl_3$, 470.0 MHz), δ –140.9 (dd, $^3J_{FF}$ = 18.8 Hz, $^3J_{HF}$ = 14.1 Hz, 2F), –157.7 (dd, $^3J_{FF}$ = 23.5 Hz, $^3J_{HF}$ = 14.1 Hz, 2F).

3-2-3-12. 4-decyloxy-2,3,5,6-tetrafluorobenzaldehyde (C10F4Ald)

Following the procedure shown in the synthesis of **C6F4Ald**, 41.2 g of residue containing **C10F4Ald** was obtained as colourless liquid by using 3-decyloxy-1,2,4,5-tetrafluorobenzene (**C10F4**) as the starting material. It was used without further purification. ^{1}H-NMR ($CDCl_3$, TMS, 500.0 MHz) δ 0.88 (t, J = 7.0 Hz, 3H), 1.28–1.34 (m, 12H), 1.46 (quintet, J = 7.6 Hz, 2H), 1.81 (quintet, J = 7.9 Hz, 2H), 4.41 (t, J = 6.5 Hz, 2H), 10.2 (s, 1H); ^{19}F-NMR ($CDCl_3$, $CFCl_3$, 470.0 MHz), δ –146.8 (dd, $^3J_{FF}$ = 25.8 Hz, $^4J_{FF}$ = 10.9 Hz, 2F), –157.7 (dd, $^3J_{FF}$ = 23.2 Hz, $^4J_{FF}$ = 10.9 Hz, 2F).

3-2-3-13. 4-decyloxy-2,3,5,6-tetrafluorophenylmethanol (C10F41OH)

C10F41OH was synthesised by the method employed for the synthesis of **C6F41OH**, 49.1 g of residue containing **C10F41OH** was obtained as colourless liquid by using 4-octyloxy-1,2,4,5-tetrafluorobenzaldehyde (**C10F4Ald**) as the starting material. It was used without further purification. ^{1}H-NMR ($CDCl_3$, TMS, 500.0 MHz) δ 0.89 (t, J =6.8 Hz, 3H), 1.29–1.33 (m, 12H), 1.46 (quintet, J = 6.6 Hz, 2H), 1.77 (quintet, J = 7.7 Hz, 2H), 2.33 (s, *OH*), 4.21 (t, J = 6.6 Hz, 2H), 4.76 (d, J = 5.5 Hz, 2H); ^{19}F-NMR ($CDCl_3$, $CFCl_3$, 470.0 MHz), δ –146.9 (d, $^3J_{FF}$ = 21.8 Hz, 2F), –157.7 (dd, $^3J_{FF}$ = 21.8 Hz, $^5J_{FF}$ = 10.9 Hz 2F).

3-2-3-14. 4-decyloxy-1,2,4,5-tetrafluorophenylbromomethane (C10F41Br)

Following the way employed for the synthesis of **C6F41Br**, 25.5 g (63.9 mmol, yield=53.2 % from **C10F4**) of **C10F41Br** was obtained as colourless liquid by using 4-decyloxy-1,2,4,5-tetrafluorophenylmethanol (**C10F41OH)** as the starting material. ^{1}H-NMR ($CDCl_3$, TMS, 500.0 MHz) δ 0.88 (t, J = 6.6 Hz, 3H), 1.28–1.35 (m, 12H), 1.45 (quintet, J = 7.7 Hz, 2H), 1.77 (quintet, J = 7.9 Hz, 2H), 4.24 (t, J = 6.5 Hz, 2H), 4.49 (s, J = 1.10 Hz, 2H); ^{19}F-NMR ($CDCl_3$, $CFCl_3$,

470.0 MHz), δ –144.9 (dd, $^{3}J_{FF}$ = 21.8 Hz, $^{5}J_{FF}$ = 10.9 Hz, 2F), –157.4 (dd, $^{3}J_{FF}$ = 21.8 Hz, $^{5}J_{FF}$ = 10.9 Hz 2F).

3-2-3-15. 2,3,6,7,10,11-hexakis(4-decyloxy-2,3,5,6-tetrafluorobenzyloxy)triphenylene (C10F41O-TP)

Following the way shown in the synthesis of **C6F41O-TP**, 3.67 g (1.64 mmol, yield=54.7 %) of **C10F41O-TP** was obtained as colourless crystalline solid by using 4-decyloxy-1,2,4,5-tetrafluorophenylbromomethane (**C10F41Br)** as the starting material. ^{1}H-NMR ($CDCl_3$, TMS, 500.0 MHz) δ 0.88 (t, J = 6.8 Hz, 18H), 1.27–1.34 (m, 72H), 1.44 (quintet, J = 7.8 Hz, 12H), 1.77 (quintet, J =8.0 Hz, 12H), 4.23 (t, J = 6.5 Hz, 12H), 5.40 (s, 12H), 8.00 (s, 6H); ^{19}F-NMR ($CDCl_3$, $CFCl_3$, 470.0 MHz), δ –144.6 (d, $^{3}J_{FF}$ = 19.1 Hz, 12F), –157.6 (d, $^{3}J_{FF}$ = 20.4 Hz, 12F) ; Anal. Calc. for $C_{108}H_{120}F_{24}O_{12}$: C, 62.78; H, 5.85; F, 22.07 %. Found: C, 63.03; H, 6.04; F, 22.09 %.

3-3. Results and discussion

3-3-1. DSC measurement

The DSC curves of all homologues synthesised are shown in Figure 3-2~3-4. In the DSC curves of **C6F41O-TP** (Figure 3-2), two endothermic peaks were observed on the first heating run at 8.9 °C and 198 °C with phase transition enthalpies (ΔH) of 2.7 and 54.7 kJmol^{-1}, respectively. However on the first cooling run, there comes up only one exothermic peak at 195 °C (ΔH: 48.1 kJmol^{-1}), and a peak corresponding to the melting point disappeared. On the second heating process, there were two endothermic peaks at 4.2 and 196 °C with the transition enthalpies of 0.73 and 50.5 kJ/mol, respectively. POM observations of the optical texture indicated the mesophase might be frozen glassy solid on cooling, though the T_g could not be detected on the DSC curves.

In the DSC curves of **C8OF41O-TP**, two endothermic peaks were observed at 4.9 °C and 190 °C (4.9 and 55.4 kJmol^{-1}, respectively) on the first heating run, and two exothermic peaks were observed on the

first cooling run at 189 °C and -1.1 °C with the phase transition enthalpies (ΔH) of 51.3 and 1.3 kJmol^{-1}, respectively.

For **C10F41O-TP**, one peak (at 186 C: ΔH =56.4 kJmol^{-1}) and one inflection point (at 1.8 °C) were observed on the first heating runs. It is the same situation that one peak and one inflection point were observed at 183 °C (ΔH: 50.0 kJmol^{-1}) and -1.2 °C. These inflection points show a glass transition takes place. This may indicate that the peripheral decyloxy groups could be bulky for packing, and these could not fix their position in a way of crystalline solid on cooling.

On the result of DSC measurement for all homologues, it is difficult to observe distinct transition behavior of crystalline state. Therefore, these results indicate that **CnF41O-TP** (n=6, 8, 10) tend not to form a crystalline state.

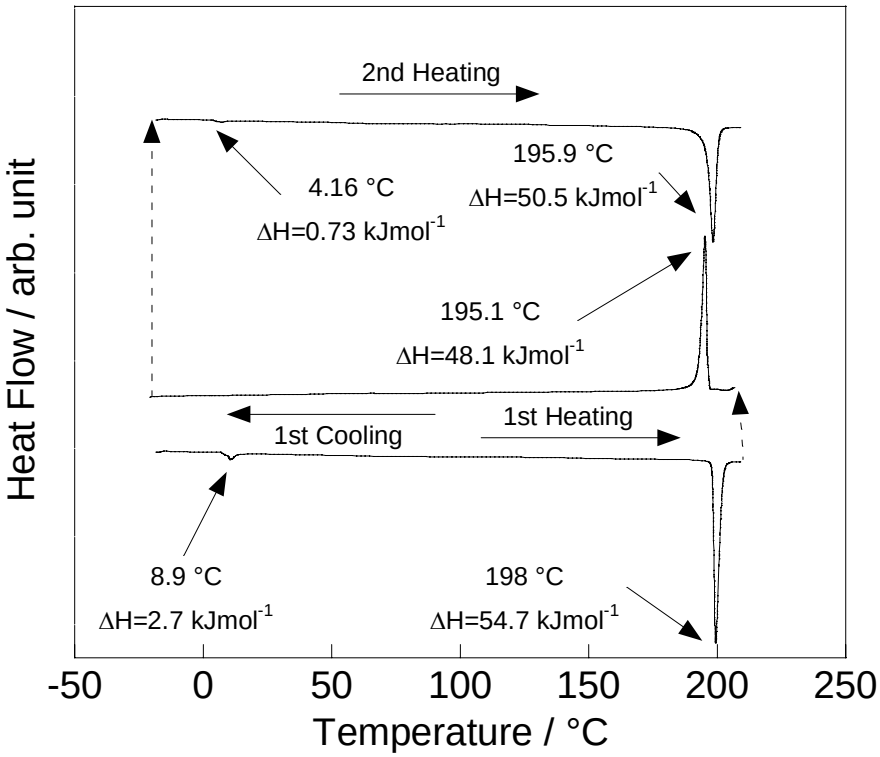

Figure 3-2 DSC curves of **C6F41O-TP** (rate: 5 °C min^{-1}).

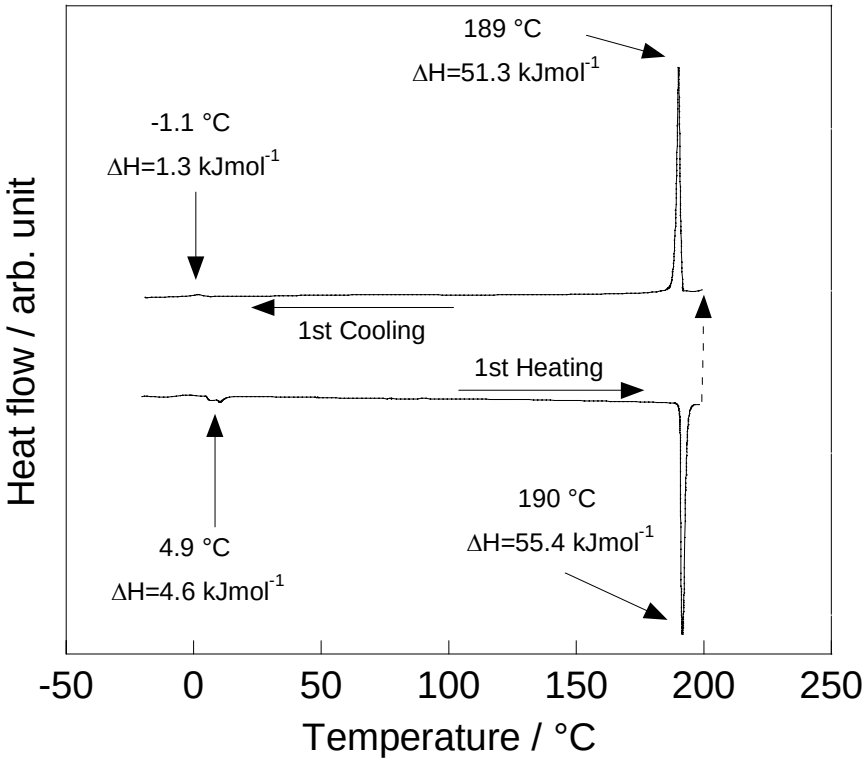

Figure 3-3 DSC curves of **C8F41O-TP** (rate: 5 °C min^{-1}).

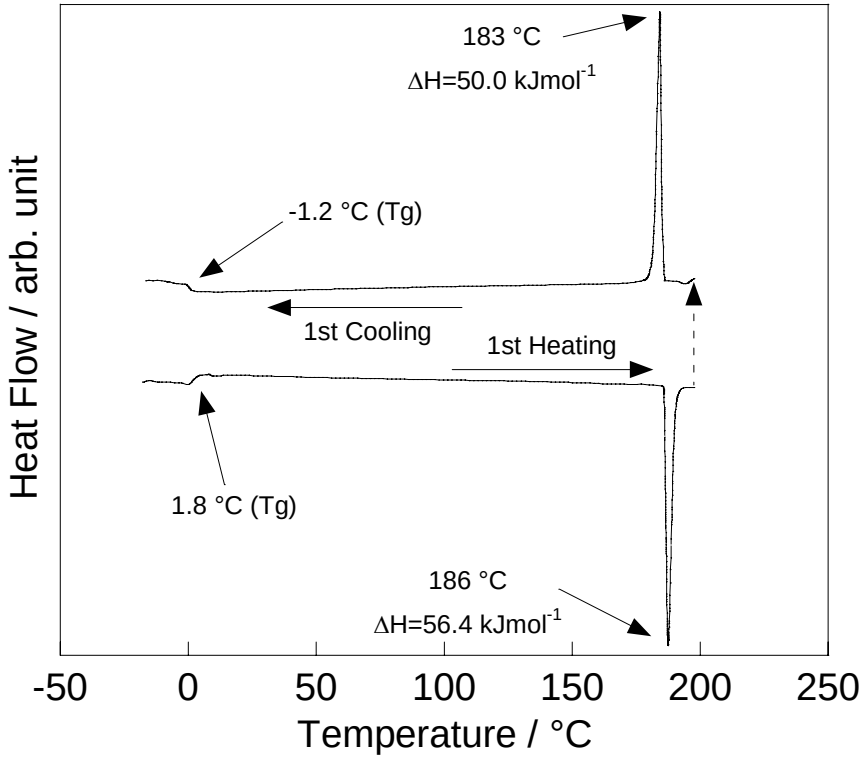

Figure 3-4 DSC curves of **C10F41O-TP** (rate: 5 °C min^{-1}).

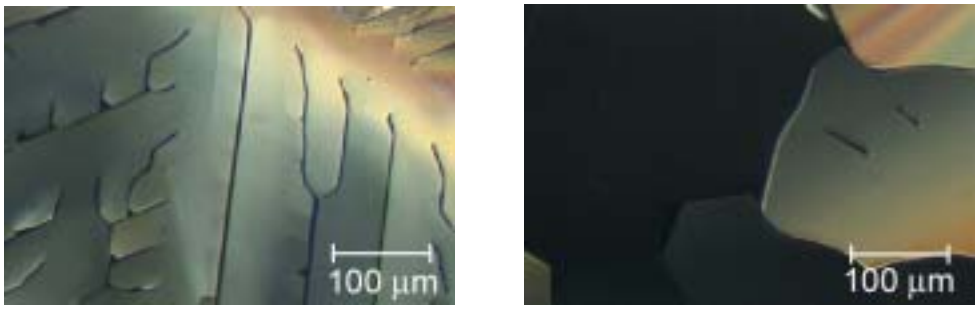

Figure 3-5 Optical textures of the mesophase for **C6F4E-TP** (left; at 180 °C) and **C8F41O-TP** (right; at 180 °C).

3-3-2. Polarized optical microscope observation

The polarized optical microscopic images of **C6F41O-TP** and **C8F41O-TP** are shown in Figure 3-5. Both compounds exhibit a dendric texture containing dark domains, indicating an optical uniaxiality of mesophase.

3-3-3. X-ray diffraction patterns

X-ray diffraction patterns of the mesophase for all compounds (for the non-aligned sample) are shown in Figure. 3-6, 3-7 and 3-8. For **C6F41O-TP**, several sharp reflections are shown at 160 °C having the spacing of 26.6, 15.0, 13.0, 9.7, 8.6, 7.4, 7.1 and 6.4 Å (Figure 3-6), corresponding to a set of the spacing ratio, 1 : 1/√3 : 1/2 : 1/√7 : 1/3 : 1/√12 : 1/√13 : 1/4, which are an evidence of a hexagonal arrangement of molecularly stacking columns. Furthermore, two halos at 5.1, 4.2 and 3.6 Å were observed in the wide-angle region. These halos centered at 5.1 Å could be assigned to the averaged molecular width of a tetrafluorophenyl moiety, according to the estimated molecular width of the molecular model (4.7-5.1 Å) by calculation using Chem3D (AM1),[2] and the halos at 4.2 Å 3.5 Å could be related to the averaged diameter of molten alkyl chains[3] and the π-π stacking distance of triphenylene cores in a column, respectively.

For the mesophases at 160 °C of **C8F41O-TP** and **C10F41O-TP** the same sets of sharp reflections were shown which have a spacing ratio of 1 : 1/√3 : 1/2 : 1/√7 : 1/3 : 1/√12 : 1/√13 : 1/4, meaning the mesophase

has a hexagonal arrangement of columns. And their halos at 5.1, 4.3 and 3.6 Å were also observed in the wide-angle region. These halos at 5.1 Å could be assigned to be the averaged molecular width of a tetrafluorophenyl moiety, and 4.3 Å could be related to the averaged diameter of molten alkyl chains, and the halo at 3.5 Å is derived from the π-π stacking periodicity of triphenylene cores in a column.

The XRD measurements of all compounds show sharp reflection peaks in the small angle region, which imply a tight long-range arrangement of columns, probably due to the rigid column structures.

The results of X-ray diffraction measurements of **CnF41O-TP**s are summarized in Table 3-1~Table 3-3. The hexagonal lattice constants ($a_{hex.}$) slightly increase with the elongation of the peripheral chains and show the similar correlation to those of other triphenylene mesogens exhibiting a hexagonal columnar phase and the observed $a_{hex.}$ are almost 70-80 % of the molecular diameters evaluated by the molecular models using AM-1.

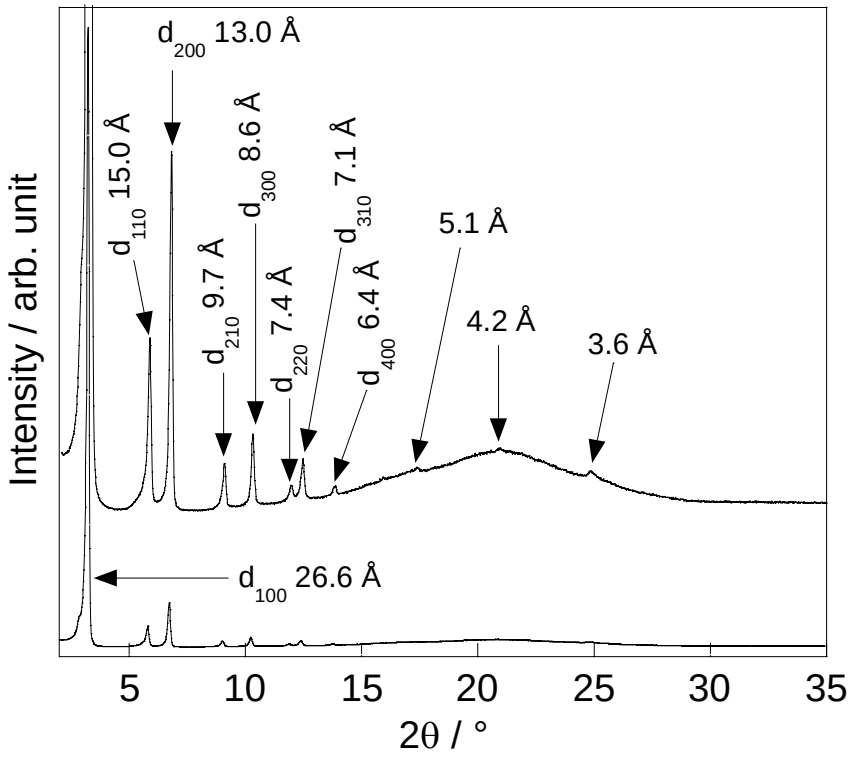

Figure 3-6 X-ray diffraction pattern of **C6F41O-TP** at 160 ºC.

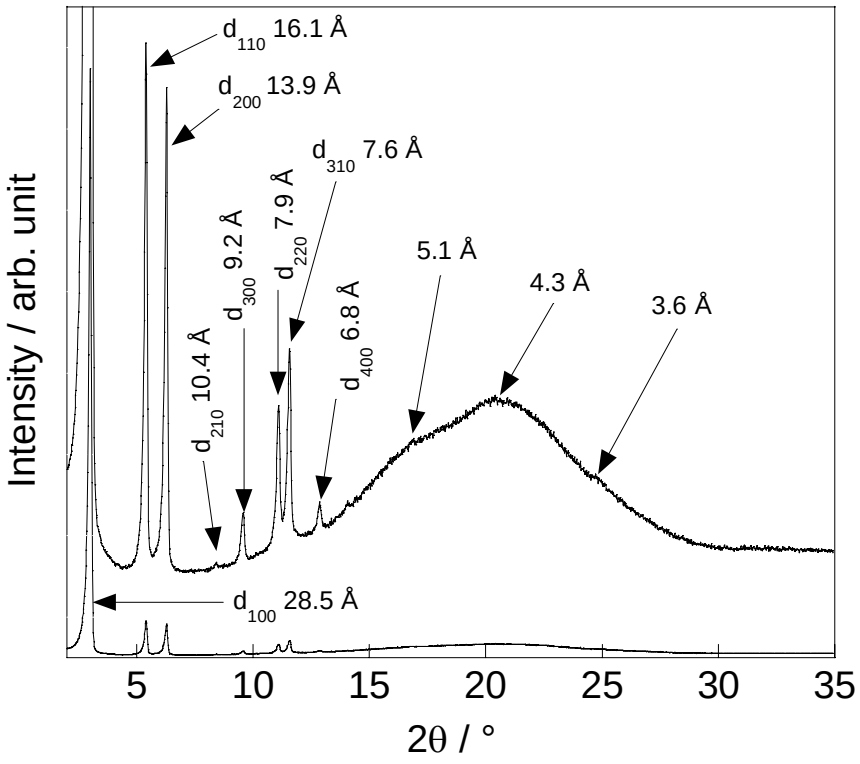

Figure 3-7 X-ray diffraction pattern of **C8F41O-TP** at 160 ºC.

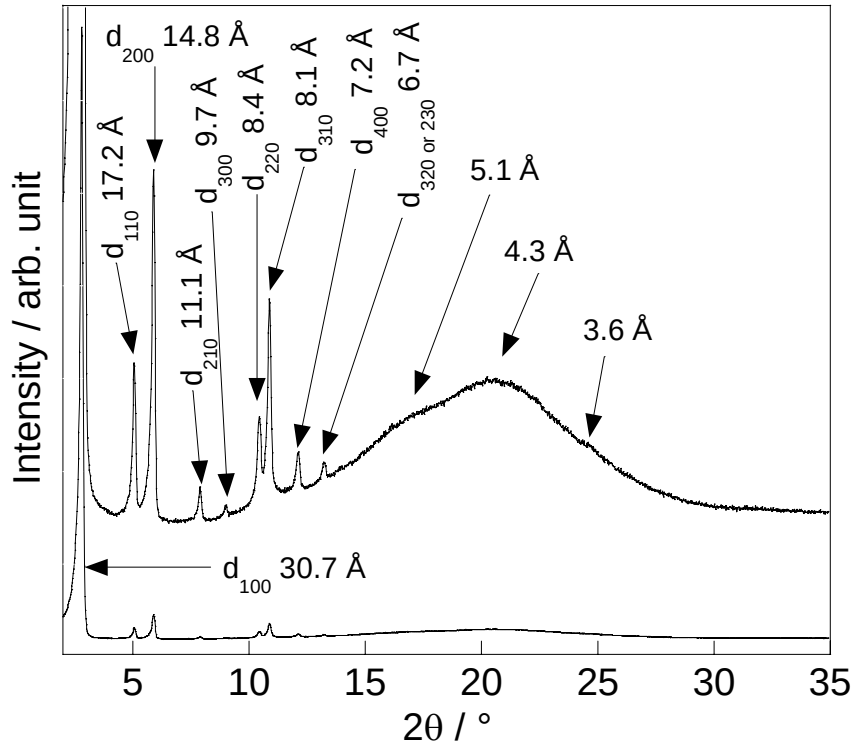

Figure 3-8 X-ray diffraction pattern of **C10F41O-TP** at 160 ºC.

Table 3-1 X-ray diffraction parameters for the mesophase of **C6F41O-TP**.

Compound	Lattice constant / Å	Molecular diameters / Å[††]	*hlk*	d_{hkl}/Å	
				Observed	Calculated
C6F41O-TP	30.0	36.2	100	26.6	26.0
(160 °C)	Z=0.5[†]		110	15.0	15.0
			200	13.0	13.0
			210	9.7	9.8
			300	8.6	8.7
			220	7.4	7.5
			310	7.1	7.2
			400	6.4	6.5
				5.1 (br) [†††]	
				4.2 (br)	
				3.6 (br)	

[†]: Calculated from the lattice constants *a*, correlation length along the *c*-axis (3.5 Å) and the postulated density ρ (1.0 g cm^{-3});[††]: calculated by AM-1; [†††]: br=Broad.

Table 3-2 X-ray diffraction parameters for the mesophase of **C8F41O-TP**.

Compound	Lattice constant / Å	Molecular diameters / Å[†]	*hlk*	d_{hkl}/Å	
				Observed	Calculated
C8F41O-TP	32.2	40.1	100	28.5	27.9
(160 °C)	Z=0.5[†]		110	16.1	16.1
			200	13.9	14.0
			210	10.4	10.5
			300	9.2	9.3
			220	7.9	8.1
			310	7.6	7.7
			400	6.8	7.0
				5.1 (br)[†††]	
				4.3 (br)	
				3.6 (br)	

[†]: Calculated from the lattice constants *a*, correlation length along the *c*-axis (3.5 Å) and the postulated density ρ (1.0 g cm^{-3});[††]: calculated by AM-1; [†††]: br=Broad.

Table 3-3 X-ray diffraction parameters for the mesophase of **C10F41O-TP**.

Compound	Lattice constant / Å	Molecular diameters / Å[†]	*hlk*	d_{hkl}/Å	
				Observed	Calculated
C10F41O-TP	34.4	45.0	100	30.7	29.8
(160 °C)	Z=0.5[†]		110	17.2	17.2
			200	14.8	14.9
			210	11.1	11.2
			300	9.7	9.9
			220	8.4	8.6
			310	8.1	8.3
			400	7.2	7.4
			320or 230	6.7	6.8
				5.1 (br) [†††]	
				4.3 (br)	
				3.6 (br)	

[†]: Calculated from the lattice constants *a*, correlation length along the *c*-axis (3.5 Å) and the postulated density ρ (1.0 g cm^{-3});[††]: calculated by AM-1; [†††]: br=Broad.

Table 3-4 Phase transition temperatures of **CnF41O-TP**s.

Compounds	Phase transition temperature / °C (ΔH: $kJmol^{-1}$ [ΔS: $Jmol^{-1}K^{-1}$])
C6F41O-TP	Cr 8.9 (2.7 [9.6]) Col_h 198 (54.7 [116]) Iso
C8F41O-TP	Cr 4.9 (4.6 [16.5]) Col_h 190 (55.4 [119]) Iso
C10F41O-TP	G 1.8 Col_h 186 (56.4 [122]) Iso
C6F4E-TP	Cr_1 130 (1.9 [4.7]) Cr_2 157 (3.6 [8.4]) Col_h 301 (25.4 [44.2]) Iso
C8F4E-TP	Cr 133 (6.2 [15.3]) Col_h 308 (28.4 [48.9]) Iso
C10F4E-TP	Cr 109 (5.1 [13.3]) Col_h 302 (26.2 [45.6]) Iso

3-3-4. Comparison of the mesomorphism

The phase transition parameters of 4-alkoxy-2,3,5,6-tetrafluorobenzyloxytriphenylenes (**CnF41O-TP**s) are summarised in Table 3-4 with those of the corresponding ester homologues (**CnF4E-TP**s). All compounds exhibit only a Col_h mesophase and this is the similar mesomorphism of the corresponding ester homologues (**CnF4E-TP**s). The clearing points of **CnF41O-TP**s slightly decrease as the peripheral chain length increases, while those for **CnF4E-TP**s exhibit almost an independent property of the peripheral chain length. The isotropification temperatures of **CnF41O-TP**s are decreased in comparison with **CnF4E-TP**s. This destabilization of the Col_h phase is probably due to the higher flexibility of ether linkage than ester one. However, the phase transition enthalpies of the clearing points for **CnF41O-TP**s are larger (over almost 50 $kJmol^{-1}$) than those of **CnF4E-TP**s. Furthermore, the phase transition entropies of the clearing point are much larger (over almost 100 $Jmol^{-1}K^{-1}$) than those of **CnF4E-TP**s. For example, ΔH of clearing point for hexabenzocoronenes[4] and metallophthalocyanines[5-7] having large π-conjugation systems were determined to be 7.8 and 9.6 $kJmol^{-1}$, respectively. Additionally, it have been reported that isotropification enthalpy (ΔH) of discotic plastic crystalline (Colp) phase which have three dimensional order alignment of columns is 18.9 $kJmol^{-1}$.[8-11] So these highly value of transition enthalpy (ΔH) and entropy (ΔS) show that column structures of Col_h phase for **CnF41O-TP**s are probably rigid. Furthermore, the XRD measurements of **CnF41O-TP**s, which show sharp reflection peaks in the small angle region, also support that the molecular dynamics in Col_h phase of **CnF41O-TP**s may be restrained. Therefore, these result indicate that a triphenylene play a role of the core part involving the peripheral tetrafluorophenyl moieties and show a strong interaction works among the stacking molecules in the Col_h mesophase. It is difficult to observe that there is significant interactions between the tetrafluorophenyl and triphenylene moieties such as hexafluorobenzene-benzene interaction[12-16] on its column order by the XRD result. However, it is reasonable to consider that tetrafluorophenylene moiety could have strong interaction to each other.

In comparison with ester homologues, the improvement of molecular order in Col_h phase for

CnF41O-TPs may be caused by the change of electric state for tetrafluorophenyl groups owing to the alteration of linkage group ester to ether, though the thermal stabilities of mesomorphism are decrease.

3-4. Conclusions

A homologue series of novel 2,3,6,7,10,11-hexakis(4-alkoxy-2,3,5,6-tetrafluorobenzyloxy)triphenylenes were synthesized and investigated on the mesomorphic behavior. All compounds exhibit Col_h phase, similarly the corresponding ester homologues (**CnF4E-TP**s) show only a Col_h phase. The phase transition enthalpy and entropy of clearing point for **CnF41O-TP**s are much larger (ΔH: over almost 50 $kJmol^{-1}$, ΔS: over almost 100 $Jmol^{-1}K^{-1}$) than those of **CnF4E-TP**s as corresponding ester homologues, although the isotropic temperature of **CnF41O-TP**s are lower thane these of **CnF4E-TP**s. This indicate that the hexagonal columnar (Col_h) phase of **CnF41O-TP**s have a very higher ordered arrangement of molecules than these of **CnF4E-TP**s, which is supported by the X-ray diffraction result.

3-5. References

[1] N. H. Tinh, H. Gasparoux, C. Destrade, *Mol. Cryst. Liq. Cryst.*, 1981, **68**, 101.

[2] *CS Chem3D Ultra*, Cambridge soft (2001).

[3] A. M. Levelut, *J. Phys., Lett.*, **1979**, 81.

[4] W. Pisula, Ž. Tomovič, B. E. Hamaoui, M. D. Watson, T. Pakula, and K. Müllen, *Adv. Funct. Mater.*, **2005**, 15, 893.

[5] J. Santiago, T. Sugino, and Y. Shimizu, *Chem. Lett.*, **1998**, 661.

[6] J. Santiago, T. Sugino and Y. Shimizu, *Mol. Cryst. Liq. Cryst.*, 1999, **332**, 497.

[7] S. Tantrawong, T. Sugino, Y. Shimizu, A. Takeuchi, S. Kimura, T. Mori and H. Takezoe, *Liq. Cryst.*, 1998, **24**, 783.

[8] C. Destrade, M. C. Mondon and J. Malthete, *J. Phys. (paris), Suppl. 40*, 1979, **C3**, 17.

[9] N. Boden, R. C. Botner, R. J. Bushby, A. N. Cammidge, M. V. Jesudason, *Liq. Cryst.*, 1993, **15**, 851.

[10] J. Simmerer, B. Glüse, W. Paulus, A. Kettner, P. Schuhmacher, D. Adam, K. H. Etzbach, K. Siemensmeyer, J. H. Wendorff, H. Ringsdorf, and D. Haarer, *Adv. Mater*, **1996**, 8, 815.

[11] B. Glusen, A. Kettner, J. H. Wendorff, *Mol. Cryst. Liq. Cryst.*, 1997, **A303**, 115.

[12] E. G. Cox, D. W. Cruickshank and J. A. Smith, *Proc. Royal Soc. London, Ser. A.*, **1958**, 274, 1

[13] C. R. Patrick and G. S. Prosser, *Nature*, **187**, 1021, (1960)

[14] J. H. Williams, *Acc. Chem. Res.*, **1993**, 26, 593

[15] J. H. Williams, J. K. Cockcroft and A. N. Fitch, *Angew. Chem. Int. Ed.*, **1992**, 31, 1655.

[16] V. B. Smith and A. G. Massey, *Tetrahedron,* 1969, **61**, 4504.

Chapter 4

Charge transport properties of the discotic liquid crystals of triphenylene mesogens peripherally attached with fluorinated phenyl rings

4-1. Introduction

Columnar structures formed by molecular stacking are one of the important features of molecular orders for liquid crystalline semiconductors based on discotic liquid crystals. In 1994, Haarer et al. reported a first discovery of liquid crystalline semiconductors of which carrier mobility reaches to almost 0.1 $cm^2V^{-1}s^{-1}$ comparable to amorphous silicon[1] for a plastic columnar mesophase having a 3-dimentional order with a helical structure.[2, 3] Also indicated that the higher ordering within the columns in both orientational and dynamical aspects is essentially important for efficient charge transport in an electronic process (charge hopping among molecules).[4] Increasing the fluctuation modes of molecules in mesophase surely leads to decreasing the efficiency, that is the lower carrier mobility is recalled.[5-7]

In Chapter 1 and Chapter3, it is reported that full fluorination on peripheral aromatic rings of discotic liquid crystals induces columnar structures on the mesomorphism and enhances the thermal stability of mesophase with highly order structures. For further studies, a homologues series of 2,3,5,7,10,11-hexakis(4-alkoxy-2,3,5,6-tetrafluorobenzoyloxy)triphenylene (**CnF4E-TP**: n=12, 14, 16) and 2,3,5,7,10,11-hexakis(4-alkoxy-2,3,5,6-tetrafluorobenzyloxy)triphenylene (**CnF41O-TP**: n=6, 8, 10) were evaluated as organic semiconductor by a Time-Of-Flight (TOF) technique,[8] which is a strong tool to estimate the drift mobility. A carrier mobility is most important property in the consideration of device applications.

Furthermore, the spectroscopic properties of these compounds were measured using a UV-Vis spectrometer and a photoelectron spectrometer surface analyzer, and their energy levels, which are important values for TOF measurements were estimated with these results.

4-2. Experimental

4-2-1. Measurement of spectroscopic properties

The UV-Visible spectra were measured by a UV-Visible spectrometer (Shimadzu UV2500pc) for the ~10^{-5} $molL^{-1}$ of cyclohexane solution. The photoelectron spectra were measured by photoelectron spectrometer surface analyzer (Riken Keiki AC-2) for the film samples on ITO glass.

4-2-2. Measurement of charge transport properties

For **CnF4E-TP**s, the sample cell was prepared using an ITO-coated glass and a TiO_2-coated ITO glass as electrodes, the TiO_2 layer is expected to behave as a charge generation layer. For **CnF41O-TP**s, the sample cell was prepared using ITO-coated glasses as electrodes. The electrodes are separated with polyimide films (12.5 μm-thick) as a spacer and fixed with silicon cement. The photoresponse of the symmetrical and asymmetrical cells were undetectable. The thickness was determined by an interferometry using a UV-Visible spectrometer (Shimadzu UV2500pc). The effective area of electrode was adjusted to 0.25 cm^2 by etching the ITO thin film. The samples were injected into the cell gap by capillarity action at the isotropic temperatures, then carefully cooled down to room temperature. The carrier mobility was measured by a TOF method. A N_2 pulse laser (λ=337 nm; pulse width of 800 ps; Laser Phototyping Inc. LP1000) was used for the photo excitation of compounds. An electric field in the cell was created using a DC power supply (NF electronics instrument, WF1941). The transient photocurrents were detected by a digital oscilloscope (HP, infinum) with the help of a wide band preamplifer (NF electronics instrument, BX-31A). The mobility μ was calculated from the equation, $\mu = d^2 / (V\tau_s)$, where d, V, τ_s are the sample thickness, the applied bias and the transit time. The transit time of photogenerated carriers were determined in the inflection point on the double-lograithmic plots of photocurrent decay curves. The experimental apparatus of TOF measurement are schematically shown in Figure 4-1.

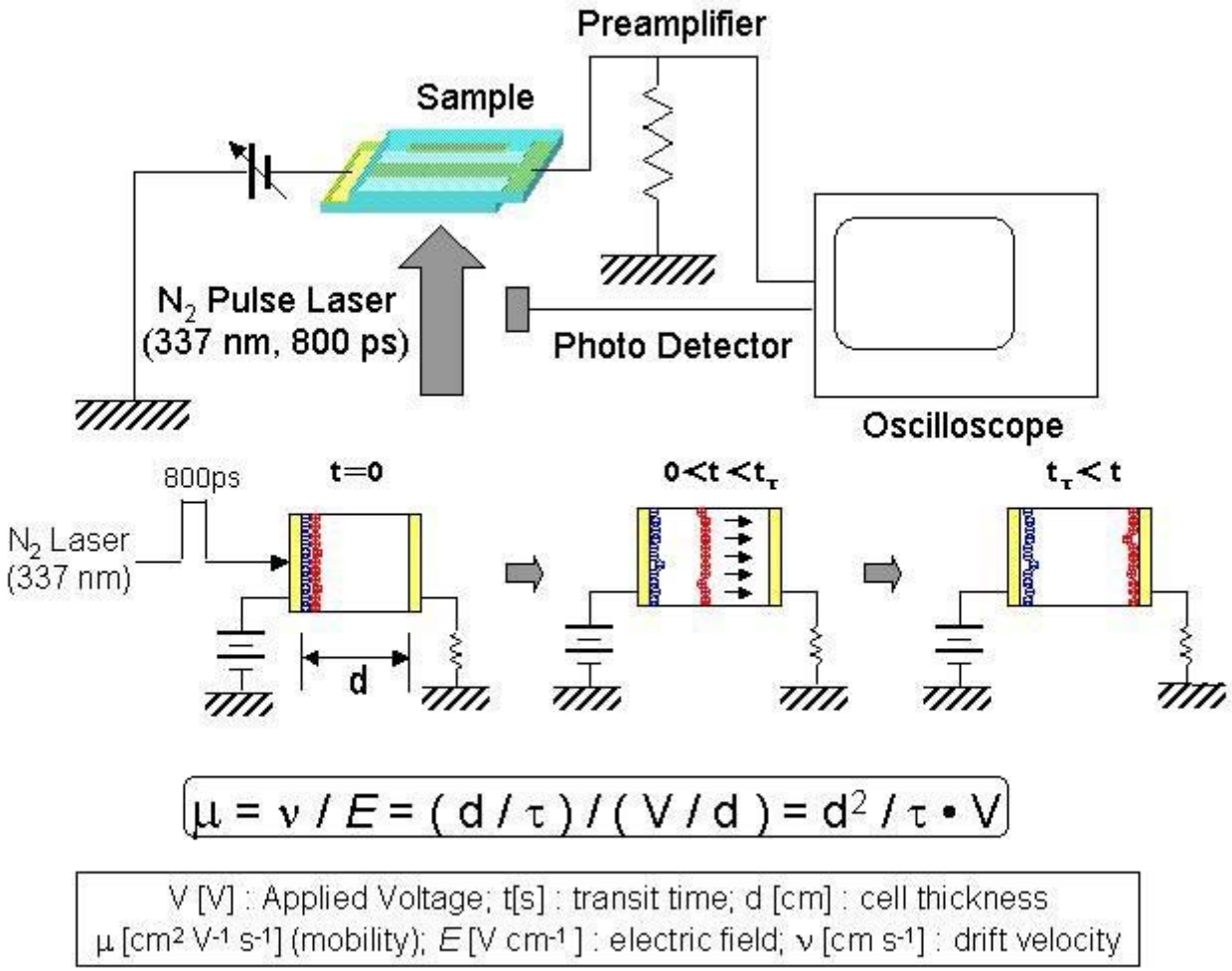

Figure 4-1 The experimental apparatus of TOF measurement.

4-3. Results and discussion

4-3-1. Electronic energy levels of the thin films

4-3-1-1. UV-Visible spectra

The UV-Vis. spectra of **CnF4E-TP**s are shown in Figure 4-2, with those of **C12H4E-TP** as the non-fluorinated homologue of **C12F4E-TP** for cyclohexane solutions.

One can see the absorptions of **CnF4E-TP**s and **C12H4E-TP** in the shorter wavelength region. The maximal absorption maxima for **CnF4E-TP**s are commonly observed at 253.5 nm, though 269.5 nm for non-fluorinated homologue. The UV-Vis. spectrum of hexakis-(4-dodecyloxybenzoyloxy)triphenylene is slightly shifted to the shorter wavelength by 16 nm due to the fluorination of the peripheral aromatic rings.

The UV-Vis. spectra of **CnF41O-TP**s are shown in Figure 4-3, with those of the ester homologue **CnF4E-TP**s for cyclohexane solution.

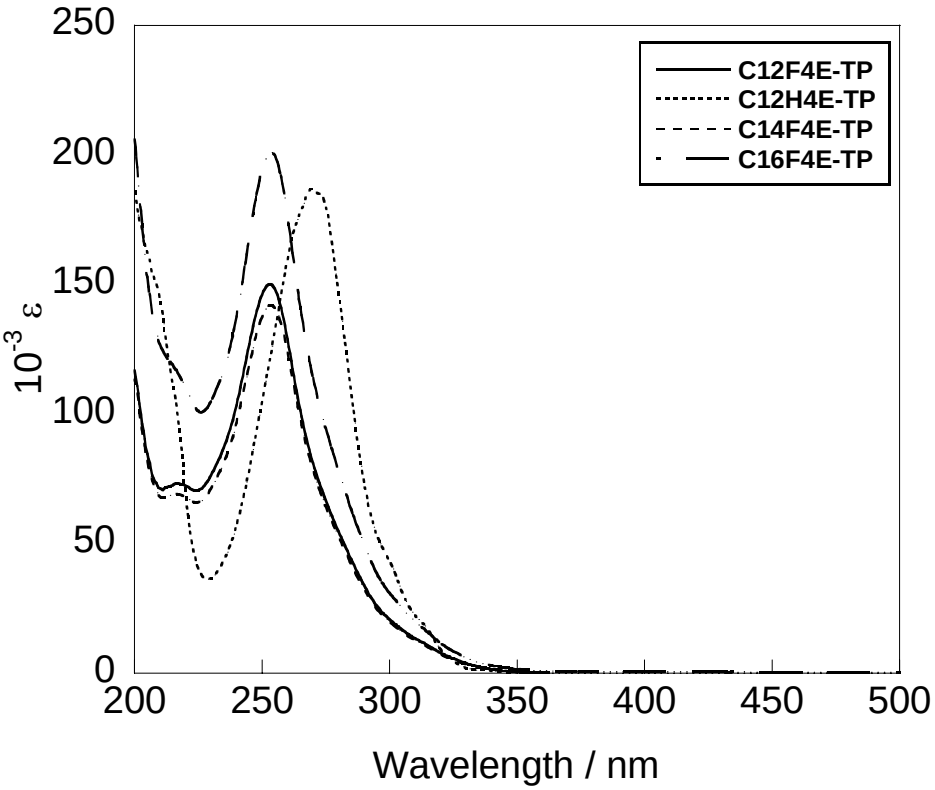

Figure 4-2 UV-Vis. spectra of **CnF4E-TP**s and **C12H4E-TP**.

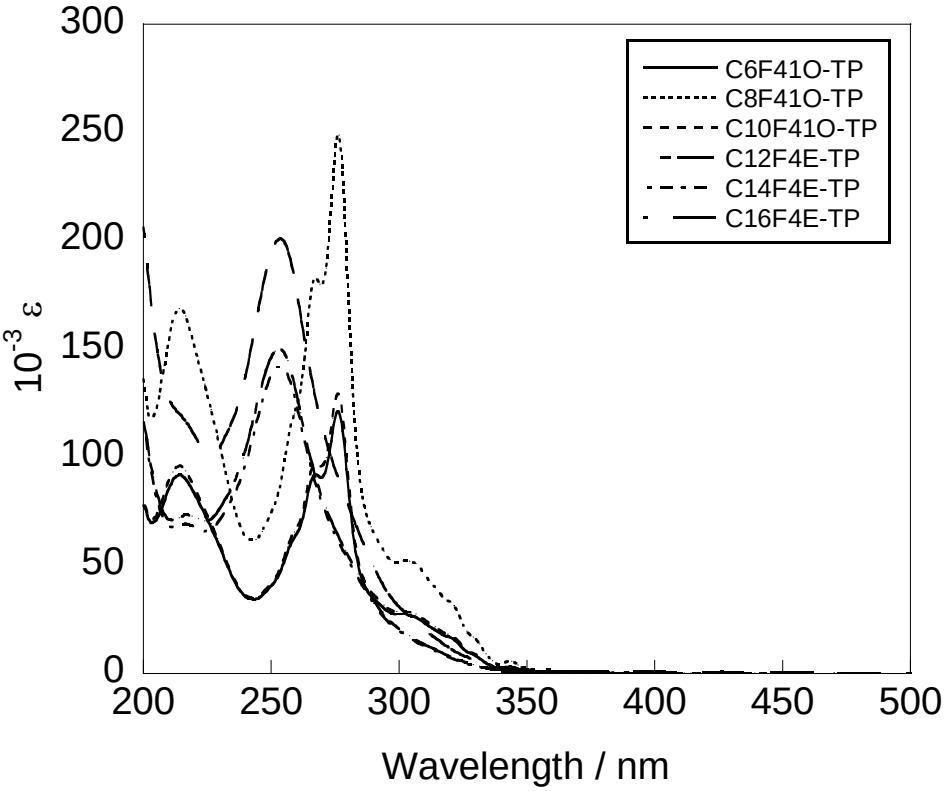

Figure 4-3 UV-Vis. spectra of **CnF41O-TP**s and **CnF4E-TP**s.

The absorption maxima for **CnF41O-TP**s commonly observed at 276 nm, though 253.5 nm for ester homologue. This result indicates that the UV-Vis. spectrum of 4-hexakis-(4-alkoxybenzoyloxy)triphenylene is shifted to the shorter wavelength by the alteration of linkage group ester to ether for triphenylene derivatives.

4-3-1-2. Electronic energy diagram of thin films

The energy diagram of **CnF4E-TP**s and **CnF41O-TP**s is shown in Figure 4-4, with the work function of ITO and TiO_2 on ITO used as the electrode and charge generation layer. The highest occupied molecular orbital (HOMO) energies of each compound were measured by a photoelectron spectrometer surface analyzer. The energy bandgaps (*Eg*) were estimated using the absorption edges of UV-Vis spectra, and the lowest unoccupied molecular orbital (LUMO) energies were calculated from the equation $E_{LUMO}=E_{HOMO}-Eg$.

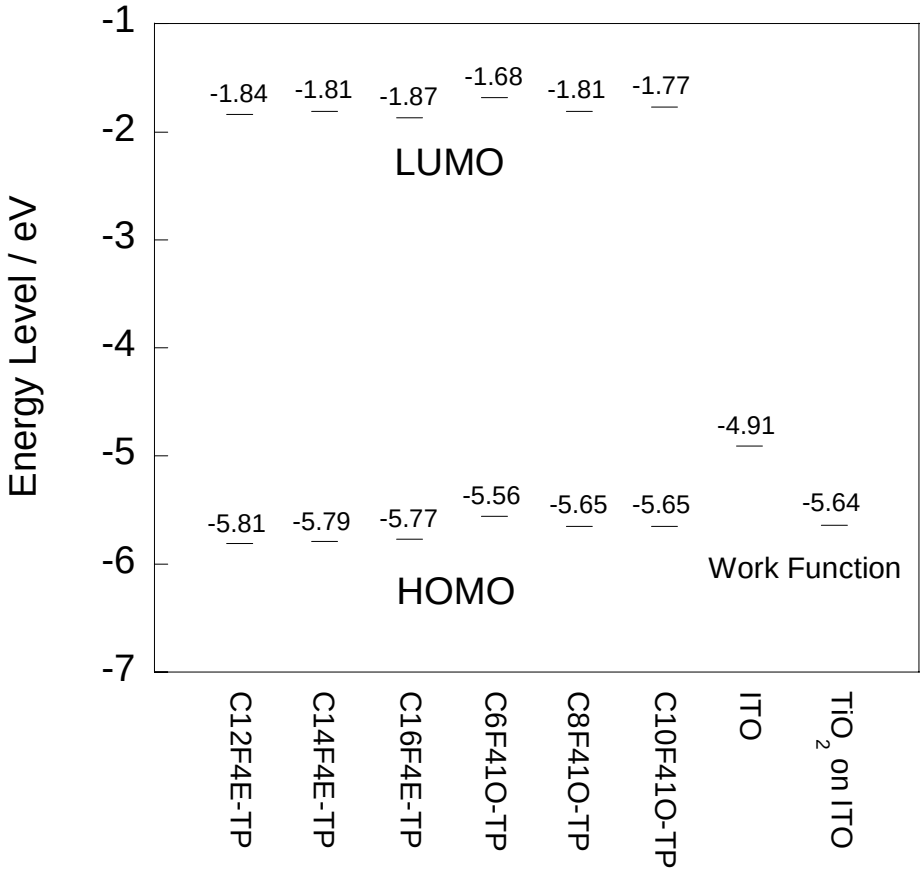

Figure 4-4 Energy diagram of **CnF4E-TP**s, **CnF4E-TP**s, ITO and TiO_2 on ITO.

The HOMO levels of **CnF41O-TP**s are relatively shallower than those of **CnF4E-TP**s. These changes were caused by the change of electronic contribution of tetrafluorophenyl groups owing to the alteration of linkage group, ester to ether. On TOF measurements, there may be not so large barrier for hole injection from ITO to **CnF4E-TP**s. **CnF4E-TP**s have deeper HOMO levels from that of ITO, although there is probably small barrier for hole injection to **CnF4E-TP**s, because TiO_2 is used for carrier generation layer, of which HOMO level lies more deeply (-5.64 eV).

4-3-2. Carrier transport properties

4-3-2-1. TOF measurements of CnF4E-TPs

The transient photocurrent decay curves for the positive carrier detected in the Col_h phase at 220 °C under different applied bias are shown in Figure 4-5, 4-6 and 4-7.

The transient photocurrent of **C12F4E-TP** shown well-defined non-dispersive transits. Furthermore, the inflection points of photocurrent decay curves could be also clearly determined on the double-logarithmic plots as shown in the inset of Figure 4-5. For **C14F4E-TP** and **C16F4E-TP**, the similar non-dispersive curves were observed in the transient photocurrent. The hole mobility was determined to be 2.6×10^{-3} $cm^2V^{-1}s^{-1}$ in $5\sim1\times10^4$ Vcm^{-1}. **C14F4E-TP** and **C16F4E-TP** also exhibited the same order of carrier mobility in the Col_h phase at 220 °C (**C14F4E-TP**: 3.9×10^{-3} $cm^2V^{-1}s^{-1}$; **C16F4E-TP**: 3.0×10^{-3} $cm^2V^{-1}s^{-1}$).The carrier mobility of **CnF4E-TP**s are almost independent of the electric field in the range 5~1 Vcm^{-1}, as shown in Figure 4-8. These field independent properties of carrier mobility are of typical for liquid crystalline semiconductors.[9]

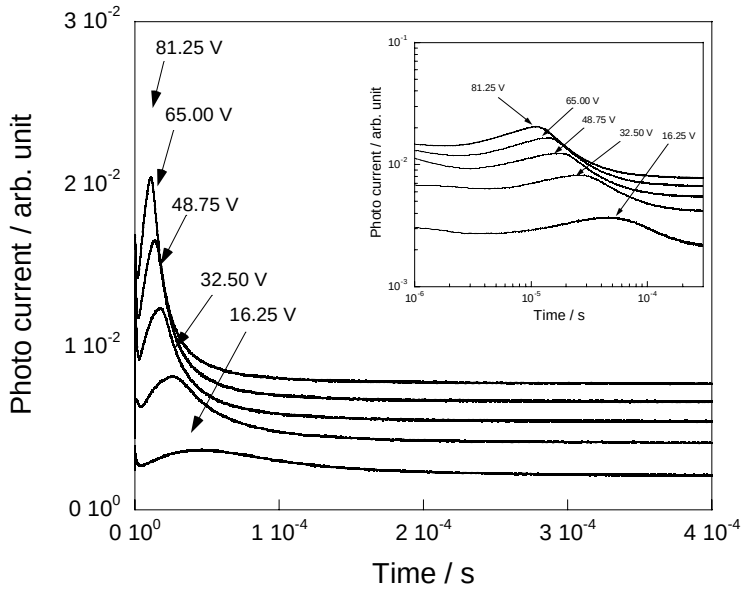

Figure 4-5 The transient photocurrents in the Col_h phase of **C12F4E-TP** at 220 °C for the positive carriers. The double logarithmic plots of the transient photocurrents in the variant electric field are shown in the inset. The sample thickness was 16.25 μm.

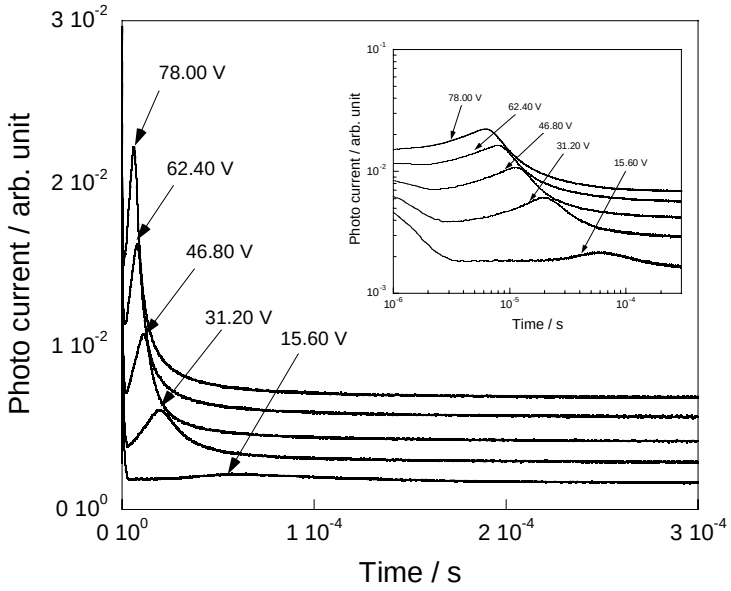

Figure 4-6 The transient photocurrents in the Col_h phase of **C14F4E-TP** at 220 °C for the positive carriers. The double logarithmic plots of the transient photocurrents in the variant electric field are shown in the inset. The sample thickness was 15.60 μm.

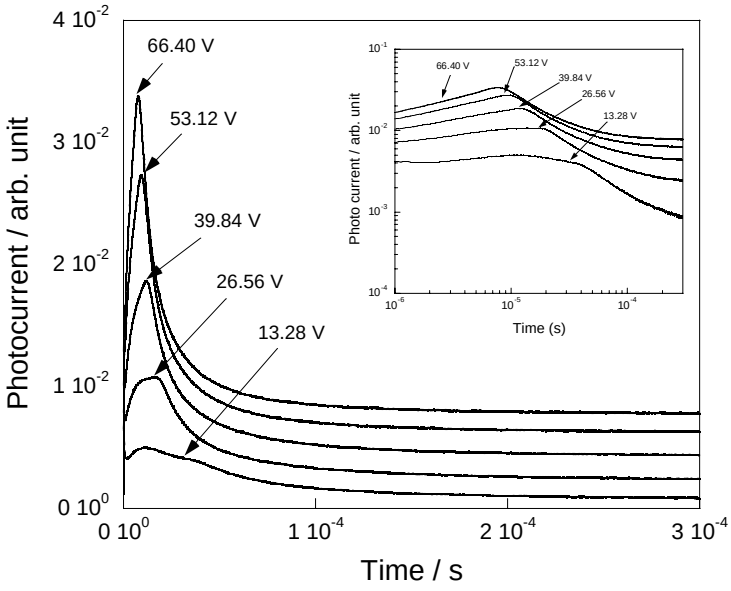

Figure 4-7 The transient photocurrents in the Col_h phase of **C16F4E-TP** at 220 °C for the positive carriers. The double logarithmic plots of the transient photocurrents in the variant electric field are shown in the inset. The sample thickness was 13.28 μm.

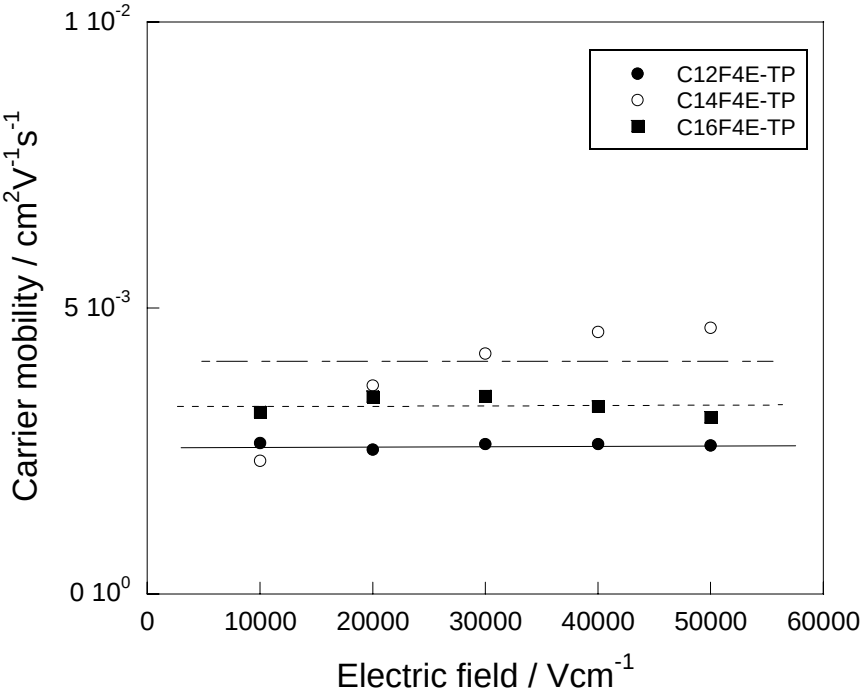

Figure 4-8 Electric field dependence of the carrier mobility of **CnF4E-TP**s at 220 °C.

4-3-2-2. Temperature dependence of carrier mobility for CnF4E-TPs

The temperature dependence of the positive carrier mobility for **C12F4E-TP** is shown in Figure 4-9. The positive carrier mobility of **C12F4E-TP** falls with the decrease of temperature and saturated, in the higher temperature region from 200 to 140 °C. The temperature dependence of carrier mobility, however, is changed at 140~150 °C and the carrier mobility more greatly falls with the decrease of temperature. The positive carrier mobility of **C12F4E-TP** is in order of 10^{-3} $cm^2V^{-1}s^{-1}$ in the higher temperature region (220-100 °C), and in order of 10^{-4} $cm^2V^{-1}s^{-1}$ in the lower (90-60 °C) temperature one. In **C16F4E-TP** and **C14F4E-TP**, almost the same temperature dependence was found (see Figure 4-10 and 4-11). The positive carrier mobility of **CnF4E-TP**s is to the similar order of that reported for the Col_h phase of hexaalkoxytriphenylenes.[10]

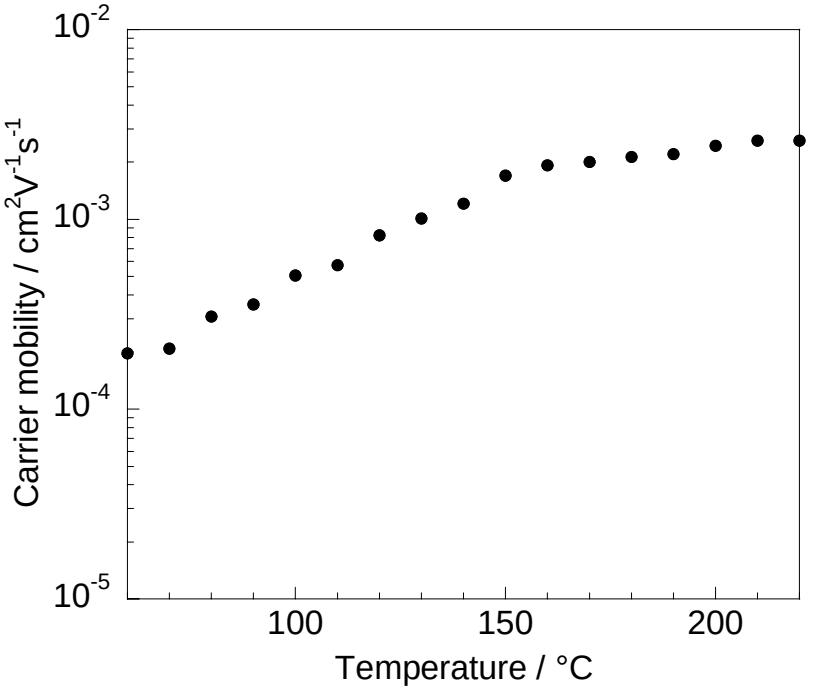

Figure 4-9 Temperature dependence of the positive carrier mobility for **C12F4E-TP** under the electric field of 5.0×10^4 Vcm^{-1}.

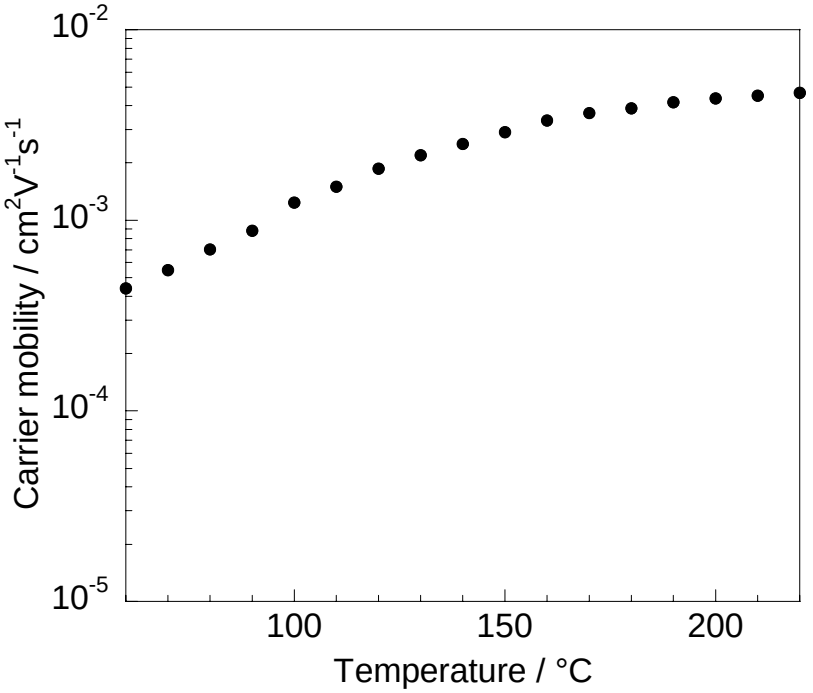

Figure 4-10 Temperature dependence of the positive carrier mobility for **C14F4E-TP** under the electric field of 5.0×10^4 Vcm^{-1}.

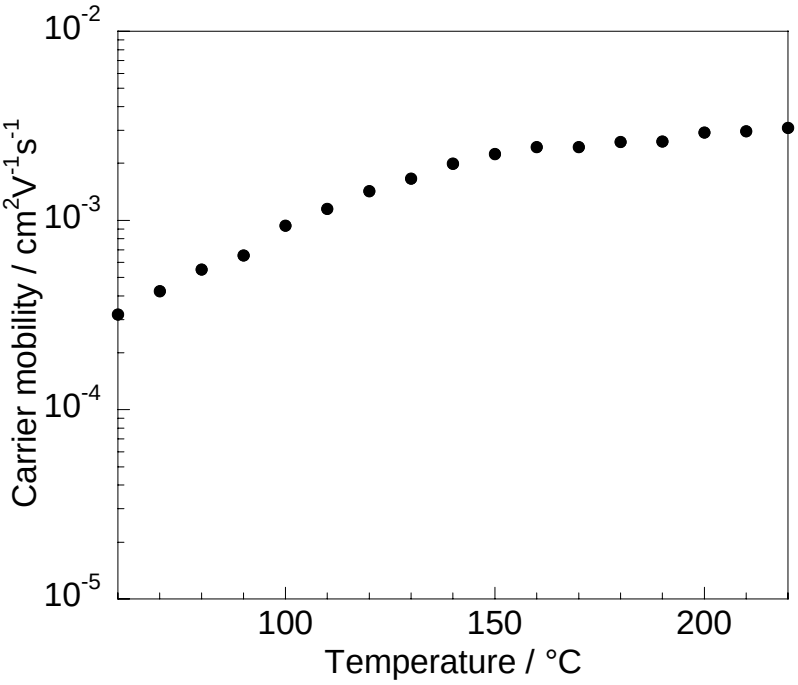

Figure 4-11 Temperature dependence of the positive carrier mobility for **C16F4E-TP** under the electric field of 5.0×10^4 Vcm^{-1}.

The Arrhenius plots of carrier mobility for **CnF4E-TP**s are shown in Figure 4-12, 4-13 and 4-14. For **C12F4E-TP**, two activation energies could be seen for the higher and lower temperature regions. The activation energy in the higher temperature region is 0.10 eV, which changes to 0.27 eV in the lower temperature one. The inflection points are commonly observed at ca. 140 °C. There are the similar behaviours in the Arrhenius plot of carrier mobility for **C14F4E-TP** and **C14F4E-TP**. For the perfluoroalkylated triphenylene mesogens, it was reported that activation energy for the carrier mobility of the Col_h phase is strongly affected by the perfluorinated chain length and a few regimes in temperature could be seen for the variant activation energy.[11]

Any significant transitions weren't observed in the DSC and XRD measurement. This indicates the activation energy change observed is not due to the structural deformations of mesophase time-averaged orders. The activation energy in the higher temperature region is the similar values to these observed the Col_h phases, which shows a slight change of mobility on temperature. Therefore, one has to consider the

change of charge transport mechanism takes place at ca. 140 °C. The variant temperature dependences of carrier mobility in the Col_h temperature range for **CnF4E-TP**s is, as one possibility to explain, caused by change of the core order.

The charge transport of negative carrier were undetectable for **CnF4E-TP**s, whilst alkoxytriphenylenes are reported to be anbipolar.[12]

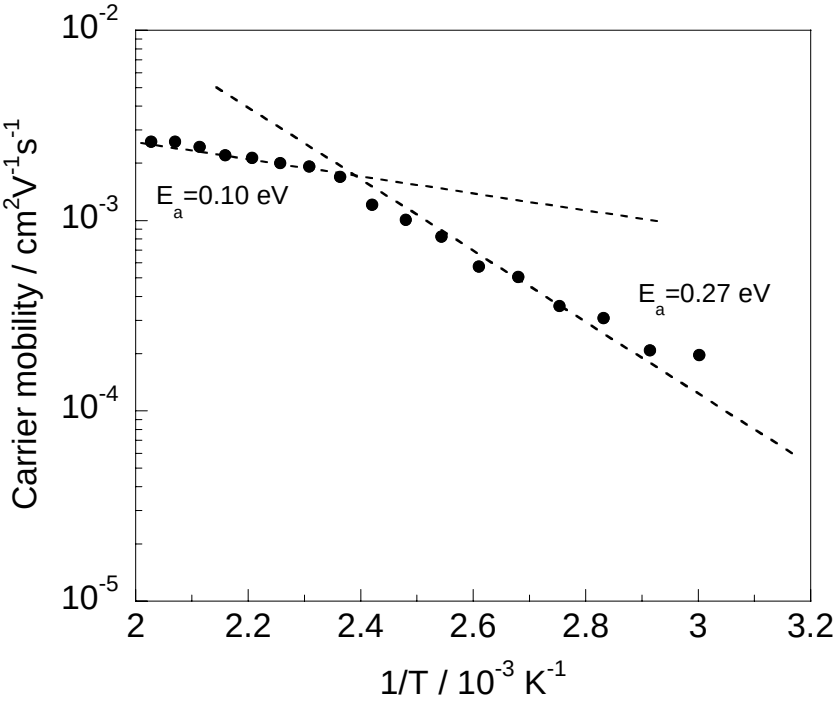

Figure 4-12 Arrhenius plot of the positive carrier mobility for **C12F4E-TP** under the electric field of 5.0×10^4 Vcm^{-1}.

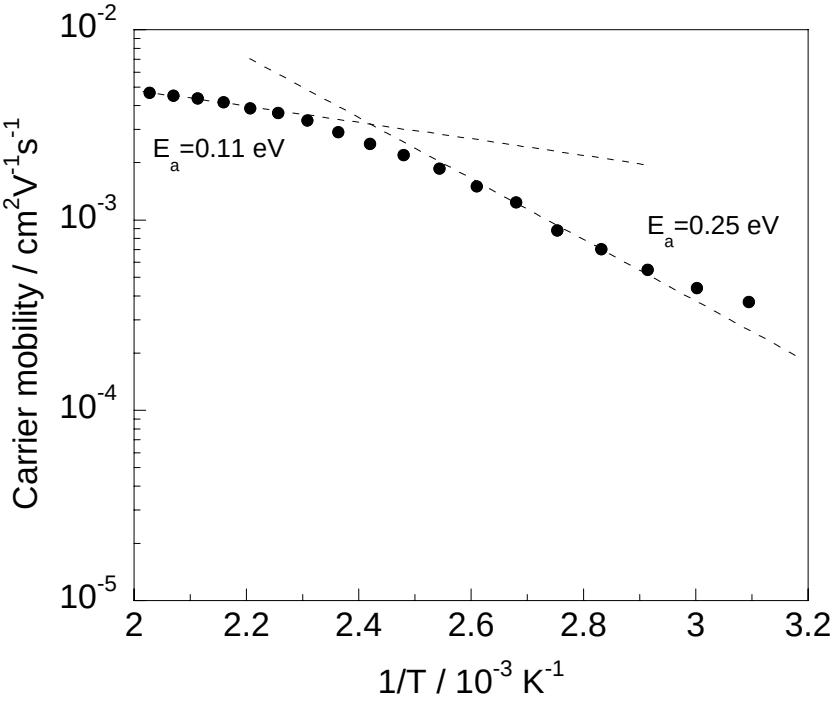

Figure 4-13 Arrhenius plot of the positive carrier mobility for **C14F4E-TP** under the electric field of 5.0×10^4 Vcm^{-1}.

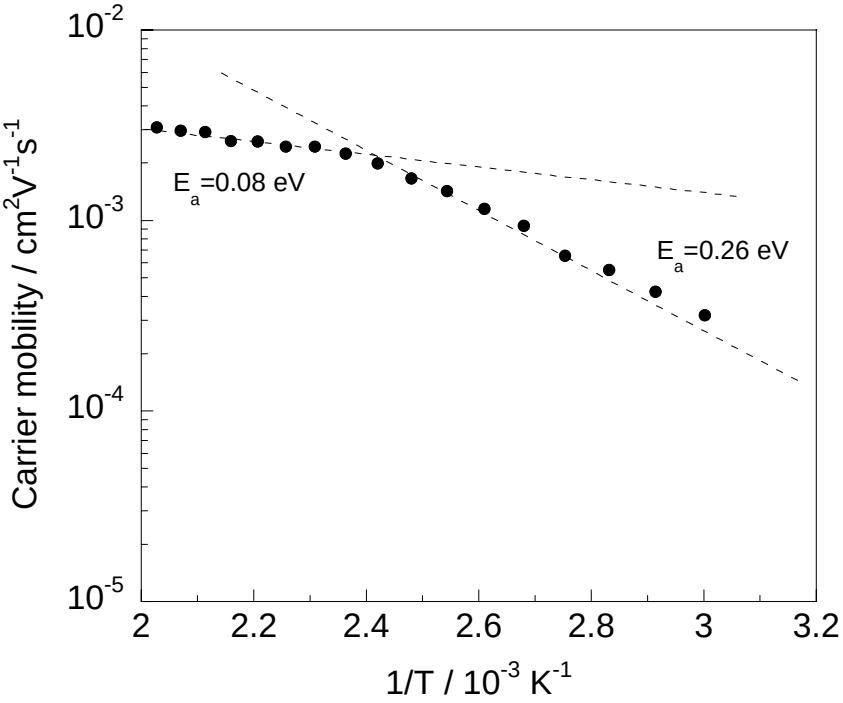

Figure 4-14 Arrhenius plot of the positive carrier mobility for **C16F4E-TP** under the electric field of 5.0×10^4 Vcm^{-1}.

4-3-2-3. TOF measurements of CnF41O-TPs

The transient photocurrent decay curves for the positive carrier detected in the Col_h phase of **CnF41O-TP**s at 170 °C under different applied bias are shown in Figure 4-15, 4-16 and 4-17.

A well-defined non-dispersive transit of **C6F41O-TP** was observed to give clear inflection points in the photocurrent decay curves of the double-logarithmic plots as shown the inset of Figure 4-15. For **C8F41O-TP** and **C10F41O-TP**, the similar non-dispersive transients and reasonable decay curves were observed in the transient photocurrents. The hole mobility was determined to be 4.9×10^{-2} $cm^2V^{-1}s^{-1}$ in the field, 20000~5000 Vcm^{-1}. **C8F41O-TP** and **C10F41O-TP** also show the same order of carrier mobility in the Col_h phase of at 170 °C (**C8F41O-TP**: 4.5×10^{-2} $cm^2V^{-1}s^{-1}$; **C10F41O-TP**: 2.1×10^{-2} $cm^2V^{-1}s^{-1}$). The carrier mobility of **CnF41O-TP**s are almost independent of the electric field in the range 20000~5000 Vcm^{-1} as shown in Figure 4-18.

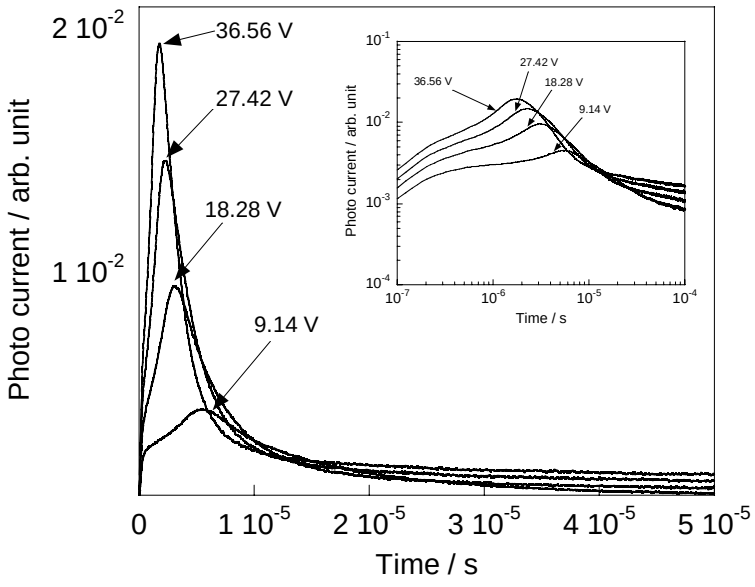

Figure 4-15 The transient photocurrents in the Col_h phase of **C6F41O-TP** at 170 °C for the positive carriers. The double logarithmic plots of the transient photocurrents in the variant electric field are shown in the inset. The sample thickness was 18.28 μm.

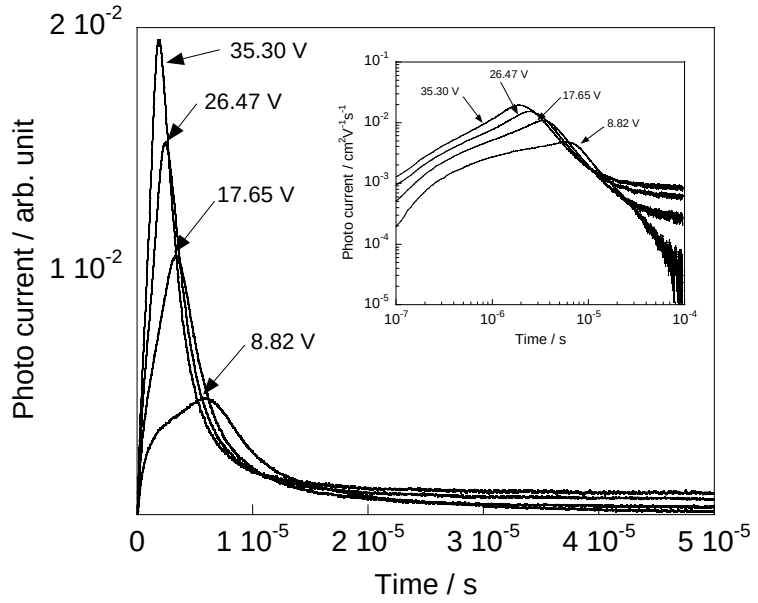

Figure 4-16 The transient photocurrents in the Col_h phase of **C8F41O-TP** at 170 °C for the positive carriers. The double logarithmic plots of the transient photocurrents in the variant electric field are shown in the inset. The sample thickness was 17.65 μm.

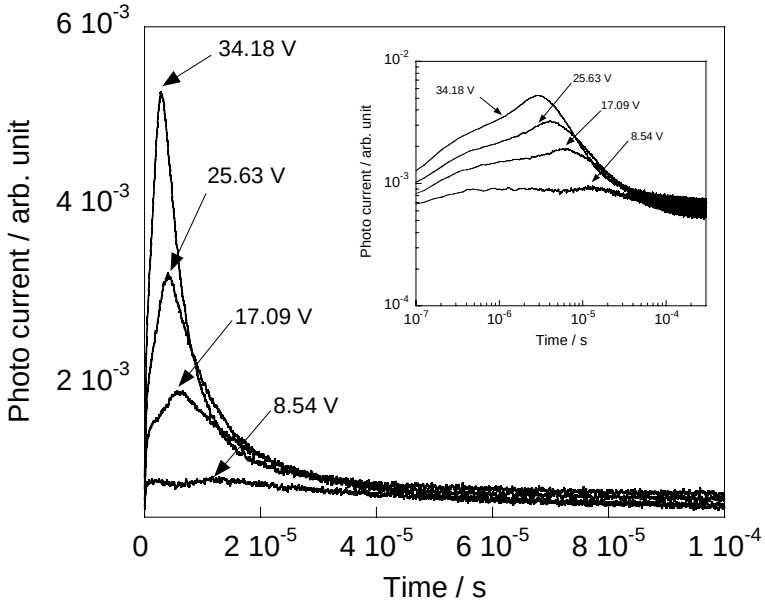

Figure 4-17 The transient photocurrents in the Col_h phase of **C10F41O-TP** at 170 °C for the positive carriers. The double logarithmic plots of the transient photocurrents in the variant electric field are shown in the inset. The sample thickness was 17.09 μm.

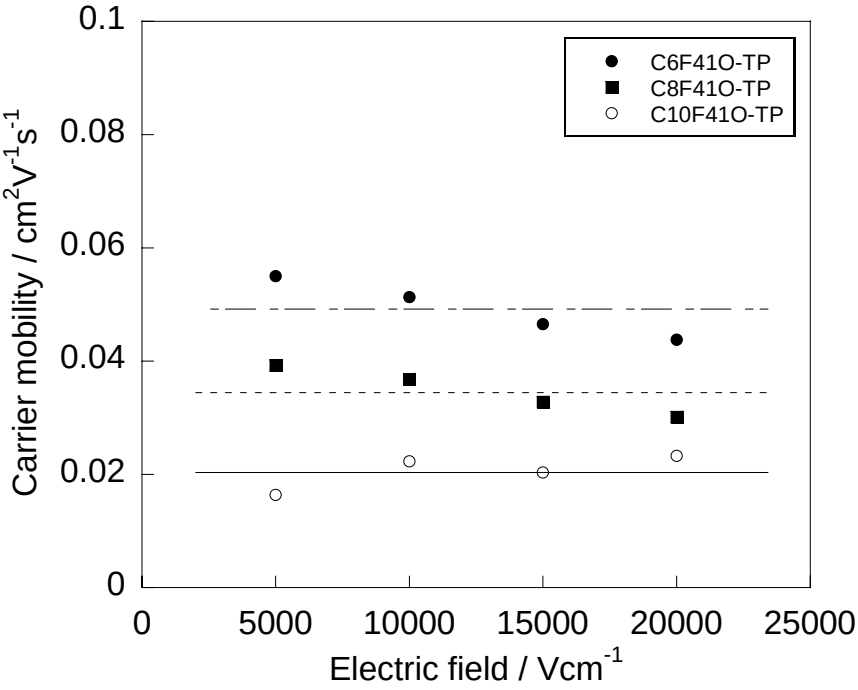

Figure 4-18 Electric field dependence of the carrier mobility of **CnF41O-TP**s at 170 °C.

4-3-2-4. Temperature dependence of carrier mobility for CnF41O-TPs

The temperature dependence of the hole mobility for **C6F41O-TP** in the range 180 to 30 °C is shown in Figure 4-19. The positive carrier mobility of **C6F41O-TP** rises with the decrease of temperature and saturated in the higher temperature region from 180 to 120 °C. The temperature dependence of carrier mobility however is changed at ca. 120 °C and the carrier mobility falls slowly with the decrease of temperature. The positive carrier mobility of **C6F41O-TP** was in order of 10^{-2} $cm^2V^{-1}s^{-1}$ in the range 180 to 30 °C, and it shows the maximum value of 7.8×10^{-2} $cm^2V^{-1}s^{-1}$ on 110 °C. In **C8F41O-TP** and **C10F41O-TP**, the similar order and temperature dependence of positive carrier mobility were observed as shown in Figure 4-20 and 4-21. These temperature dependences of carrier mobility are different from the case of ester homologues **CnF4E-TP**s. The drift mobility of positive carrier for **CnF41O-TP**s (>5.0×10^{-2} $cm^2V^{-1}s^{-1}$) were faster than that in the conventional Col_h phase[6, 12-16] and the Col_p phase[2, 17-18] having the three dimensional alignment. In the X-ray diffraction patterns of **CnF41O-TP**s, there are lots of sharp peaks in the small angle region, indicating the more highly order of molecules as intercolumnar manners,

though any significant reflection peaks due to three dimensional order of molecules isn't observed (see Chapter 3). The high carrier mobility of **CnF41O-TP**s is probably due to their high inter-columnar alignment, which is induced by strong interactions working among the peripheral tetrafluorophenyl moiety.

Furthermore, the carrier mobility of **CnF41O-TP**s decreases with elongation of the peripheral chain length. This temperature dependence of the carrier mobility is probably due to the increase of excluded volume effect with elongation of the peripheral chain length.

The Arrhenius plots of carrier mobility for **CnF41O-TP**s are shown in Figure 4-22, 4-23 and 4-24. For **C6F41O-TP**, two activation energies could be observed the activation energy of -0.15 eV in the high temperature region, which change to 0.09 eV in the lower temperature one. In addition, a sign of the activation energy is changed positive to negative with decrement of temperature. There are the similar behaviour in the Arrhenius plot for **C8F41O-TP** and **C10F41O-TP**. The inflection points are observed around 120 °C in common.

Any significant transitions could no be observed around 120 °C in the DSC and XRD measurement. So, this change of activation energy is not due to the structural deformations of mesophase time-averaged orders. Therefore, these result indicate that the change of the molecular fluctuation take place around 120 °C, so the inclination of temperature dependence of carrier mobility may be changed.

The variant temperature dependences of carrier mobility in the Col_h temperature range for **CnF41O-TP**s is probably caused by change of the core dynamics, implying intermolecular specific interaction could be an important factor to control the dynamical situations of ordered fluid state as mesophase.

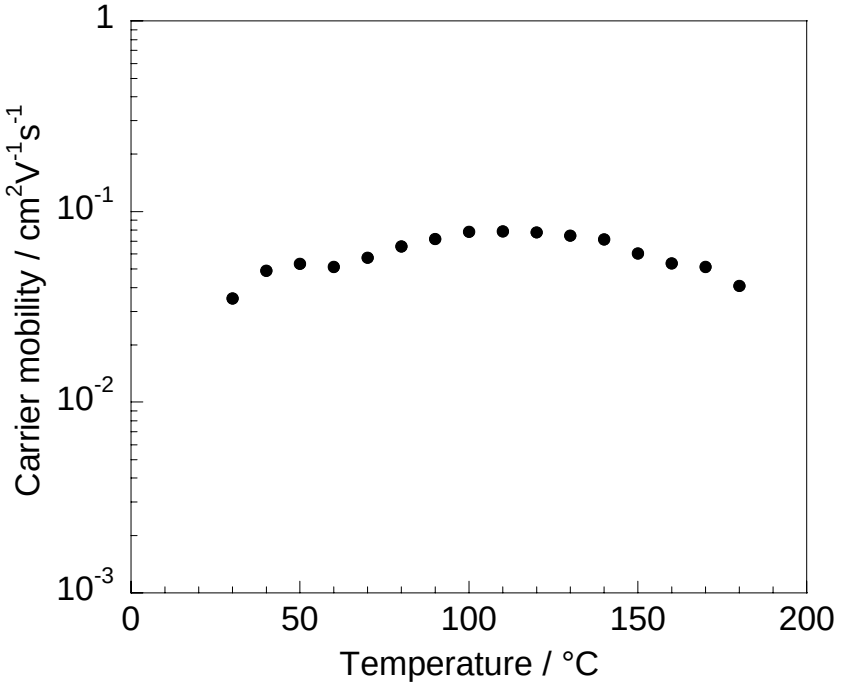

Figure 4-19 Temperature dependence of the positive carrier mobility for **C6F41O-TP** under the electric field of 1.0×10^4 Vcm^{-1}.

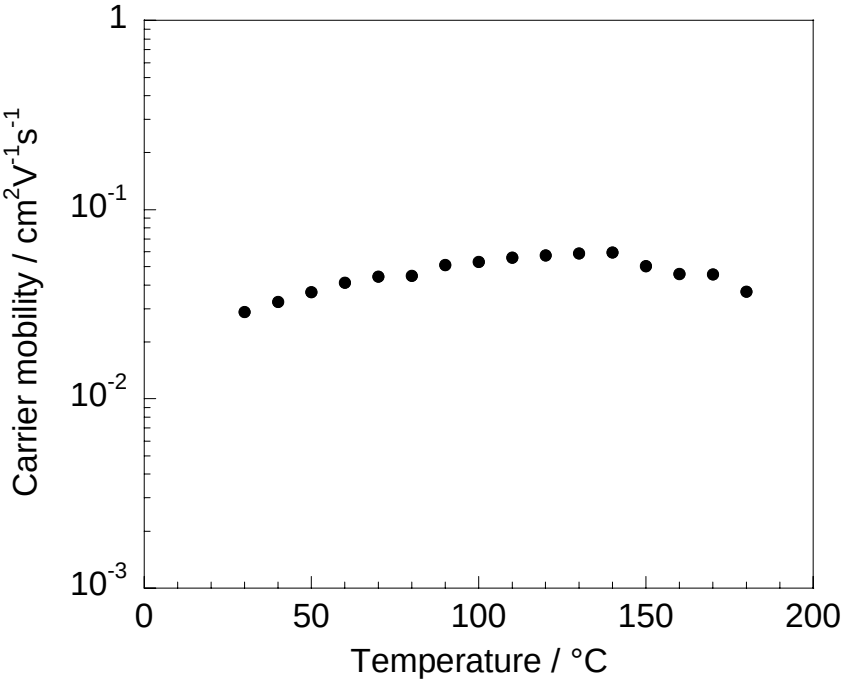

Figure 4-20 Temperature dependence of the positive carrier mobility for **C8F41O-TP** under the electric field of 1.0×10^4 Vcm^{-1}.

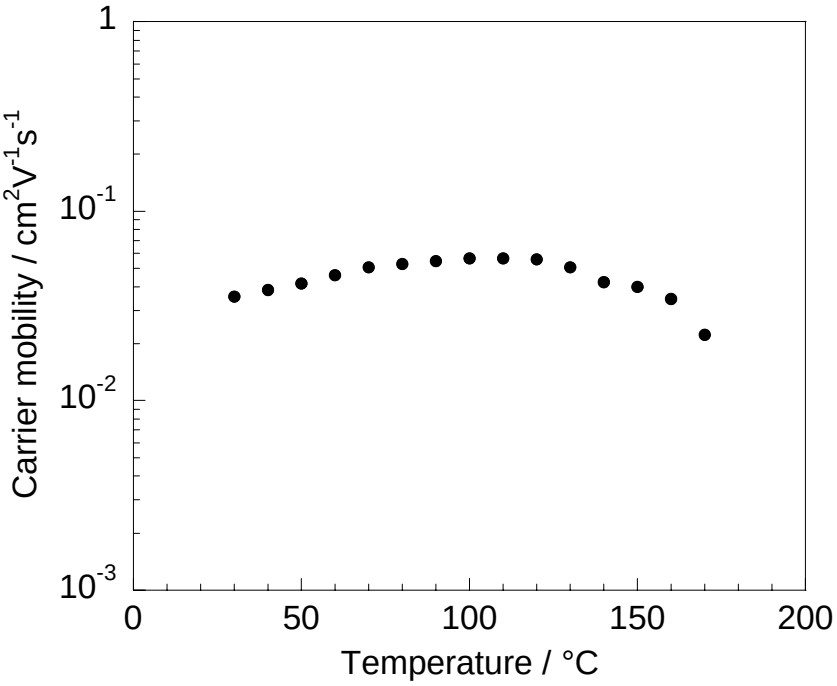

Figure 4-21 Temperature dependence of the positive carrier mobility for **C10F41O-TP** under the electric field of 1.0×10^4 Vcm^{-1}.

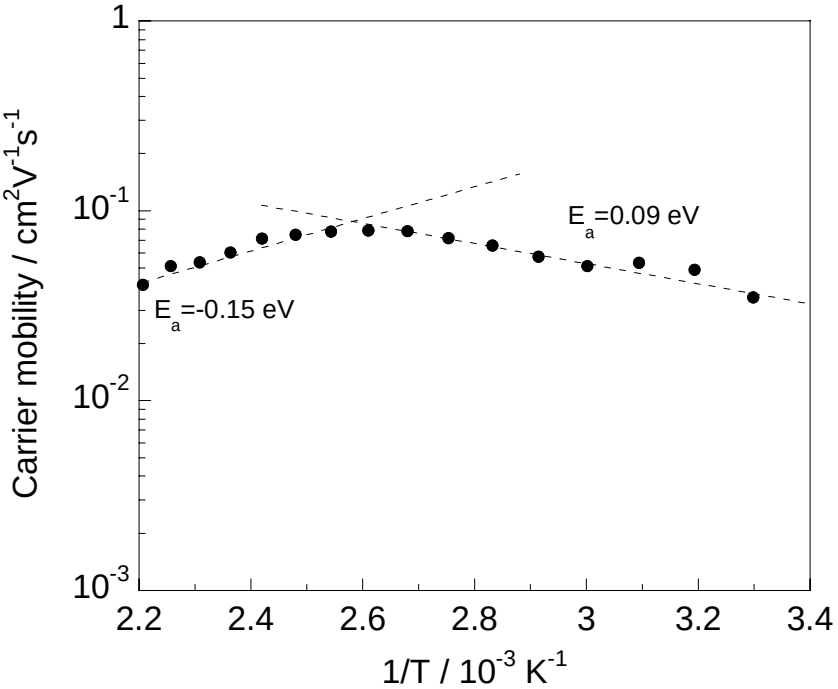

Figure 4-22 Arrhenius plot of the positive carrier mobility for **C6F41O-TP** under the electric field of 1.0×10^4 Vcm^{-1}.

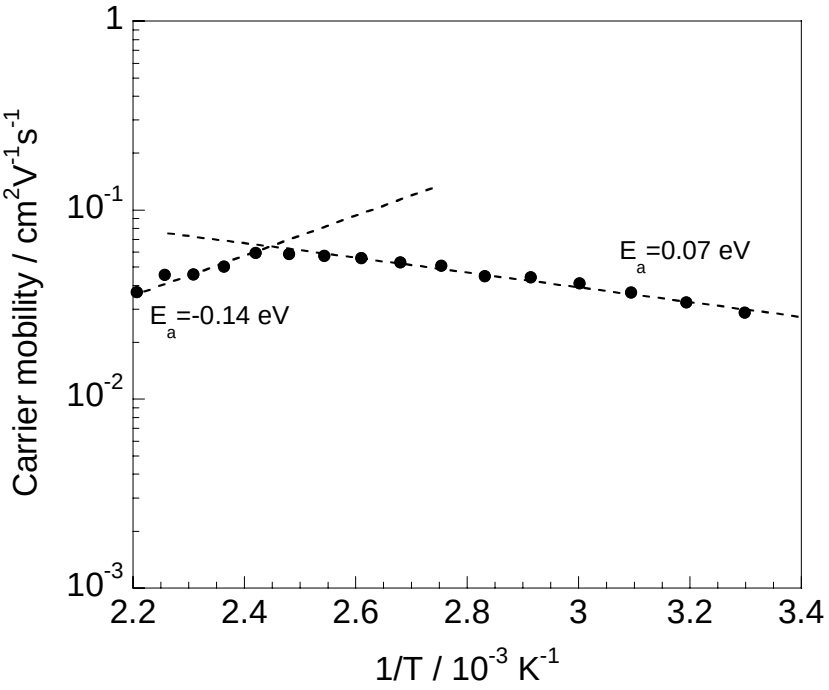

Figure 4-23 Arrhenius plot of the positive carrier mobility for **C8F41O-TP** under the electric field of 1.0×10^4 Vcm^{-1}.

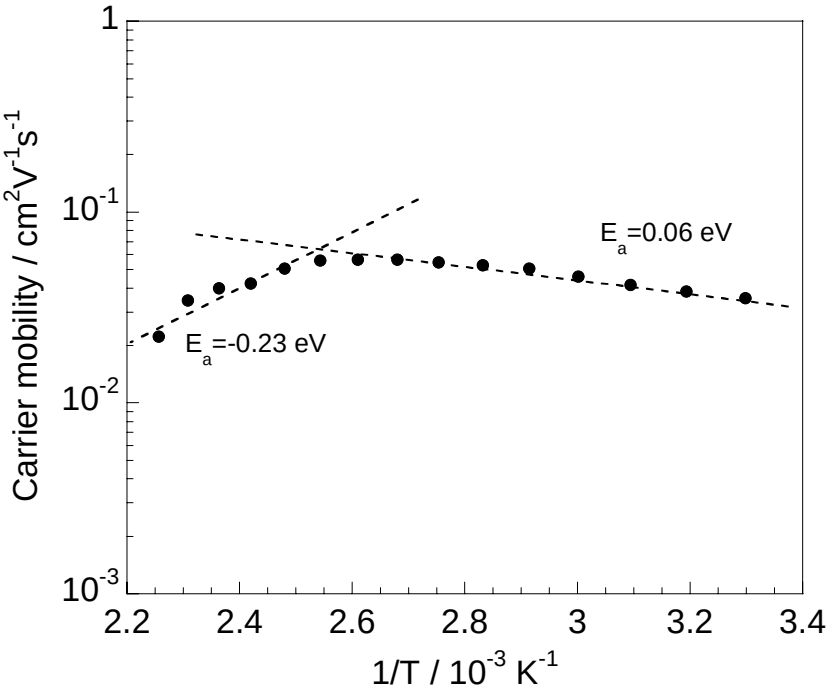

Figure 4-24 Arrhenius plot of the positive carrier mobility for **C10F41O-TP** under the electric field of 1.0×10^4 Vcm^{-1}.

4-4. Conclusion

Drift mobility of a homologues series of 2,3,5,7,10,11-hexakis(4-alkoxy-2,3,5,6-tetrafluorobenzoyloxy)-triphenylene (**CnF4E-TP**: n=12, 14, 16) and 2,3,5,7,10,11-hexakis(4-alkoxy-2,3,5,6-tetrafluorobenzyloxy)-triphenylene (**CnF41O-TP**: n=6, 8, 10) were evaluated by Time-Of-Flight (TOF) technique. Furthermore, the spectroscopic properties of these compounds were measured using UV-Vis spectrometer and photoelectron spectrometer surface analyzer, and the their electronic energy levels were estimated.

The absorption maxima for **CnF4E-TP**s and **CnF41O-TP**s located at the same wavelength of 253.5 nm and 276 nm, respectively. The highest occupied molecular orbital (HOMO) energy of **CnF4E-TP**s and **CnF41O-TP**s were -5.77~-5.81 eV and -5.56~-5.65 eV, respectively, and the lowest unoccupied molecular orbital (LUMO) of each compounds were -1.81~-1.87 eV (**CnF4E-TP**s) and -1.68~ -1.81 eV, respectively.

In TOF measurements, the transient photocurrent showed well-defined non-dispersive transits. The positive carrier mobility of **CnF4E-TP**s were determined to be in the order of 10^{-3} $cm^2V^{-1}s^{-1}$ in the higher (220-100 °C), and in order of 10^{-4} $cm^2V^{-1}s^{-1}$ in the lower (90-60 °C) temperature regions, respectively. In the Arrhenius plots of carrier mobility for **CnF4E-TP**s, it is observed that the activation energy change at ca. 140 °C. The variant temperature dependences of carrier mobility in the Col_h temperature may be caused by change of the core order.

On the other hand, the positive carrier mobility of **CnF41O-TP**s, which are determined to be more than 5.0×10^{-2} $cm^2V^{-1}s^{-1}$ in the range of Col_h phase were relatively fast as carrier mobility of discotic liquid crystal. The high carrier mobility of **CnF41O-TP**s may be due to their high inter-columnar order, which is induced by strong interactions working among the peripheral tetrafluorophenyl moiety. In the Arrhenius plot of carrier mobility for **CnF41O-TP**s, two activation energies could be observed, and the inflection points are commonly observed around 120 °C.

This result indicate that tetrafluorophenyl moiety on the peripheral aromatic ring of **CnF41O-TP**s has very strong interactions of inter-column ways, and this is very interesting property of new molecular design concept for liquid crystalline organic semiconductors of discotics.[19-20]

4-5. References

[1] P. G. LeComber and W. E. Spear, *Phys, Rev. Lett.*, 1970, **25**, 509.

[2] D. Adam, F. Closs, T. Frey, D. Funhoff, D. Haarer, H. Ringdorf, P. Schuhmacher, K. Siemensmeyer, *Phys. Rev. Lett*., 1993, **70**, 457.

[3] D. Adam, P. Schuhmacher, J. Simmerer, L. Häulβing, K. Siemensmeyer, K. Etzbach, H. Ringdorf, and D. Haarer, *Nature*, **1994**, *371*, 141.

[4] H. Bässler, *Mater, Phys. Stat. Solid. B*, 1993, **175**, 15.

[5] J. Simmerer, B. Glüsen, W. Paulus, A. Kettner, P. Schuhmacher, D. Adam, K. H. Etzbach, K. Siemensmeyer, J. H. Wendorf, H. Ringsdorf, and D. Haarer, *Adv. Mater*., **1996**, *8*, 815.

[6] H. Iino, J. Hanna and D. Haarer, *Phys. Rev. B*, 2005, **72**, 193203.

[7] R. J. Bushby and O. R. Lozman, *Current Opinion in Colloid & Interface Science 7*, **2002**, 343.

[8] H. Scherand and E. W. Montroll, *Phys. Rev. B*, 1975, **12**, 2455.

[9] T. Kreouzis, K. Donovan, N. Boden, R. J. Bushby, O. R. Lozman and Q. Liu, *J. Chem. Phys.*, 2001, **114**, 1797.

[10] H. Iino, Y. Takayashiki, J. Hanna, R. J. Bushby and D. Haarer, *Appl. Phys. Lett.*, 2005, **87**, 192105.

[11] Y. Miyake, A. Fujii, M. Ozaki and Y. Shimizu, submitted.

[12] H. Monobe, Y. Shimizu, S. Okamoto, and H. Enomoto, *Mol. Cryst. Liq. Cryst.*, 2007, **476**, 31.

[13] M. Kastler, F. Laquai, K. Müllen, and G. Wegner, *Appl. Phys. Lett.*, 2006, **89**, 252103.

[14] M. J. Sienkowska, H. Monobe, P. Kaszynski, and Y. Shimizu, *J. Mater. Chem.*, 2007, **17**, 1392.

[15] F. Nekelson, H. Monobe, M. Shiro and Y. Shimizu, *J. Mater. Chem.*, 2007, **17**, 2607.

[16] T. Kreouzis, K. Scott, K. J. Donovan, N. Boden, R. J. Bushby, O. R. Lozman, and Q. Liu, *Chem. Phys*. 2000, **262**, 489.

[17] H. Iino, J. Hanna, C. Jäger, D. Haarer, *Mol. Cryst. Liq. Cryst.*, 2005, **436**, 217.

[18] N. Boden, R. J. Bushby, O. R. Lozman, Z. Lu, A. McNeill, B. Movaghar, K. Donovan, and T. Kreouzis, *Mol. Cryst. Liq. Cryst.*, 2004, **410**, 13.

[19] Y. Shimizu, K. Oikawa, K. Nakayama and D. Guillon, *J. Mater. Chem.*, 2007, **17**, 4223.

[20] S. Sergeyev, W. Pisula and Y. H. Geerts, *Chem. Soc. Rev.*, 2007. **36**, 1902.

Concluding Remarks

In this thesis, fluorinated phenyl groups are introduced to discotic liquid crystal molecules aiming the induction of molecular level segregation, which is expected to show in a columnar order by strong attractive interactions. Three types of discotic liquid crystals, which are fluorinated on the peripheral aromatic rings, were synthesized and the mesomorphic and charge transport properties was investigated.

A homologue series of novel 2,3,6,7,10,11-hexakis(4-alkoxy-2,3,5,6-tetrafluorobenzoyloxy)triphenylenes having non-branched and branched peripheral chains were synthesized to study the aromatic fluorination effect on the mesomorphic properties of discotic liquid crystals in **Chapter 1**; All compounds exhibit Col_h phase with higher thermal stabilities which have relatively higher clearing points (>270 °C) with large transition enthalpies. In non-branched homologues, their clearing points were slightly decreased with elongation of peripheral chain length. On the other hand for branched homologues, their clearing points were higher than corresponding non-branched peripheral chain homologues. These results indicated strong interaction among cores with the peripheral tetrafluorophenylene groups.

Hexakis (4-octyloxybenzoyloxy) triphenylene derivatives with mono- or di-fluorinated at the inner (2- and/or 6-), outer (3- and/or 5-) or inner and outer (2- and 5-) positions in the peripheral aromatic rings were synthesised and investigated on the mesomorphic behaviour to reveal the alteration of fluorinated positions in the phenyl rings leads to a drastic change of the mesomorphism involving the thermal stability in **Chapter 2**; Their mesomorphism show the variation of the position and the number of fluorine atoms on the peripheral phenyl rings leads to a drastic change of mesomorphism. Especially, the thermal stability of the columnar mesophase are extremely stabilized over 400 ºC in the homologues, for which peripheral phenylene groups are fluorinated at the outer positions. Thermal stability of mesophase above 400 ºC has been reported only for compounds having large π-conjugation systems, such as hexabenzocoronenes, and carbonaceous mesophase. It is quite interesting that mesomorphic properties drastically change by the tiny difference of the position in fluorination on peripheral aromatic rings.

The results of Chapter 1 and Chapter 2 strongly show that a certain attractive force works around the

fluorinated peripheral phenylene moieties, so a triphenylene plays a role of the large core part involving the peripheral fluorinated phenyl rings and indicate a strong interaction works among the stacking molecules.

A homologue series of novel 2,3,6,7,10,11-hexakis(4-alkoxy-2,3,5,6-tetrafluorobenzyloxy)triphenylenes were synthesised to investigate a change of mesomorphic behaviour by the alteration of linkage group, and investigated on the mesomorphic behavior in **Chapter 3**; All compounds exhibit Col_h phase, similarly the corresponding ester homologues show only a Col_h phase. The phase transition enthalpies and entropies of clearing point for these homologues are much larger (ΔH: over 50 $kJmol^{-1}$, ΔS: over 100 $Jmol^{-1}K^{-1}$) than these of not only the corresponding ester homologues but also conventional discotic liquid crystals. In comparison with ester homologues, the improvement of molecular order in the Col_h phase may be caused by the change of electric state for tetrafluorophenyl groups owing to the alteration of linkage group ester to ether, though the thermal stabilities of mesomorphism are decrease.

A homologues series of 2,3,5,7,10,11-hexakis(4-alkoxy-2,3,5,6-tetrafluorobenzoyloxy)triphenylene and 2,3,5,7,10,11-hexakis(4-alkoxy-2,3,5,6-tetrafluorobenzyloxy)triphenylene were evaluated as organic semiconductor with Time-Of-Flight (TOF) technique in **Chapter 4**; The positive carrier mobility of the benzoyl homologues were in order of 10^{-3} $cm^2V^{-1}s^{-1}$ on the higher (220-100 °C), and in order of 10^{-4} $cm^2V^{-1}s^{-1}$ on the lower (90-60 °C) temperature regions, respectively. On the other hand, the positive carrier mobility of the benzyl homologues which are more than 5.0×10^{-2} $cm^2V^{-1}s^{-1}$ were very fast as carrier mobility in discotic liquid crystalline phase. The high carrier mobility of the benzyl homologues may be due to their highly inter-columnar alignment, which is induced by tetrafluorophenyl moiety. The homologues series of 2,3,5,7,10,11-hexakis(4-alkoxy-2,3,5,6-tetrafluorobenzyloxy)triphenylene should be useful materials for liquid crystalline organic semiconductor.

Therefore in this thesis it was successfully clarified that new strategies of molecular design for liquid crystalline semiconductor by fluorination on peripheral aromatic rings of discotic liquid crystals is possible and the fluorination effect on the peripheral aromatic rings of discotic liquid crystals gives stabilized columnar structure with the higher molecular order.

List of achievement

§ Dissertation

Chapter 1:

Aromatic Fluorination Effect on the Mesomorphic Properties of Discotic Liquid Crystal of Alkoxybenzoyloxytriphenylene

Yasuyuki Sasada, Hirosato Monobe, Yasukiyo Ueda, and Yo Shimizu

Chemistry Letters, 2007, **36**, 584.

Aromatic Fluorination Effect on the Mesomorphic Properties of Discotic Liquid Crystal of Alkoxybenzoyloxytriphenylene

Yasuyuki Sasada, Hirosato Monobe, Yasukiyo Ueda, and Yo Shimizu

Molecular Crystals and Liquid Crystals, in press.

Chapter 2:

Drastic enhancement of discotic mesomorphism induced by fluorination of the peripheral phenyl groups in triphenylene mesogens

Yasuyuki Sasada, Hirosato Monobe, Yasukiyo Ueda, and Yo Shimizu

Chemical Communications, **2008**, 1452.

Chapter 3:

Mesomorphic and charge transport properties of

2,3,6,7,10,11-hexakis(4-alkoxy-2,3,5,6-tetrafluorobenzyloxy)triphenylenes

Yasuyuki Sasada, Hirosato Monobe, Yasukiyo Ueda, and Yo Shimizu

To be prepared.

Chapter 4:

Mesomorphic and charge transport properties of

2,3,6,7,10,11-hexakis(4-alkoxy-2,3,5,6-tetrafluorobenzoyloxy)triphenylenes

Yasuyuki Sasada, Hirosato Monobe, Yasukiyo Ueda, and Yo Shimizu

Chemistry of Materials, submitted.

§ Patent applications

Liquid crystal organic semiconductor material and organic semiconductor device using the same

Yasuyuki Sasada, Yo Shimizu, and Hirosato Monobe

JP2008085289, EP1894984, US2008058544.

§ Presentation in symposium

1) Change of phase transition behavior by fluorination of the phenyl groups in alkoxybenzoyloxytriphenylen discotic liquid crystals

Yasuyuki Sasada, Hirosato Monobe, Yasukiyo Ueda, and Yo Shimizu

Japanese Liquid Crystal Conference 2006, **3B01**, Akita University, Akita, Japan, September, 2006.

2) Discotic liquid crystals having fluorinated aromatic rings: mesomorphic properties of fluorobenzoyltripehnylene.

Yasuyuki Sasada, Hirosato Monobe, Yasukiyo Ueda, and Yo Shimizu

The 87th spring meeting 2007; The Chemical Society of Japan, **2E2-04**, Kansai University, Osaka, Japan, March, 2007.

3) Effect of type and length of peripheral alkoxy group on the mesomorphic properties in alkoxytetrafluorobenzoyloxytripehnylene discotic liquid crystals.

Yasuyuki Sasada, Hirosato Monobe, Yasukiyo Ueda, and Yo Shimizu

Japanese Liquid Crystal Conference 2007, **1pC03**, Tokyo Institute of Technology, Tokyo, Japan, September, 2007.

4) Charge transport properties of alkoxytetrafluorobenzoyloxytriphenylenes

Yasuyuki Sasada, Hirosato Monobe, Yasukiyo Ueda, and Yo Shimizu

The 12th symposium; The society for the study of liquid crystalline chemistry, **P20**, The University of Tokyo, Tokyo, Japan, June, 2008.

5) Mesomorphic and charge transport properties of alkoxytetrafluorobenzyloxytriphenylenes

Yasuyuki Sasada, Hirosato Monobe, Yasukiyo Ueda, and Yo Shimizu.

Japanese Liquid Crystal Conference 2008, **1b02**, Campus plaza Kyoto, Kyoto, Japan, September, 2008.

6) Discotic liquid crystals having fluorinated aromatic rings: mesomorphic properties of fluorobenzoyltripehnylene.

Yasuyuki Sasada, Hirosato Monobe, Yasukiyo Ueda, and Yo Shimizu

The 89th spring meeting 2009; The Chemical Society of Japan, **3E3-11**, Nihon University, Chiba, Japan, March, 2009.

§ Presentation in international symposium

1) Aromatic Fluorination Effect on the Mesomorphic Properties of Discotic Liquid Crystals of Alkoxybenzoyloxytriphenylenes.

Yasuyuki Sasada, Hirosato Monobe, Yasukiyo Ueda, and Yo Shimizu

9th European Conference on Liquid Crystals, **PA22**, Lisbon, Portugal, July, 2007.

2) Mesomorphic and Charge Transport Properties of Alkoxytetrafluorobenzoyloxytriphenylenes.

Yasuyuki Sasada, Hirosato Monobe, Yasukiyo Ueda, and Yo Shimizu

The European Materials Research Society 2008 Spring Meeting, **SymposiumQ-16-65**, Strasbourg, France, May, 2008.

3) Aromatic Fluorination Effect on the Mesomorphic Properties of Discotic Liquid Crystals of Alkoxybenzoyloxytriphenylene

Yasuyuki Sasada, Hirosato Monobe, Yasukiyo Ueda, and Yo Shimizu

22nd International Liquid Crystal Conference, **P3-MA41**, Jeju, Korea, June, 2008.

4) Charge transport properties of alkoxybenzoykoxytriphenylenes

Yasuyuki Sasada, Hirosato Monobe, Yasukiyo Ueda, and Yo Shimizu

The 4th Japanese-Italian Workshop on Liquid Crystals, **P42**, Nara-ken New Public Hall, Nara, Japan, July, 2008.

5) Triphenylene mesogens with peripherally attached fluorinated phenyl groups: columnar mesomorphism and mobility behaviour.

Yasuyuki Sasada, Hirosato Monobe, Yasukiyo Ueda, and Yo Shimizu

4th International Meeting on Molecular Electronics, **T5-OC15**, Grenoble, France, December, 2008.

Acknowledgement

I wish to express my deep gratitude to Professor Yasukiyo Ueda, Department of Molecular Science and Material Engineering, Graduate School of Science and Technology, Kobe University for his grateful direction and discussion in this work.

I grateful acknowledge Dr. Yo Shimizu, Synthetic Nano-Function Group, Nanotechnology Research Institute, Advanced Industrial Science and Technology for his essential direction and helpful discussion in this work.

I wish to express my sincere gratitude to Associate Professor Kenji Ishida and Research Assistant Ms. Yasuko Koshiba, Department of Molecular Science and Material Engineering, Graduate School of Science and Technology, Kobe University for their useful suggestion and helpful support.

I deeply appreciate Dr. Hirosato Monobe and Dr. Takuya Ohzono, Synthetic Nano-Function Group, Nanotechnology Research Institute, Advanced Industrial Science and Technology for their useful suggestion and discussion.

I grateful appreciate Dr. Yasuyuki Goto, Liquid Crystals Division, Chisso Corporation, and Dr. Kazutoshi Miyazawa, Ms. Atsuko Fujita, Mr. Shizuo Murata, and Dr. Ryushi Shundo, Research Laboratory I, Goi Laboratory, Chisso Petrochemical Corporation for giving me the opportunity for this study and their helpful support. I also deeply appreciate Chisso Corporation Liquid Crystals Division for their financial support.

I wish to thank my wife Kumiko and our dear children Kouta and Manami for their continuous encouragement and thoughtful support.

January, 2009

Yasuyuki SASADA